GEORGIOS LAZAROU

IMPLICATIONS OF MILITARY AIRCRAFT'S MISSION OPTIMAL PERFORMANCE ON GAS TURBINE ENGINE LIFE EXPECTANCY

SCHOOL OF AEROSPACE, TRANSPORT AND MANUFACTURING

MSc by Research Thesis

Academic Year: 2020 - 2023

Supervisor: Dr Theoklis Nikolaidis

Associate Supervisor: Dr Nalianda Devaiah

August 2023

SCHOOL OF AEROSPACE, TRANSPORT AND MANUFACTURING

MSc by Research Thesis

Academic Year 2020 - 2023

GEORGIOS LAZAROU

IMPLICATIONS OF MILITARY AIRCRAFT'S MISSION OPTIMAL PERFORMANCE ON GAS TURBINE ENGINE LIFE EXPECTANCY

Supervisor: Dr Theoklis Nikolaidis
Associate Supervisor: Dr Nalianda Devaiah

August 2023

© Cranfield University 2023. All rights reserved. No part of this publication may be reproduced without the written permission of the copyright owner.

Academic integrity declaration

I declare that:

- the thesis submitted has been written by me alone.
- the thesis submitted has not been previously submitted to this university or any other.
- that all content, including primary and/or secondary data, is true to the best of my knowledge.
- that all quotations and references have been duly acknowledged according to the requirements of academic research.

I understand that to knowingly submit work in violation of the above statement will be considered by examiners as academic misconduct.

Abstract

Gas turbine engines have a crucial role in evaluating military aircraft performance. Operating in a range of missions and environmental conditions, they are subjected to an excessively demanding usage often reaching their operating limits. The impact prediction on engine components degradation of this adverse usage requires a multi-disciplinary approach to best capture its effects.

This master thesis investigates the implications of optimal mission performance on the degradation of military gas turbine engines. The research focuses on the degradation of first stage of the high-pressure turbine caused by the failure mechanisms of creep, low cycle fatigue and high cycle fatigue, each acting independently on the turbine blades.

By exploring the implications of mission performance on engine degradation, this study provides valuable insights for optimizing mission execution strategies and improving operational efficiency in military aviation.

Through a comprehensive analysis, several key findings have been identified. It was observed that as the turbine entry temperature (TET) decreases, the stresses on the turbine blade have a disproportionately greater effect on the overall damage. This suggests that maintaining optimal TET levels is crucial for mitigating engine degradation, as an increase of 0.005% in blade temperature can lead to 40% more thrust, 100% more fuel consumption but can reduce life by 18% in Creep, 15% in LCF and 14% in HCF.

In addition, the study reveals that the use of afterburner though having similar thermo-mechanical stresses upon the blades with the maximum dry setting, the extensive usage in a mission can significantly impact the life consumption. A mission with 40% less overall duration can present an up to 40% reduced life expectancy.

Lastly, the investigation highlights the significant differences in life consumption during several optimal climb paths. A time optimized profile is found to be the most damage inflicting having 3 times less lifespan than noise and IR optimized

paths. A life expectancy of only 80 flight hours is predicted for the usage applied on this profile resulting from the impact of low cycle fatigue contribution.

This research contributes to the field of military-related costs by shedding light on the operational availability of gas turbine engines.

Keywords: military aircraft, gas turbine engine degradation, low bypass ratio, high-pressure turbine, creep, low cycle fatigue, high cycle fatigue, afterburner, operational availability.

Acknowledgements

It has been exactly three years since I started my journey into research and even though I had previously been in touch with small projects, I could never imagine the commitment and sheer will required to fulfill a research like this. Though it has been so long time I write these words as a last remark to express my happiness that I was given this opportunity.

This would have never been possible had not been my close friend Aristeidis Antonakis who has mentored me all these year through my academic and professional career. I will be forever thankful for his efforts and advice.

My supervisors, Dr Theoklis Nikolaidis and Dr Nalianda Devaiah, who have guided me and offered valuable advice, that were crucial for this research. In addition, I would like to express them my gratitude for the understanding they have showed these years for the personal issues I went through.

Finally, I want to thank all the people who have stood by me, motivated me and encouraged me to continue this work during difficult times. One should always have family and friends that can rely upon and be influenced by.

Table of Contents

Academic integrity declaration i
Abstract ii
List of Figures vii
List of Tables ix
List of Equations x
Nomenclature xii
List of Abbreviations xiv
1 Introduction 1
2 Literature review 4
2.1 Introduction to Techno-economic and Environmental Risk Assessment (TERA) 5
2.2 Aircraft Performance 6
2.2.1 Aircraft Performance Modelling 7
2.2.2 Flight Path Analysis and Mission Simulation 8
2.3 Gas Turbine Life Estimation 10
2.4 Research gap 13
3 Methodology 15
3.1 Aircraft modelling 18
3.2 Gas turbine modelling 18
3.3 Mission Simulation 20
3.3.1 Optimal climb paths 24
3.4 Gas turbine design 25
3.4.1 HPT blade sizing 25
3.4.2 Aerodynamic calculations 26
3.5 Heat transfer analysis 27
3.5.1 Heat transfer coefficient and blade temperature 28
3.5.2 Radial temperature distribution factor (RTDF) 28
3.5.3 Blade cooling performance 29
3.5.4 Blade temperature at coolant side 29
3.6 Mechanical stress 31
3.6.1 Centrifugal force 31
3.6.2 Gas bending stress 32
3.7 Failure mechanisms 35

3.7.1 Creep 35
3.7.2 Fatigue 36
3.8 Total damage 44
4 Case Studies 45
4.1 Optimal climb profiles 58
5 Results Discussion 75
6 Future work 77
7 References 79

List of Figures

Figure 2-1: TERA Philosophy [8] 5
Figure 2-2: Typical fighter speed-altitude envelopes superimposed on contours of constant specific energy [16] 8
Figure 2-3: Comparison of minimum time to climb paths for typical subsonic fighter [16]. 9
Figure 2-4: Comparison of engine power settings [3] 11
Figure 2-5: Blade damage life for mission type [12]. 13
Figure 3-1: Project methodology 15
Figure 3-2: Block diagram of the aircraft performance model showing the data flow between the aircraft, engine and interference modules [18]..... 18
Figure 3-3: Input and output in TURBOMATCH modules [32] 19
Figure 3-4: Engine thermodynamic modules and station numbering..... 19
Figure 3-5: Cruise Optimization for maximum range. The red circle denotes the optimal solution whereas red dots account for intermediate solutions generated during an optimization process. [18] 23
Figure 3-6: Nominal velocity triangle for the 1st stage HPT rotor [42] 26
Figure 3-7: Spanwise blade temperature distribution for different engine ratings 30
Figure 3-8: Centrifugal force acting on blade sections. 31
Figure 3-9: Spanwise blade Centrifugal Stress for different engine ratings 32
Figure 3-10: Spanwise blade Bending Stress for different engine ratings 34
Figure 3-11: Spanwise blade Total Stress for different engine ratings 34
Figure 3-12: Spanwise Creep life in Log(hr) for different engine ratings 36
Figure 3-13: Fatigue life method of Universal Slopes [47] 37
Figure 3-14: Idealized fatigue hysteresis loop displaying Nuebler's Rule [48] .. 38
Figure 3-15: Spanwise LCF life in Log(Nf) for different engine ratings 39
Figure 3-16: Combined Goodman/S-N diagram [48] 40
Figure 3-17: Approximation of S-N curve for steel [48] 40
Figure 3-18: Representation of combined cyclic loading [28] 41
Figure 3-19: Major cycle Goodman diagram [25] 42
Figure 3-20: Minor cycle Goodman diagram [25] 43
Figure 3-21: S-N/R-M diagram [25] 43
Figure 3-22: Spanwise HCF life in Log(Nf) for different engine ratings 43
Figure 4-1: Training mission: Alt - Range 45
Figure 4-2: Training mission: Alt & Mach - Time 45
Figure 4-3: Training mission: Fuel Flow – Time 46
Figure 4-4: Training mission: TET – Time 46
Figure 4-5: Training mission: AB temperature – Time 47
Figure 4-6: Supersonic interception: Alt - Range 47
Figure 4-7: Supersonic interception: Alt – Mach 48
Figure 4-8: Supersonic interception: Fuel Flow – Time 48
Figure 4-9: Supersonic interception: TET – Time 49
Figure 4-10: Supersonic interception: AB temperature – Time 49

Figure 4-11: High AoA BFM: Alt – Range 50
Figure 4-12: High AoA BFM: Alt – Mach 50
Figure 4-13: High AoA BFM: Fuel Flow – Time 51
Figure 4-14: High AoA BFM: TET – Time 51
Figure 4-15: High AoA BFM: AB Temperature – Time 52
Figure 4-16: Thermo-mechanical analysis at "Idle" rating 53
Figure 4-17: Thermo-mechanical analysis at "Intermediate" rating 53
Figure 4-18: Thermo-mechanical analysis at "Max" rating 54
Figure 4-19: Thermo-mechanical analysis at "AB" rating 54
Figure 4-20: Training mission cycles to failure 55
Figure 4-21: Supersonic interception cycles to failure 55
Figure 4-22: High AoA BFM cycles to failure 56
Figure 4-23: Training mission life consumption 57
Figure 4-24: Supersonic interception life consumption 57
Figure 4-25: High AoA BFM life consumption 58
Figure 4-26: Max Range: Alt-Range 59
Figure 4-27: Max Range: Alt-Mach 59
Figure 4-28: Max Range: Fuel Flow-Time 60
Figure 4-29: Max Range: TET-Time 60
Figure 4-30: Max Range: AB Temperature-Time 61
Figure 4-31: Min Fuel: Alt-Range 62
Figure 4-32: Min Fuel: Alt-Mach 62
Figure 4-33: Min Fuel: Fuel Flow-Time 63
Figure 4-34: Min Fuel: TET-Time 63
Figure 4-35: Min Fuel: AB Temperature - Time 64
Figure 4-36: Min IR:Alt-Range 64
Figure 4-37: Min IR: Alt- Mach 65
Figure 4-38: Min IR: Fuel Flow-Time 65
Figure 4-39: Min IR: TET-Time 65
Figure 4-40: Min IR: AB Temperature-Time 66
Figure 4-41: Min Noise: Alt-Range 66
Figure 4-42: Min Noise: Alt-Mach 67
Figure 4-43: Min Noise: Fuel Flow-Time 67
Figure 4-44: Min Noise: TET-Time 68
Figure 4-45: Min Noise: ABT-Time 68
Figure 4-46: Min Time: Alt-Range 69
Figure 4-47: Min Time: Alt-Mach 69
Figure 4-48: MIn Time: Fuel Flow-Time 70
Figure 4-49: Min Time: TET-Time 70
Figure 4-50: Min Time: AB Temperature-Time 71
Figure 4-51: Minimum Time Climb cycles to failure 71
Figure 4-52: Minimum Noise Climb cycles to failure 72
Figure 4-53: Minimum IR signature Climb cycles to failure 72
Figure 4-54: Minimum Fuel Climb cycles to failure 73
Figure 4-55: Maximum Mission Range cycles to failure 73

List of Tables

Table 3-1: Engine performance characteristics 20
Table 3-2: Engine design point 20
Table 3-3: Cruise optimization objectives 22
Table 3-4: Energy Transition optimization objectives 23
Table 4-1: Life critical points 56
Table 4-2: Life critical points 74

List of Equations

(3-1)…….. 21
(3-2)……..... 21
(3-3)..... 22
(3-4)……. 22
(3-5)…….. 24
(3-6)..... 24
(3-7)…….. 24
(3-8)..... 24
(3-9)……. 24
(3-10)……..... 24
(3-11)…….. 24
(3-12)..... 26
(3-13)..... 26
(3-14)..... 27
(3-15)..... 27
(3-16)..... 27
(3-17)..... 27
(3-18)..... 27
(3-19)..... 28
(3-20)..... 28
(3-21)..... 28
(3-22)..... 28
(3-23)..... 28
(3-24)..... 28
(3-25)..... 29
(3-26)..... 29
(3-27)..... 29
(3-28)..... 29
(3-29)..... 29
(3-30)..... 29
(3-31)..... 30
(3-32)..... 30
(3-33)..... 30
(3-34)..... 31
(3-35)..... 31
(3-36)..... 31
(3-37)..... 31
(3-38)..... 32
(3-39)..... 32
(3-40)..... 33
(3-41)..... 33
(3-42)..... 33
(3-43)..... 33

(3-44)..... 33
(3-45)..... 33
(3-46)..... 33
(3-47)..... 33
(3-48)..... 35
(3-49)..... 37
(3-50)..... 37
(3-51)..... 38
(3-52)..... 38
(3-53)..... 38
(3-54)..... 38
(3-55)..... 40
(3-56)..... 41
(3-57)..... 41
(3-58)..... 41
(3-59)..... 41
(3-60)..... 41
(3-61)..... 42
(3-62)..... 42
(3-63)..... 42
(3-64)..... 44
(3-65)..... 44

Nomenclature

A	Area	m2
Bi	Biot number	-
Cd	Drag coefficient	-
Cl	Lift coefficient	-
Cp	Specific heat in constant pressure	J/K*kg
D	Drag	N
d	Diameter	m
D	True fracture ductility	-
D	Damage fraction	-
E	Young’s modulus material property	GPa
Es	Specific Energy	-
F	Force	N
FAR	Fuel Air Ratio	-
g	gravitational acceleration	m/sec2
h	Heat transfer coefficient	W/m2*K
Hp	Pressure Altitude	m
I	Inertia	mm4
k	Fluid thermal conductivity	W/m*K
Kf	Fatigue concentration factor	-
Kt	Stress concentration factor	-
m	mass	kg
m	mass flow	kg/s
M	Moment	N*m
Nf	Number of cycles to failure	-
Nu	Nusselt number	-
nz	Load factor	-
p	Static Pressure	Pa
Pr	Prandtl number	-
Ps	Specific Power	m/s
Pst	Static Pressure	Pa
Pt	Total Pressure	Pa
q	heat energy	J
Qf	Fuel flowrate	kg/s
r	radius	m
R	Universal gas constant	J/(kg*K)
Re	Reynolds number	-

S	Surface area	m2
St	Stanton number	-
T	Thrust	kN
T	Total Temperature	K
tf	time to failure	Hrs
Tst	Static Temperature	K
Tt	Total Temperature	K
U	linear speed	m/s
V	Velocity	m/s
W	Mass flow (for Turbomatch)	kg/s
WAR	Water/Air mass	-
X	cooling technology factor	-
X (turbomatch)	Water phase	-
γ	Flight path angle	deg
γ	Heat capacity ratio	-
ε	Strain	MPa
η	cooling efficiency	-
Λ	Reaction degree	-
μ	dynamic viscocity	N*sec/m2
ρ	density	kg/m2
σ	Stress	MPa
ω	rotational speed	rad/s

List of Abbreviations

A/B	Afterburner
AoA	Angle of Attack
ATC	Air Traffic Control
BD	Bending
BFM	Basic Fight Maneuvers
CC	Combustion Chamber
CF	Centrifugal Force
DOF	Degrees Of Freedom
E-M	Energy - Maneuverability
EMS	Equivalent Mena Stress
FT	Feet
HCF	High Cycle Fatigue
HPC	High Pressure Compressor
HPT	High Pressure Turbine
IR	Infrared Radiation
IRSL	Infra-Red Signature Level
LCC	Life Cycle Costs
LCC	Life Cycle Costs
LCF	Low Cycle Fatigue
LMP	Larson Miller Parameter
LPC	Low Pressure Compressor
LPT	Low Pressure Turbine
MS	Mean Stress
NOZ	Nozzle
OASPL	Overall Sound Pressure Level
OAT	Outside Air Temperature
RA	Redaction Area
RPM	Rounds Per Minute
RTDF	Radial Temperature Distribution Factor
SFC	Specific Fuel Consumption
SVR	Shop Visit Rate
SVR	Shop Visit Rate

T/O	Take-Off
TBC	Thermal Barrier Coating
TDD	Throttle Dependent Drag
TERA	Techno-economic and Environmental Risk Assessment
TLA	Throttle Lever Position
TMF	Thermo-mechanical Fatigue
USAF	United States Air Force
UTS	Ultimate Tensile Strength
VSV	Variable Stator Vane

1 Introduction

In military aviation, the optimal performance and operational readiness of aircraft and engines are of ultimate significance. Although a great amount of research has been conducted in engine life prediction for civil aircraft, little resources are available in the open domain about military applications. Research so far has predominantly focused on analyzing specific aspects of aircraft or engine performance and lifing studies were based on certain engine performance degradation. Nevertheless, a noticeable gap remains in assessing military operational costs and doing a more detailed evaluation of mission performance on engine deterioration. This study aims to address these critical gaps by investigating the implications of mission performance in military aircraft on the degradation of low bypass ratio gas turbine engines, with a specific focus on the first stage of the high-pressure turbine.

Until today, military aircraft studies have primarily focused on assessing aerodynamic capabilities and flight dynamics, often bypassing the crucial aspect of operational costs. Although the economic implications of gas turbine engines in civil aviation have been extensively researched due to their direct impact on profitability and efficiency, the understanding of operational costs associated with engine degradation in the military domain remains limited.

Furthermore, existing studies on gas turbine engine lifing have mostly relied on predetermined levels of engine performance degradation, failing to account for the dynamic nature of engine operation in fighter aircrafts and the mission profiles encountered in military applications. As a result, the comprehensive assessment of the relationship between mission performance and engine degradation in military aircraft to optimize mission planning and improve operational efficiency can form a useful tool.

In addition, previous research has not adequately addressed the integrated performance of aircraft and engines as a system, largely overlooking the links between aircraft mission profiles and their impact on engine degradation. By introducing an aircraft/engine integrated system point of view into the analysis, a

wider understanding of operational costs and performance degradation in military aviation can be achieved.

In this context, this project focuses on the introduction of an approach for military mission assessment in terms of engine availability deterioration as part of a highly integrated suite for aircraft/engine configurations. It aims to bridge the highly developed “Economics” module for civil aircraft of Cranfield University’s Techno-economic Environmental Risk Assessment (TERA) framework with the military applications.

To investigate this research topic, the main objectives of this study are as follows:

1. Examine the relationship between engine degradation and overall performance deterioration of the aircraft/engine system through the sequence of a range of missions flown by a multirole fighter: This aims to establish correlations between mission sequences, engine life, and the overall performance of the aircraft/engine integrated system. By analyzing various mission profiles and their impact on engine degradation, valuable insights are gained about the effects of mission profiles on engine degradation and the subsequent influence on overall performance.

2. Evaluate the effect of optimized climb path profiles on engine performance deterioration: This objective aims to assess the impact of optimized climb path profiles (time, fuel, noise) on engine degradation mechanisms. By studying the relationship between optimal climb paths and engine degradation, this research aims to showcase that by modifying the climb path followed operational lifespan of the engine can be extended. Insights gained from this objective can contribute to climb path optimization strategies that minimize engine degradation and improve operational efficiency.

To achieve these objectives, this study will use a well-established methodology involving data collection from simulated mission profiles, analysis, and modelling. A multirole fighter aircraft is selected for investigation, and a range of mission profiles will be analyzed to assess their impact on engine degradation. The fighter class that will be used is that of Eurofighter/Rafale/F18 and the engine model that will be used is derived from the sizing of their engines (M88, EJ200, F404).

Detailed data on the high-pressure turbine blades will be collected for a set of operating conditions corresponding to required mission performance parameters. Data for HPT will include mechanical and thermal stresses on the blades which will be fed into the mission simulation algorithm to predict the severity of each mission. The severity calculation is based on three major failure mechanisms: creep, low cycle fatigue and high cycle fatigue.

Furthermore, advanced modelling techniques will be utilized to simulate and optimize climb path profiles. By integrating acquired data and applying advanced modelling tools, this study will examine the effects of optimized climb paths on engine performance deterioration. The objective is to identify climb path profiles that minimize engine degradation and enhance the operational lifespan of the engine.

Through addressing these objectives, this research aims to contribute to a better understanding of the implications of mission performance in military aircraft on the degradation of low bypass ratio gas turbine engines. The study specifically focuses on the first stage of the high-pressure turbine, a critical component influencing overall engine performance and longevity. By analyzing a range of mission sequences and optimized climb path profiles, this study seeks to provide valuable insights into the relationships between mission performance, engine degradation and their implications on life expectancy.

Overall, this research represents a significant step towards bridging the gap between military aircraft performance, operational costs, engine degradation, and optimized mission profiles. By addressing the system integrated performance and exploring the relationship between mission performance and engine degradation, this study aims to provide valuable insights that can inform decision-making processes, enhance operational availability and optimize resource allocation in military aviation.

2 Literature review

In military aviation, the primary goal is the optimization of operational readiness, ensuring the capability to perform assigned flight missions. Operational readiness encompasses three crucial components: availability, serviceability, and sustainability. Unfortunately, serviceability and sustainability are heavily dependent on the design of the aircraft and thus defined by the manufacturer.

Availability by mission scheduling is often managed manually on a day-to-day basis. This reactive approach to aircraft flight hour allocation can lead ton non-optimal use of available resources. While there have been efforts for the development optimization models to address this problem, the notion for this type of research on military aircraft is still being tackled [1].

One of the key factors that significantly impacts engine life is how the engines are used during field operations. Engine life is affected by various factors, such as design practices, manufacturing processes, materials, engine installations, usage, and maintenance system practices. While maintenance optimization has been addressed [2], users are only contributing to usage and maintenance interventions. Research has shown that engine power usage is a major contributing factor to engine life in field operations [3]. Through a better understanding of engine usage in relation to aircraft characteristics and the nature of missions flown, it has become evident that engine life can vary significantly based on usage patterns. Over the years, increasing amounts of data have been collected, providing valuable insights into the magnitude and variability of engine life across various aircraft roles. [4]

By incorporating these insights into the development of comprehensive optimization models, military aviation can be more efficient during the system selection process [5], can achieve more efficient flight hour allocation, enhance operational readiness, and prolong the life of critical aircraft components, including engines. This proactive approach can lead to safer and more reliable flight operations, ultimately contributing to the success of military missions.

2.1 Introduction to Techno-economic and Environmental Risk Assessment (TERA)

The aviation market is characterized by high competitiveness, where costs and risks that are associated with new projects are significant as they always include the safety factor and thus industries have to evaluate very carefully each choice they make upon new projects or upgrading old ones since seemingly similar options can lead to either success or pose a threat to a company's survival.

Preliminary design is of paramount importance in the success of an aircraft and research institutions have put effort in developing corresponding frameworks to facilitate the evaluation and selection process of new designs especially concerning the propulsion system. [6, 7]

To address the need for assessing multidisciplinary problems around gas turbine engine integration and generally preliminary design, Cranfield University has developed its own modular framework for gas turbine and aircraft performance evaluation. Techno-economic and environmental risk assessment (TERA) framework is a modular suite that was developed to provide insight into the economic, environmental and performance impact during the conceptual and preliminary design of new aviation projects [8].

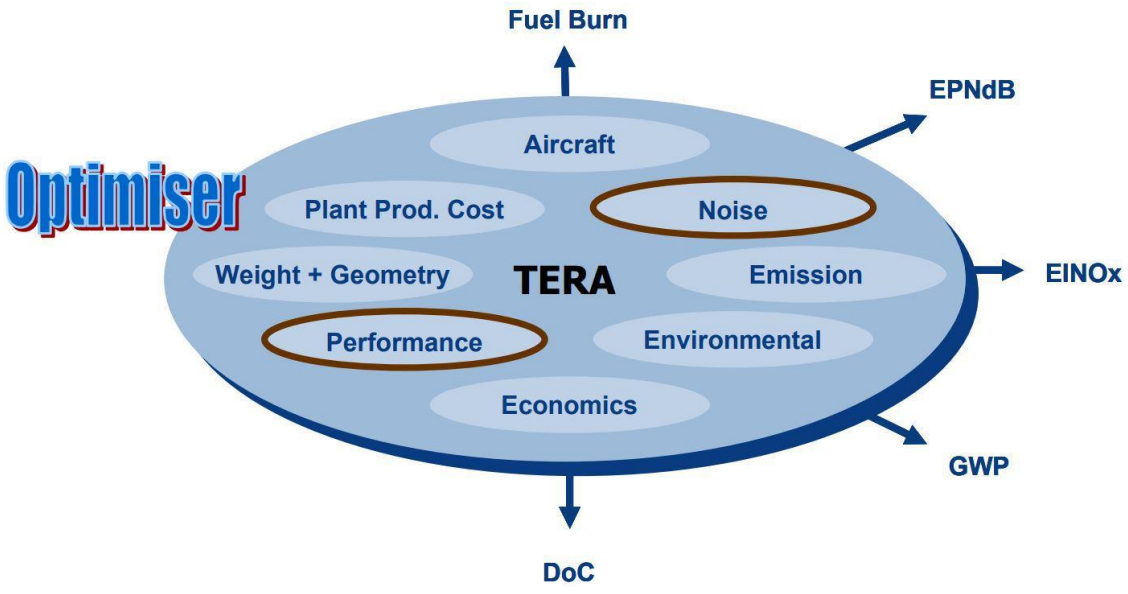

Figure 2-1: TERA Philosophy [8]

It is a project conceived to provide insight into the acquisition and usage costs of modern gas turbine engine. To address the highly demanding market of gas turbines, a multi-dimensional approach was required for the assessment of new technologies. TERA is comprised of a set of computational modules, each one dedicated to a different aspect of a complex engine ecosystem but provides an integrated point of view. Coupled with an optimizer, it can provide valuable information for decision making.

Although TERA was conceived as a tool for civil usage, in the past few years there is a great deal of effort to expand its modules for use in the military domain. In the core of TERA framework lies the HERMES [9] module is used for aircraft performance evaluation simulating the engine's installed performance on generic airliner airframes and is combined with the University's in-house engine performance code, TURBOMATCH [10] which performs the engine modelling. These modules are the ones that research done in recent years is trying to adapt to military applications [11, 12]. A critical addition in this domain is effort to adapt the "Economics" module to military applications. This module addresses the direct and indirect costs of engine ownership and its adaptation to military applications will help introduce the notion of "military related costs".

2.2 Aircraft Performance

Flight mechanics is a critical aspect of aircraft design, encompassing various disciplines such as aircraft performance, stability and control, and flight simulation. These disciplines govern the design and operation parameters of an aircraft, including take-off, climb, and the conditions necessary for successful flight. Four fundamental forces - lift, drag, thrust, and weight - dictate the aircraft's performance characteristics.

Achieving the necessary levels of thrust for feasible flight relies on employing engines that meet the requirements effectively. The turbofan engine plays a crucial role in this regard, with important control parameters such as shaft speed and combustor outlet temperature contributing to thrust adjustments.

This chapter delves into the aspects of aircraft performance and gas turbine performance, which serve as fundamental inputs for estimating severity and

predicting shop visits. By understanding and optimizing these performance aspects, aircraft designers and engineers can enhance the overall efficiency and reliability of the aircraft, ensuring a balanced and effective combination of performance and design.

2.2.1 Aircraft Performance Modelling

From the early days of aerial warfare, it became apparent that good handling skills weren't sufficient to prevail in sustained battlefield operations. Aircraft that had better performance specifications were more successful and as the range of missions flown was expanding, it became clear that whoever had the correct combination of airframe design and engine would hold the key to victory [13].

World War II saw tremendous advancements in aircraft technology and performance. Fighter planes like the British Spitfire and the German Messerschmitt Bf 109 became faster and more agile. The introduction of jet engines during the war marked a significant leap in aircraft speed and performance. The German Me 262, the world's first operational jet-powered fighter aircraft, reached unprecedented speeds.

During the early development of military aviation, engineers and pilots were primarily concerned with aircraft stability and control. As aircraft designs evolved, there was a growing need to understand and improve the performance characteristics of fighter aircraft.

In the 1950s, William F. Loftin, an aeronautical engineer, began investigating the relationship between aircraft performance and maneuverability and the first handbooks for aircraft performance were developed [14]. He conducted pioneering research on energy-state and maneuverability trade-offs, laying the foundation for Energy-Maneuverability Theory which was later established by USAF pilot J. R. Boyd in the mid-1960s [15]. Making use of an earlier study conducted by Rutowski [16] they suggested that aircraft performance can be quantified by its total energy state and that maneuverability can be measured in terms of energy rate exchange between altitude and speed. In this way, an "energy" flight envelope can be easily constructed and comparisons can be made by superimposing different flight envelopes in the same chart.

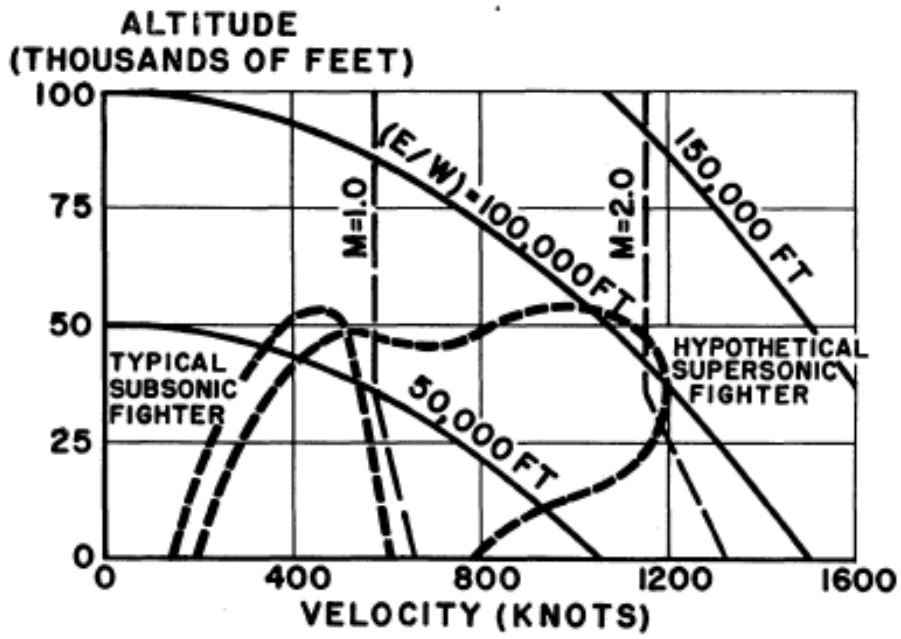

Figure 2-2: Typical fighter speed-altitude envelopes superimposed on contours of constant specific energy [16]

2.2.2 Flight Path Analysis and Mission Simulation

In the pursuit of finding a measure to identify, evaluate and compare the performance of aircraft in complex scenarios such as combat missions, more detailed tools had to be developed. Being a multi-disciplinary problem, the evaluation of an aircraft/engine combination in a mission requires the use of a simulation tool. These tools are particularly suited to evaluate the complicated events that occur on the course of an aircraft mission. By executing multiple simulation runs of a combat scenario under variable initial conditions, aircraft performance can be statistically isolated and quantitative conclusions may be reached upon the effect of various design parameters on an airframe's combat effectiveness. To provide a common reference for aircraft developers, the US department of Defense issued specifications [17] introducing standardized mission profiles to be used for assessing the performance of military aircraft.

Engine-airframe integration requires careful evaluation of an aircraft's performance in executing the mission it has been designed for. In principle flight path simulation can be approached in two distinct ways. The first method relies solely on the aircraft's equations of motion and can produce detailed results for

steady state and transient phases of the aircraft [18]. The second presents an energy-point-of-view approach that makes use of E-M theory.

2.2.2.1 Optimal Flight Profiles

Optimal flight profiles are specific flight paths or trajectories that are carefully designed to achieve the best possible performance and efficiency for an aircraft during different phases of flight. These profiles are developed based on various factors, including aircraft type, mission requirements, fuel efficiency, safety, and environmental considerations. Optimal flight profiles aim to minimize time-to-target, fuel consumption, reduce emissions, maximize range, and ensure the aircraft operates within safe and efficient limits.

They belong to the category of trajectory optimization problems which are mathematical challenges that involve finding the optimal path or trajectory for a system subject to certain constraints and objectives. It is a problem that can be approached by a variety of solutions, some of which can be of low fidelity but computationally inexpensive like the pioneering work of Rutowski [16]. It involves managing the aircraft's energy state, which is a combination of its kinetic energy (associated with its speed) and potential energy (associated with its altitude).

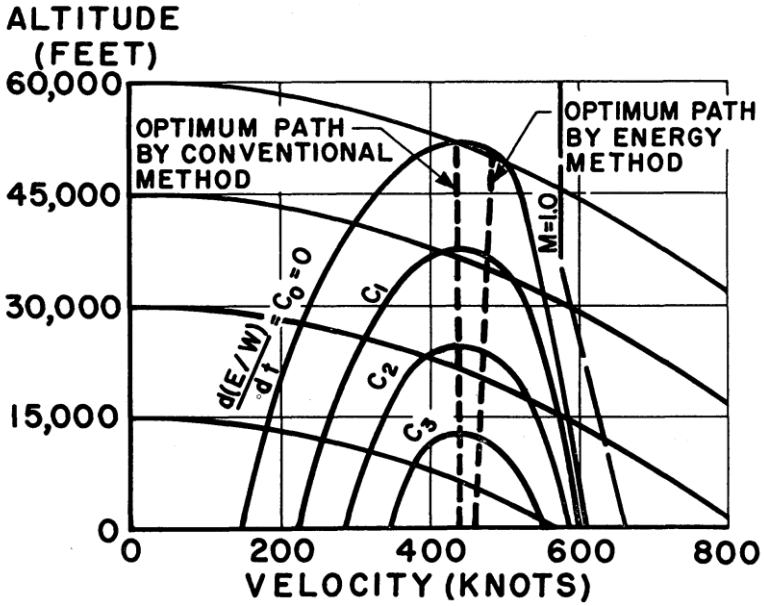

Figure 2-3: Comparison of minimum time to climb paths for typical subsonic fighter [16].

By carefully controlling the aircraft's energy state, pilots and flight planners can achieve more fuel-efficient, time-efficient, and environmentally friendly flight

profiles. Others require complex numerical solutions and programming techniques to produce detailed results [19]. Various methods such as direct shooting, indirect shooting, collocation, genetic algorithms, or gradient-based approaches can be employed depending on the problem's dimensions, nonlinearity, and accuracy requirements [20].

2.3 Gas Turbine Life Estimation

Gas turbine life estimation is a critical aspect of ensuring the reliable and efficient operation of gas turbine engines used in military aircraft. Their engines are subjected to a wide range of mission profiles, from combat missions to reconnaissance and transport operations, each involving unique demands on the engine components. Accurate life estimation, considering mission-specific operating conditions, is vital to optimize maintenance schedules, manage life cycle costs, and maintain the highest level of mission readiness. Not long after the establishment of solid foundation about military aircraft performance assessment, the need for a unified life-cycle analysis for aircraft turbine engines was recognized. USAF in cooperation with Rand Corporation proposed a way to evaluate the life-cycle process by utilizing earlier research into weapon systems and reviewing commercial life-cycle practice [21].

This mission-centric approach involves integrating mission profiles and operational data into life estimation methodologies. In addition, military mission profiles present the inherent modelling difficulty that thrust input during flight changes based on the flight phase. A standard ferry flight that constitutes a simple transportation between two airports without any operational maneuvers presents an entirely different power setting profile from an operational evaluation flight that different scenarios and maneuvers are performed in the duration of the flight. This means that, in contrast with civil aviation [3], Throttle Lever Position (TLA) must be taken into consideration to capture the full dynamics of a mission.

Furthermore, modern multirole fighter jets can change role each mission and thus the stresses they are subjected to, cannot be considered constant throughout their life. This poses the challenge that mission sequence must be considered to evaluate the overall engine degradation.

Though civil and military applications share the same philosophy for aircraft and engine modelling as well as failure mechanisms, the underlying mission approach is completely different. Naeem [22] was one of the first researchers to investigate the engine degradation in relation to flight profiles. In his research the implications of engine deterioration on both operational effectiveness (Time-to-climb, Fuel consumption, Net thrust) and failure mechanisms (Creep, LCF, TMF) are evaluated for different mission profiles. His approach uses predefines deterioration levels of erosion in LPT/HPT and fouling in LPC/HPC to simulate the performance deterioration that a gas turbine is subjected to over time and evaluates the impact on operational metrics. In addition, he measures the effects of performance deterioration and resulting gas path temperature rise in the degradation of the 1st HPT stage.

In a similar approach, Rolph [12] studies the Shop Visit Rate (SVR) of a military turboprop for a set of missions that are executed in different sequences by a cargo airplane. In this way he is trying to capture the life-cycle-costs (LCC) of a military engine and incorporate the notion of fleet optimization in military organizations.

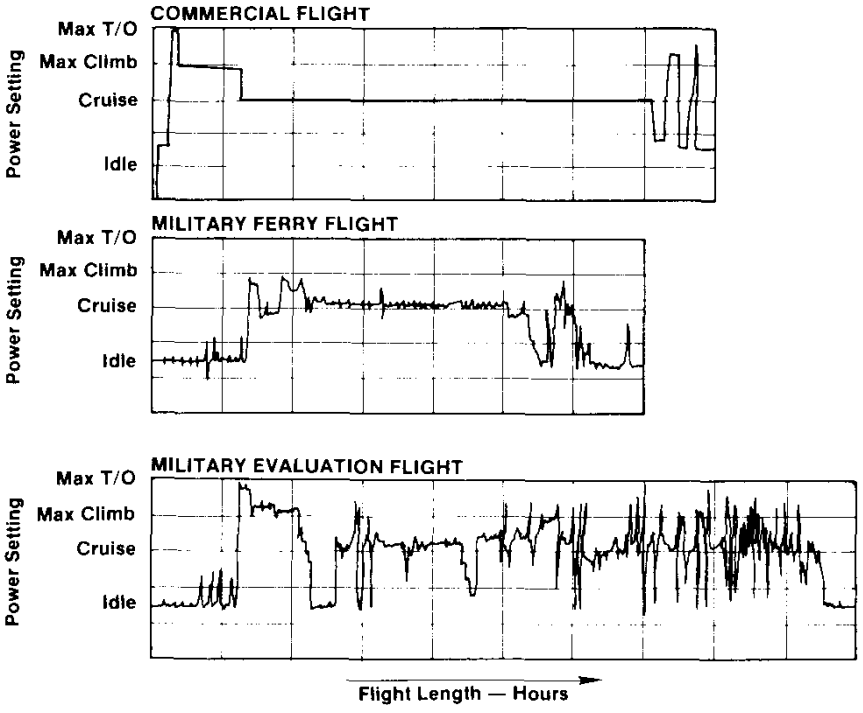

Figure 2-4: Comparison of engine power settings [3]

In the same framework, Matchett [23], evaluates the implications of a variety of mission profiles of a twin spool turbofan engine without afterburner into the damage inflicted by them in HPT 1st stage blade. Similarly, Maxwell [24] calculates the HPT blade life based on four failure mechanisms for a standard interception mission. In addition, he makes comparative case studies for different blade materials. The same objectives are being tackled by Tamma [25] in his thesis where he studies an interception mission and its effects in damage. He is also performing optimization analysis for different blade materials.

Being of sensitive nature, sources around military turbines are limited and data in the open-source domain are classified. Due to this fact, institutions are putting effort into developing in-house evaluation suites. In this context, Cranfield University is trying to expand its TERA module for military applications. Sharing the same underlying principles, military TERA can profit from the comparatively larger pool of available data for civil applications.

Mission flight profiles have been the subject of research in civil aviation for apparent reasons. To enhance its TERA framework, Cranfield University's researchers have been tackling this issue to get a better understanding of how a jet engine reacts under different operating conditions. Khani [26] is investigating the influence of operation parameters such as airport factors on engine life. In his research both environmental parameters (OAT, altitude) and operational decision such as Take-Off derate are taken into consideration. The results present a correlation between required thrust and increased engine degradation due to higher gas path temperatures. Similarly, Hanumanthan [27] is investigating different civil flight profiles with a combination of operational and technological factors. His sensitivity analysis between engines of different rating provides insight into comparative damage caused by operational factors. A different approach is presented by An [28] where in addition to operational factors, she examines the effects of technological factors like flame pattern profiling, stress concentration factor and thermal barrier coating for a civil aircraft performing a standard mission profile. The engine technological factors are also researched by Xu [29] for high-bypass ratio turbofan.

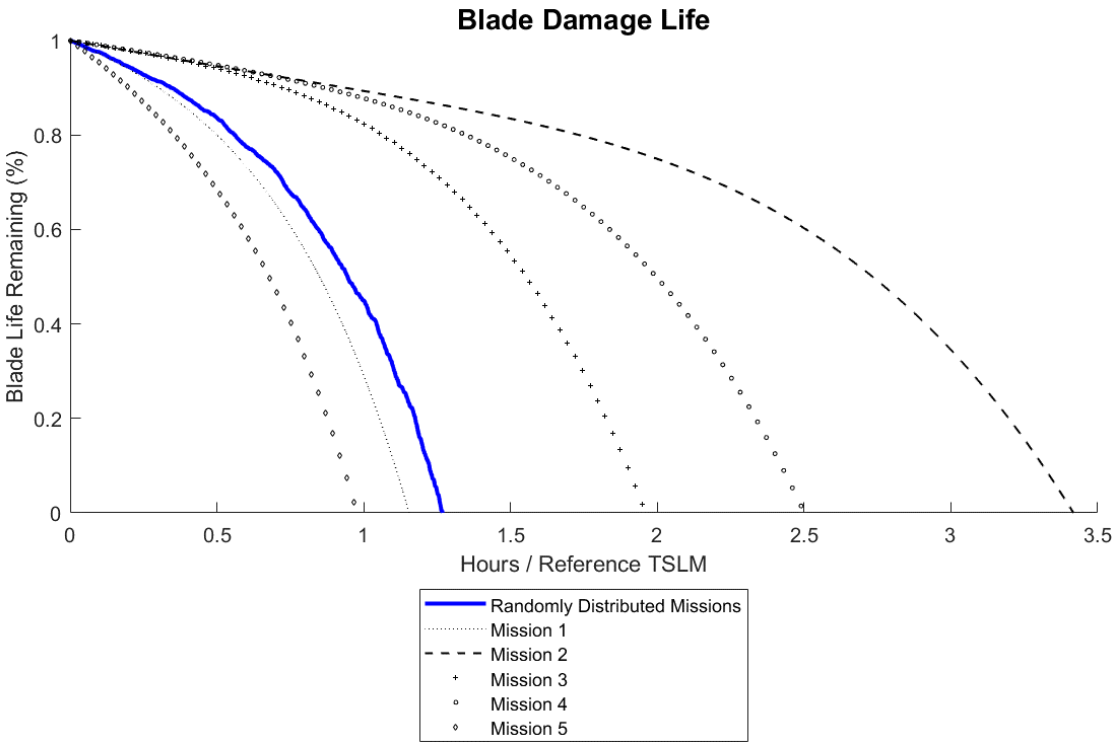

Figure 2-5: Blade damage life for mission type [12].

2.4 Research gap

In the domain of military gas turbine lifing applications, current research shows distinct gaps that require further investigation to optimize engine and aircraft usage. The existing focus often leans towards either aircraft deterioration or engine degradation separately, without considering their integrated system performance correlation with damage accumulation. Additionally, assessments of operational costs, such as availability and maintenance rates, are often overlooked. Lifing studies tend to concentrate on specific engine performance degradation factors, neglecting the combined effects of multiple mechanisms on over a set of diverse missions. Moreover, aircraft/engine integrated system performance degradation studies are scarce, despite their critical influence on mission effectiveness and longevity.

To address these gaps, essential research questions emerge. One such question explores how the set of executed missions and their sequence affects gas turbine life consumption. Investigating the cumulative impact of mission profiles on engine life can lead to increased fleet availability. Another important question revolves around the relationship between the aircraft's mission performance and

the engine's degradation. Understanding this interplay could optimize mission planning and decision-making. Lastly, researchers should explore the correlation between optimized mission profiles and gas turbine performance and longevity. By identifying links between mission-specific optimization and engine efficiency, better operational strategies and cost-effectiveness can be achieved in military gas turbine applications.

3 Methodology

In this chapter, the methodology that was employed for this research is described and the methods that were used are analyzed together with the assumptions that were made. The result is an extension of TERA economics module coupled with research recently done by Antonakis [18]. His module for Aircraft model was used together with the mission and optimal flight path simulation. More specifically, the aircraft model remained the same, the engine model was re-built with reference to the one built by him to match the demands of the missions simulated. In addition, the “High AoA BFM” mission profile was developed for the needs of this research. An overview of this methodology is shown in Figure 3.1.

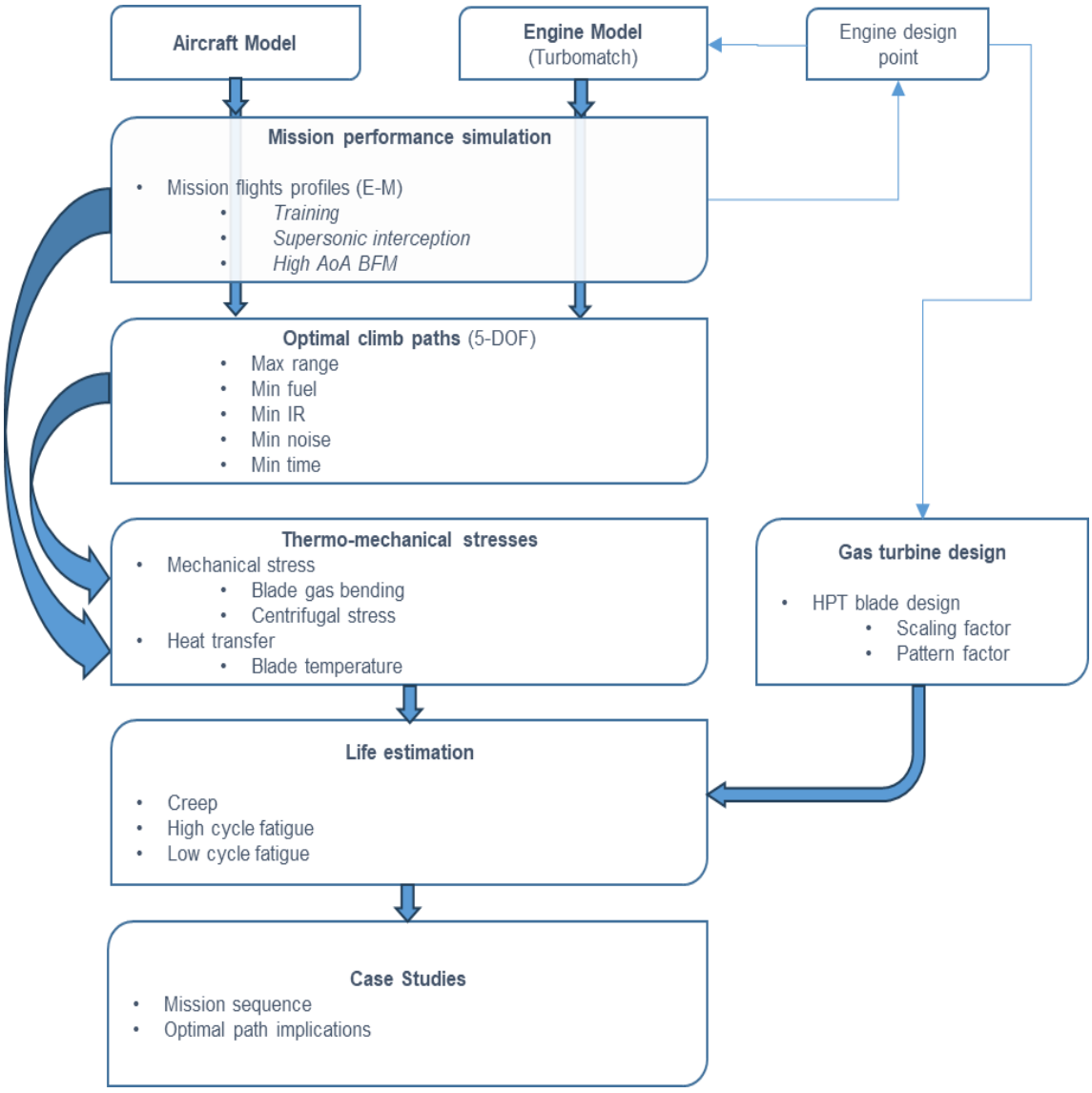

Figure 3-1: Project methodology

For the reader to have an overview of the data flow path, a brief description follows about the data interaction and outcome of each module.

Both aircraft and engine models serve as an aircraft integrated system model. The aircraft model provides the aerodynamics behavior of the aircraft in each flight condition and the engine model, after being fed the initial conditions for the engine sizing, provides data for the operational point parameters (temperature, pressure, fuel flow, thrust, air mass flow, VSV angle, nozzle area) at each engine station. These two modules are fed into the flight profile simulation modules (mission and climb path) to produce the performance equilibrium at each flight condition.

The data produced, contain the gas flow path conditions in each engine station, which will in turn be used by the mechanical and thermal stress modules. In this this step of the data flow path, the analysis focuses on the 1st stage of the HPT. This engine module is sized based on the conditions used to produce the initial engine operation maps and will give the geometry of the blades as well as the cooling technology used.

Combining the thermo-mechanical stresses with the blade geometry, the impact of each failure mechanism upon the blade is calculated. Based on the material properties of the blade, a maximum operational lifecycle under each failure mechanism is derived.

Finally, the life consumption of each flight path is estimated as a sum of the damage induced in every point during flight by each failure mechanism acting on the blade. This life consumption is compared to a reference mission to acquire the relative impact of each flight path and give comparative conclusions of the missions performed.

This thesis consists of six chapters whose description follows below.

Chapter 1: Gives an overview of the domain that this research investigates and sets the background for the objectives based on the research gap. Finally, it presents in a brief philosophy the methodology that will be used.

Chapter 2: In this chapter the literature review that was performed, is presented. It is divided into subsections that each one of them covers a submodule of the general methodology. In these sections, sources relevant to its topic are analyzed and a brief overview of their approach is presented. In the last paragraph, the research gap that was identified is described and the objectives to be aimed at are set.

Chapter 3: In chapter 3 the detailed methodology that was adopted for the needs of this research, is presented. Similarly with chapter 2, it is divided into subsections each of whom lays the foundation of the underlying methodology followed to formulate the interim modules and objectives of this research. In addition, ad-hoc models that were developed in the context of this research are analyzed and validated.

Chapter 4: This chapter includes the case studies that were analyzed and their results are presented in order for a comparison to be done. Furthermore, brief comments on the results are made that will later be formulated in the findings of this work.

Chapter 5: In this chapter the summary of conclusions is presented. Observations are made based on the results and the capabilities of the framework are analyzed.

Chapter 6: In the last chapter of this thesis, a general discussion of the framework is made. The restrictions are noted and recommendations are made for future development of the frameworks capabilities.

3.1 Aircraft modelling

A reliable aircraft aerodynamic model ensures the robustness and high functionality of any framework that includes aircraft simulation as it is in the core of the modelling. It enables key parameters to be easily calculated across the flight envelope and guarantees compatibility with other connecting modules.

For these reasons, in this research the aerodynamic model of Antonakis [18] is used. It derives from data available in table formats in the open-source domain [30, 31]. They were used to model the aircraft's behavior in terms of lift and drag coefficients (C_L, C_D).

In addition, Antonakis in his research introduced an add-on module for interference drag prediction. This approach is used to model the drag contribution of engine integration with the airframe. Most notably this contribution is caused by inlet drag and afterbody interaction of the nozzle.

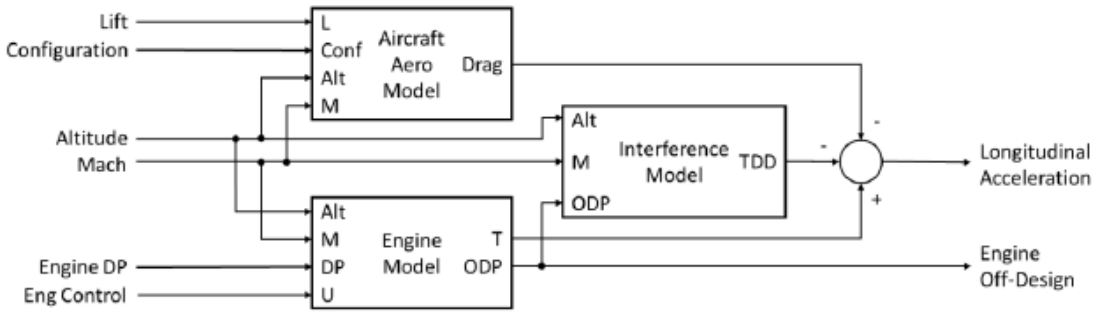

Figure 3-2: Block diagram of the aircraft performance model showing the data flow between the aircraft, engine and interference modules [18].

3.2 Gas turbine modelling

According to the requirements of the simulated missions and aircraft model, a twin-spool low by-pass ratio turbofan engine with afterburner configuration was employed for the context of this research.

The engine was simulated using a 0-D approach by TURBOMATCH [32], Cranfield's in-house developed software for performance simulation. Turbomatch models the engine as a set of thermodynamic models, each one corresponding to a respective engine compartment. Figure 3-3 represents an arbitrary engine compartment with the inputs it requires and the outputs produced.

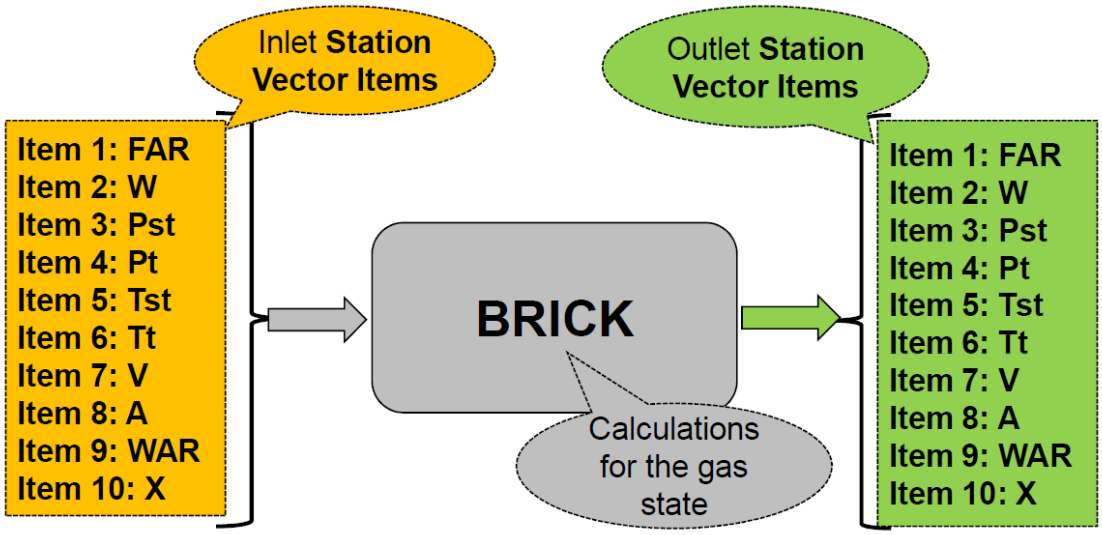

Figure 3-3: Input and output in TURBOMATCH modules [32]

The configuration used for this research can be visualized in Figure 3-4 where the station numbers are displayed for the corresponding thermodynamic modules.

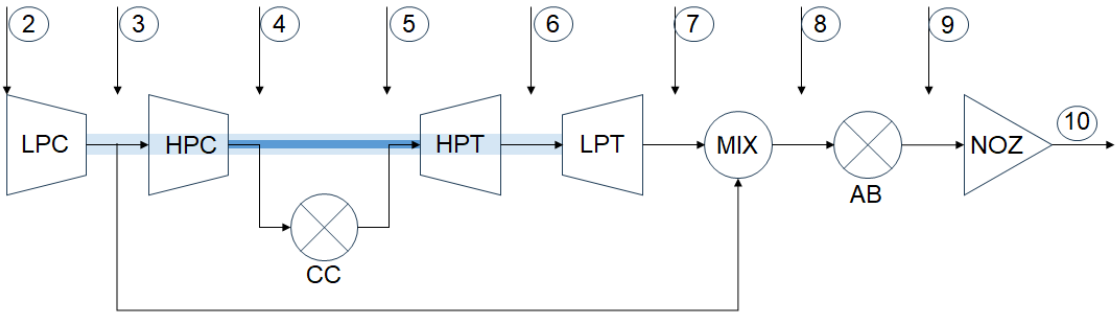

Figure 3-4: Engine thermodynamic modules and station numbering

To capture the physics in a most efficient and accurate way, certain assumptions needed to be made in TURBOMATCH, for the engine to match the characteristics of the simulated military turbofans (EJ200, M88, F404).

The characteristics of the engine model used, are presented in Table 3-1 and the design point definition in Table 3-2.

Component	Parameter	Value
Low Pressure Compressor	Pressure Ratio	4
	Isentropic Efficiency	0.8
High Pressure Compressor	Pressure Ratio	6
	Isentropic Efficiency	0.8
	Bleed Extraction	0.01
	VSV Angle	0-20 degrees
Combustion Chamber	Combustion Efficiency	0.99
	Pressure Loss	0.05
	Max Combustion Temperature	1700K
Low Pressure Turbine	Isentropic Efficiency	0.85
High Pressure Turbine	Isentropic Efficiency	0.85
Heat Exchanger	Pressure Loss	0.01
Afterburner	Combustion Efficiency	0.9
	Pressure Loss	0.02
	Max Combustion Temperature	2000K

Table 3-1: Engine performance characteristics

Air Mass Flow	80 kg/s
Bypass Ratio	0.4
Thrust	90 kN
SFC	45 mg/N*sec

Table 3-2: Engine design point

3.3 Mission Simulation

Mission simulation plays a critical role in aircraft performance assessment since it provides the representation of the actual flight profile and gives insight into this multi-disciplinary subject. It provides a cost-effective and safe way to test aircraft performance and make comparisons.

Military flight profiles though being versatile and varying in phase during one mission, they tend to be independent of ATC restrictions and thus rely mostly on maximizing performance metrics.

In terms of modelling there are numerous approaches; the two most common are:

1 Numerical simulation based
2 Energy based

In the context of this research, to simulate full mission profiles the approach from Antonakis [18] was chosen as a tested and robust way. In his approach, an extended version of the traditional Energy-Maneuverability [15] method is used due to lower computational costs involved in simulating full mission profiles. Though being subject to know limitations, this method was deemed suitable for this research due to its simplicity and low computational cost.

Based on MIL-STD-3013 [17], mission profiles can be classified into three distinct segments:

1. Energy transitions
2. Cruise
3. Combat

By utilizing the integral:

$$Q = \int_{E_{S_1}}^{E_{S_2}} \frac{dQ/dt}{P_S} dE_S \tag{3-1}$$

several performance metrics can be analyzed. Defining Q as the quantity to be optimized, Rutowski's methodology [16] can be applied for different flight segments requiring energy transitions with their respective objectives to obtain optimal flight paths and simulate full mission profiles.

By discretizing the integral from Eq. (3-1) we can break down the mission profile and analyze it individually. This approach can be visualized as follows:

$$Q = \sum_{i=1}^{N} \frac{1}{q_i} \Delta E_{S_i} \tag{3-2}$$

and leads to N optimization problems for the quantity:

$$q_i = \frac{P_S}{dQ/dt}$$

subject to $$D_j(\bar{x}) \leq 0,\ \mathrm{j} = 1, \ldots, \mathrm{M} \quad (3\text{-}3)$$

where $D_j(\bar{x})$ is the aircraft's flight envelope.

Similarly, for the cruise segments of the mission profile, it is possible to formulate an optimization problem to acquire optimal performance solutions. In this case, the cruise problem is formulated as follows:

$$Q(\bar{x}), \bar{x} = \{h, M, T\}$$

subject to $$D_j(\bar{x}) \leq 0,\ \mathrm{j} = 1, \ldots, \mathrm{M}$$

and $$C(\bar{x}) = 0 \quad (3\text{-}4)$$

where $C(\bar{x})$ represents the aircraft's trim condition.

Applying this approach for all flight phases leads to the generation of a set of optimal mission profile points.

The individual objectives that were optimized for each flight segment by Antonakis [18] are presented in Table 3-3 for Cruise, Table 3-4 for Energy Transitions and Figure 3-5for sustained turn rates charts during combat.

Cruise Type	***Q***
Max Range	$Q(\bar{x}) = \frac{\dot{Q}_F}{V_x}$
Max Endurance (Loiter)	$Q(\bar{x}) = \dot{Q}_F$
Minimum Noise	$Q(\bar{x}) = \log(P_{OASPL})$
Minimum IRSL	$Q(\bar{x}) = \log(IRSL)$

Table 3-3: Cruise optimization objectives

Trajectory Type	***Objective Function***	***Remarks***
Minimum Time	$q_i = \max_{\bar{x}} P_S$	
Minimum Fuel	$q_i = \max_{\bar{x}} \frac{P_S}{\dot{Q}_F}$	$\dot{Q}_F$: *Fuel Flowrate*
Maximum Range	$q_i = \max_{\bar{x}} \frac{P_S}{\dot{Q}_F - \left[\frac{\dot{Q}}{V_x}\right]_{cr} V_x}$	$\left[\frac{\dot{Q}}{V_x}\right]_{cr}$: *Cruise fuel consumption per unit distance*
Minimum Noise	$q_i = \max_{\bar{x}} \log\left(\frac{P_S}{P_{OASPL}}\right)$	P_{OASPL}: *Aicraft Noise Sound Pressure w.r.t.ground observer*
Minimum IRSL	$q_i = \max_{\bar{x}} \log\left(\frac{P_S}{IRSL}\right)$	$IRSL$: *Aicraft IR Signature Level w.r.t.ground observer*

Table 3-4: Energy Transition optimization objectives

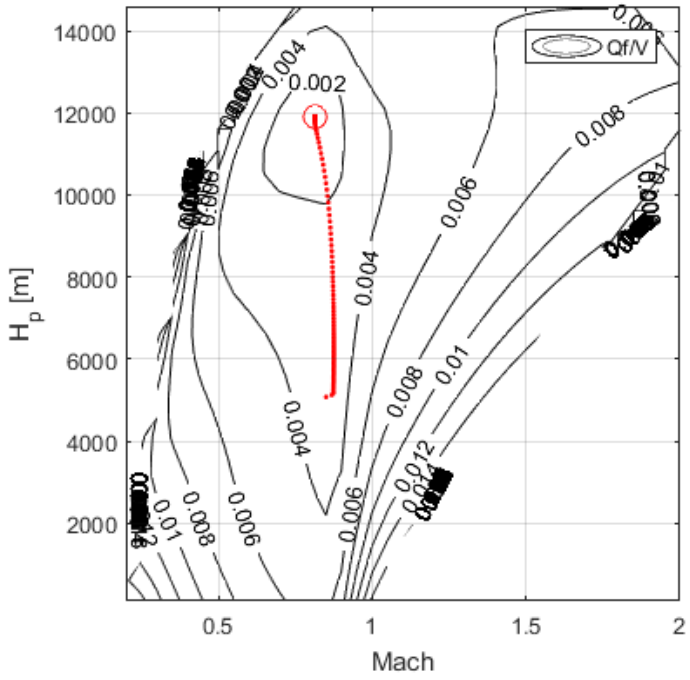

Figure 3-5: Cruise Optimization for maximum range. The red circle denotes the optimal solution whereas red dots account for intermediate solutions generated during an optimization process. [18]

3.3.1 Optimal climb paths

The pursuit of optimal climb paths is a multidimensional challenge, encompassing a range of factors that influence an aircraft's trajectory. From the selection of the suitable climb gradients to considering aircraft performance capabilities, weight variations, atmospheric conditions, and air traffic constraints, a multitude of variables must be harmoniously balanced to achieve the most efficient climb.

Though being a flight phase easily overlooked for its importance in mission performance, optimal climb paths can have a significant impact on the engine as the routine in terms throttle input can vary depending on the objective of the climb path.

To capture this variance, Antonakis [18] introduced a novel way for simulating optimized climb paths. His numerical based approach is based on a 5-DOF aircraft model that uses a guidance algorithm to follow generated optimal climb paths.

His aircraft model show in Equations 3-5 to 3-11 is guided upon Bezier generated splines [33] that are optimized with a use of Multi-Objective Particle Swarm Optimization (MOPSO) [34]. The guidance is achieved by Carrot chasing algorithm [35] inspired model specifically developed for the needs of his research.

$$\dot{x} = V cos\gamma \tag{3-5}$$

$$\dot{h} = V sin\gamma \tag{3-6}$$

$$\dot{V} = \frac{T-D}{m} - g sin\gamma \tag{3-7}$$

$$\dot{\gamma} = \begin{cases} \min\left\{\frac{\gamma_c-\gamma}{\tau}, \frac{L_{max}}{mV} - \frac{gcos\gamma}{V}\right\} & \gamma_c > \gamma \\ \max\left\{\frac{\gamma_c-\gamma}{\tau}, \frac{-L_{max}}{mV} - \frac{gcos\gamma}{V}\right\} & \gamma_c < \gamma \end{cases} \tag{3-8}$$

$$\dot{m} = -SFC \times T \tag{3-9}$$

$$L_{max} = \min\left\{\frac{1}{2}\rho S C_{L_{max}} V^2, n_{Z_{max}} mg\right\} \tag{3-10}$$

$$D = \frac{1}{2}\rho S V^2 C_D \tag{3-11}$$

3.4 Gas turbine design

This section refers to the process of sizing an engine based on certain requirement criteria. It is an essential procedure to understand the physics taking place inside the engine components and extract the thermal and mechanical loads that act upon these components. The need for obtaining physical dimensions of engine components is required to have a comprehensive view of the exact points of stress concentration.

The components that are most often critical in terms of failure are the hot section ones and the most notable one is the High Pressure Turbine (HPT) since it is located after the combustion chamber. In particular, the 1st stage of the HPT is, as a rule of thumb, the most stressed engine component and thus requires focus in terms of sizing.

In this research the focus is shifted towards the design of blades of the 1st stage of HPT using publicly available data for similar engines and correlating with procedures civil applications.

3.4.1 HPT blade sizing

Blade sizing is important in the process of understanding the impact a mission has on turbine life. In the absence of publicly available data, the approach followed in this research is a combination of data available for civil aviation turbines sized for the performance metrics required by low by-pass ratio turbofan used in military applications. The level of detail in this stage will remain at the preliminary stage, as it was deemed sufficient for the purpose of this research.

In this context, the preliminary blade design was conducted based on well documented generic methods from Cohen et. Al. [36], Walsh et. al. [37], Horlock [38] and McManus [39]. In addition, data from NASA's E3 Engine [40] and General Electric's F404 [41] were used as baseline coordinates for the blade's geometry.

Under this concept, certain assumptions had to be made:

- The design is based on Mean Line Analysis to reduce the complexity.

- The stage to be analyzed is designed for constant mean radius.

$$U_{mean} = \frac{2\pi N_G r_{mean}}{60} = const \tag{3-12}$$

- The reaction degree of the rotor is fixed at 50%.

$$\Lambda = \frac{T_{t2} - T_{t3}}{T_{t1} - T_{t3}} \tag{3-13}$$

- Constant stagnation enthalpy, constant axial velocity throughout the annulus area of turbine and the whirl velocity varies inversely to the radius of the turbine according to the Free Vortex Theory [36].

3.4.2 Aerodynamic calculations

After the geometry of blade has been defined, the loads acting on the blade can be calculated for the different engine ratings using thermodynamic relations for pressure, temperature and air mass flow.

3.4.2.1 Velocity Triangles

The gas velocity triangles shown in Figure 3-6 are used to calculate the axial and tangential velocity on the blades of the 1st stage HPT rotor and determine the blade's chord.

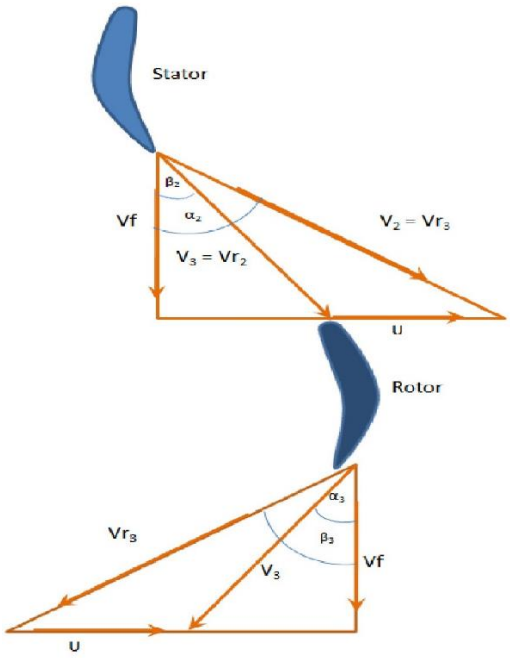

Figure 3-6: Nominal velocity triangle for the 1st stage HPT rotor [42]

Since the reaction degree is 50%, the two triangles are similar so the axial velocity can be considered constant. To calculate V_f, an iterative process is needed since both average temperature *t* and average pressure *p* are unknown.

$$t = \frac{T}{1+\frac{\gamma-1}{2}M^2} \tag{3-14}$$

$$p = \frac{P}{\left(1+\frac{\gamma-1}{2}M^2\right)^{\frac{\gamma}{\gamma-1}}} \tag{3-15}$$

Mach number (M) is calculated by iteration from:

$$Q = \sqrt{\frac{\gamma}{R}}\frac{M}{\left(1+\frac{\gamma-1}{2}M^2\right)^{\frac{(\gamma+1)}{2(\gamma-1)}}} = \frac{m\sqrt{T}}{PA} \tag{3-16}$$

Having obtained the average pressure and temperature the gas density can be calculated:

$$\rho = \frac{p}{Rt} \tag{3-17}$$

And V_f can be finally calculated:

$$V_f = \frac{\dot{m}Rt}{pA} \tag{3-18}$$

Combining the axial velocity with information for the baseline coordinates of the blades, all triangle velocities can be calculated.

3.5 Heat transfer analysis

Gas flowing throw the core of modern GTE can reach temperatures up to 1700K. Materials under this temperature undergo severe stress and their life would be extremely short in the absence of cooling. Accurately estimating the heat interchange between the coolant in the blade and gas heat is essential in achieving lifing models closely resembling reality.

In the context of this research conduction and convection were the two mechanisms that were studied for heat transfer as an assumption was made that there are no points of the rotor blade in sight with the flame from the combustor and hence radiation is negligible.

In addition, the coolant passage is a straight circular tube running throw the blade providing uniform coolant temperature distribution throughout the flow. The presence of cooling holes on the blades surface produces a uniform cooling film and the presence of a Thermal Barrier Coating (TBC) is considered.

3.5.1 Heat transfer coefficient and blade temperature

In order to calculate the temperature distribution across the blade's surface the calculation of heat exchange between the surface and the gas is needed. Heat transfer coefficient gives insight into the boundary layer between these them. This can be calculated through the Nusselt number:

$$Nu = \frac{h\,d}{k} \tag{3-19}$$

where $Nu = f(Re)$ [43]:

$$Nu = 0.15Re^{0.7} \tag{3-20}$$

and

$$Re = \frac{\rho\,V\,d}{\mu} \tag{3-21}$$

For the hot side of rotor blade a similar approach is applied with the use of Stanton number [44].

$$St = 0.285Re^{-0.37}Pr^{\left(-\frac{2}{3}\right)} \tag{3-22}$$

where

$$\mathrm{Pr} = \frac{\mu\,C_p}{k} \tag{3-23}$$

Finally with the use of Equation 3-24 the heat transfer coefficient is calculated.

$$h = St\,C_p\,\rho\,V \tag{3-24}$$

3.5.2 Radial temperature distribution factor (RTDF)

Gas coming out of the combustor is not uniform as incomplete mixing takes place. This is the leading cause for non-uniform temperature radial distribution [37]. The introduction of RTDF accounts for the difference between mean and max gas temperatures usually action on NGVs. As indicated by Horlock et. al. [45] this

number should be around 0.1 and kept below 0.2. It is assumed that maximum temperature in the axial direction of the blade occurs between 0.5 and 0.75 of the blade span.

$$RTDF = \frac{T_{combustor,,max} - T_{combustor,mean}}{\Delta T_{combustor}} \quad (3\text{-}25)$$

3.5.3 Blade cooling performance

The performance of cooling on a blade can be described as the quantity of heat absorbed by the coolant relative to gas temperature [37]. It can be calculated by the temperature absorption effectiveness:

$$\varepsilon = \frac{T_{gas} - T_{blade,out}}{T_{gas} - T_{coolant,in}} = \frac{\dot{m}\,\eta}{1 + \dot{m}\,\eta} \quad (3\text{-}26)$$

Where $\dot{m}$ is the coolant mass flow, calculated from:

$$\dot{m} = (1 + Bi)\frac{m_{cb}\,C_p}{h_{gas}\,S_{gas}\,U_{gas}} \quad (3\text{-}27)$$

Since a TBC has been incorporated, the Biot number accounts for this adjustment.

$$Bi = \frac{h_{gas}\,L}{k} \quad (3\text{-}28)$$

In Equation (3-26), η accounts for the cooling efficiency of the cooling system:

$$\eta = 1 - exp\left(-\frac{X}{\dot{m}}\right) \quad (3\text{-}29)$$

The technology factor X determines the cooling passage design and its effectiveness in terms of heat absorption.

$$X = \left(\frac{n_c h_c S_c}{U_{gas} S_{gas}}\right) \quad (3\text{-}30)$$

3.5.4 Blade temperature at coolant side

Blade temperature can be calculated by using the thermal energy balance. The heat difference between the gas side and coolant side results in the heat energy absorbed by the blade and thus its temperature raises.

The heat input from gas on the blade is:

$$q_{in} = h_{gas} S_{gas} \left(T_{gas} - T_{blade,gas} \right) \quad (3\text{-}31)$$

And the heat absorbed by the coolant is:

$$q_{out} = m_{coolant,blade} C_{p,coolant} \left(T_{coolant,out} - T_{coolant,in} \right) \quad (3\text{-}32)$$

Using the thermal balance equation, the temperature rise of the blade is the resultant from the accumulated thermal energy.

$$q_{in} - q_{out} = q_{acc} = mass_{blade} C_{p,blade} \left(T_{blade,gas} - T_{blade,coolant} \right) \quad (3\text{-}33)$$

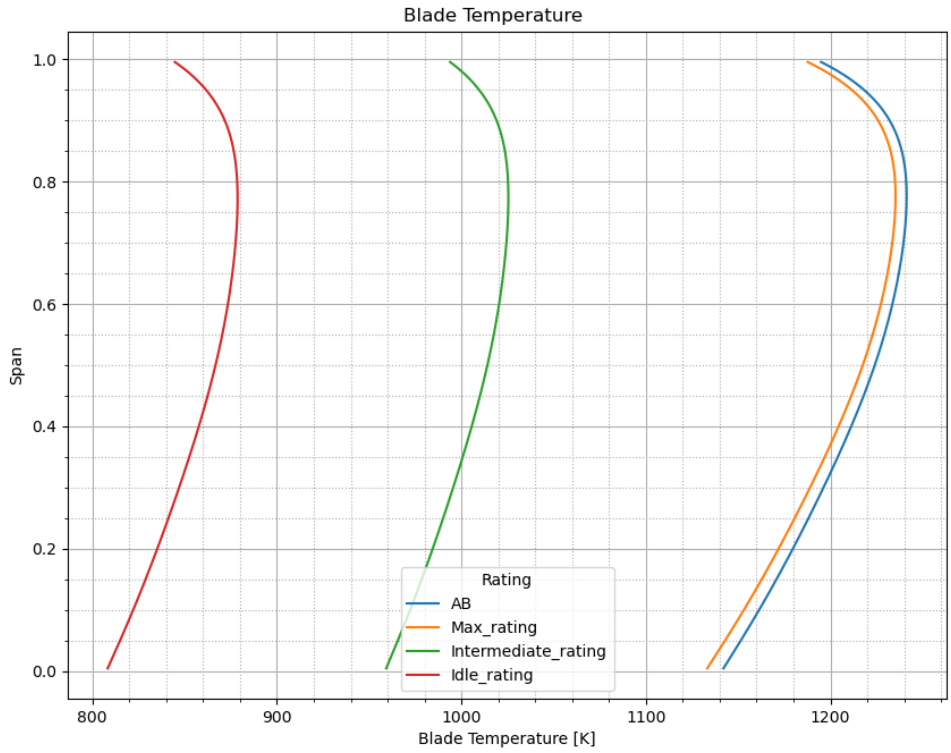

Figure 3-7: Spanwise blade temperature distribution for different engine ratings

In Figure 3-7 the temperature profile of the blade's surface is shown. As observed, the maximum blade temperature is around 80% of the span. After that point, there is a steady decrease in temperature until the blade tip. Notably the temperature at the tip is not the minimum as theoretically supposed due to reduced efficiency of the coolant as it flows through the blade and absorbs heat. In addition, it is noted that for an average increase of about 7°C between "Max" and "AB" ratings, or 0.005%, there is a thrust increase of about 40% and fuel consumption increase of almost 100%.

3.6 Mechanical stress

Mechanical stresses acting on the blade can be divided into two main categories:

1. Centrifugal loads acting on the blade due to inertial forces of rotating mass.
2. Bending moments due to differential gas linear speed caused by blade twisting.

3.6.1 Centrifugal force

Centrifugal Force (CF) is exerted on the blades as a result of their rotation around the engine shaft. The force acting on the blades has a radial direction and tends to force masses away from the center of rotation. The equation for CF is:

$$CF = m\, r_{CG} \omega^2 \tag{3-34}$$

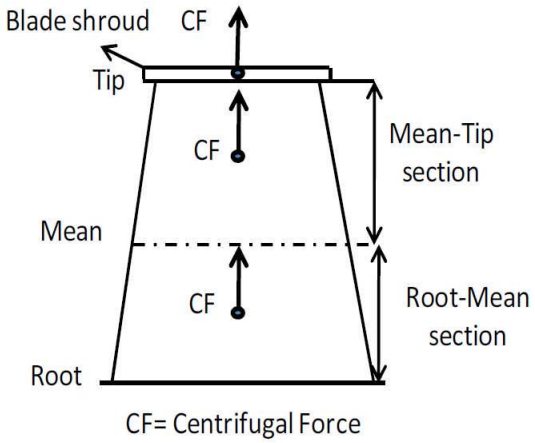

Figure 3-8: Centrifugal force acting on blade sections.

This force can be considered to act upon the individual masses of the blade's sections. The mass of each section is:

$$m_i = vol_i \times \rho \tag{3-35}$$

where vol_i is the volume of each considered section and ρ is the material's density and

$$\omega^2 = \left(\frac{2\pi RPM}{60}\right)^2 \tag{3-36}$$

The stress acting on each section of the blade is calculated from:

$$\sigma_{CF} = \frac{\sum CF_i}{A_{root}} \tag{3-37}$$

From Eq. 3-37 it is apparent that the maximum CF occurs at the blades root.

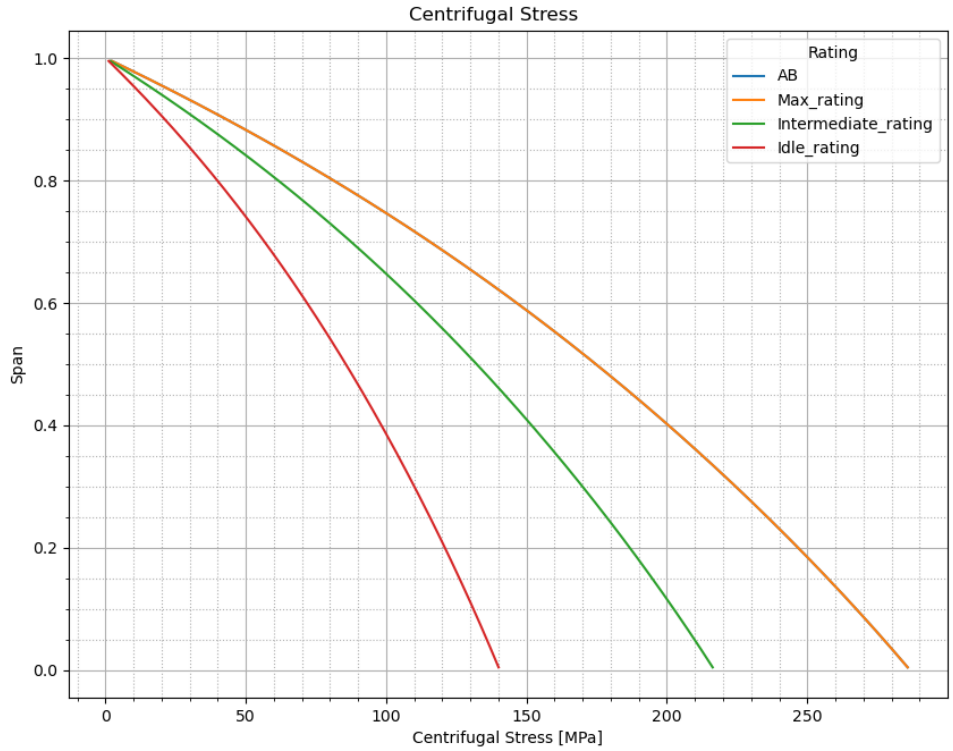

Figure 3-9: Spanwise blade Centrifugal Stress for different engine ratings

A notable observation in this graph is that the curves “AB” and “Max_rating” coincide since the shaft speed between these two is the same and thus the same centrifugal force is exerted on the blades.

3.6.2 Gas bending stress

Gas bending stress is the result of gas interaction with blades. As the rotor turns, pressure and temperature gradients across the blade cause energy reaction between the gas and the blade. This process causes bending moments on the blade.

The bending moment caused by changes of pressure gradients can be expressed as:

$$M_{dp} = F_{dP}\, r_{cg} \tag{3-38}$$

where r_{cg} is the distance from the blade root to the section CG and

$$F_{dp} = \frac{dp\ (2\pi r_{AV} dr)}{N} \tag{3-39}$$

Similarly, the bending moment caused by momentum change is expressed as:

$$M_{\Delta V\theta} = mass_{section}\, \Delta V_{\theta} r_{cg} \tag{3-40}$$

where ΔV_{θ} is the axial and tangential velocity gradients.

Using the “Engineers Bending Theory” the resulting bending stress σ_{BD} can be calculated after the bending moments M in axial and tangential directions are obtained:

$$\frac{M}{I} = \frac{\sigma_{BD}}{y} \tag{3-41}$$

Assuming the effects of thermal stress are independent, the mechanical load can calculated for all blade sections on LE, TE and SUCTION respectively.

$$\sigma_{LE} = \frac{M_{XX} Y_{LE}}{I_{XX}} + \frac{M_{YY} X_{LE}}{I_{YY}} \tag{3-42}$$

$$\sigma_{TE} = \frac{M_{XX} Y_{TE}}{I_{XX}} - \frac{M_{YY} X_{TE}}{I_{YY}} \tag{3-43}$$

$$\sigma_{suction} = \frac{M_{XX} Y_{suction}}{I_{XX}} - \frac{M_{YY} X_{suction}}{I_{YY}} \tag{3-44}$$

Axial (M_A) and tangential (M_T) bending moments are converted about the XX and YY axis:

$$M_{XX} = M_T cos\theta - M_A sin\theta \tag{3-45}$$

$$M_{YY} = M_T sin\theta + M_A cos\theta \tag{3-46}$$

After calculating both bending and centrifugal stresses, the calculation of total stress is possible and expressed as follows:

$$\sigma_{total} = \sigma_{CF} + \sigma_{BD} \tag{3-47}$$

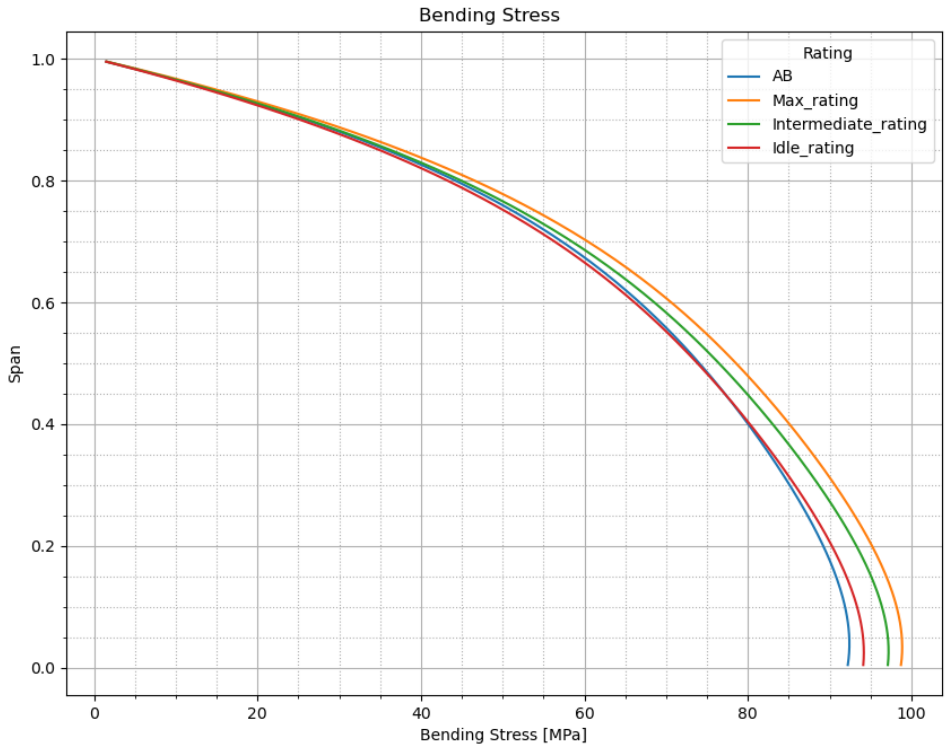

Figure 3-10: Spanwise blade Bending Stress for different engine ratings

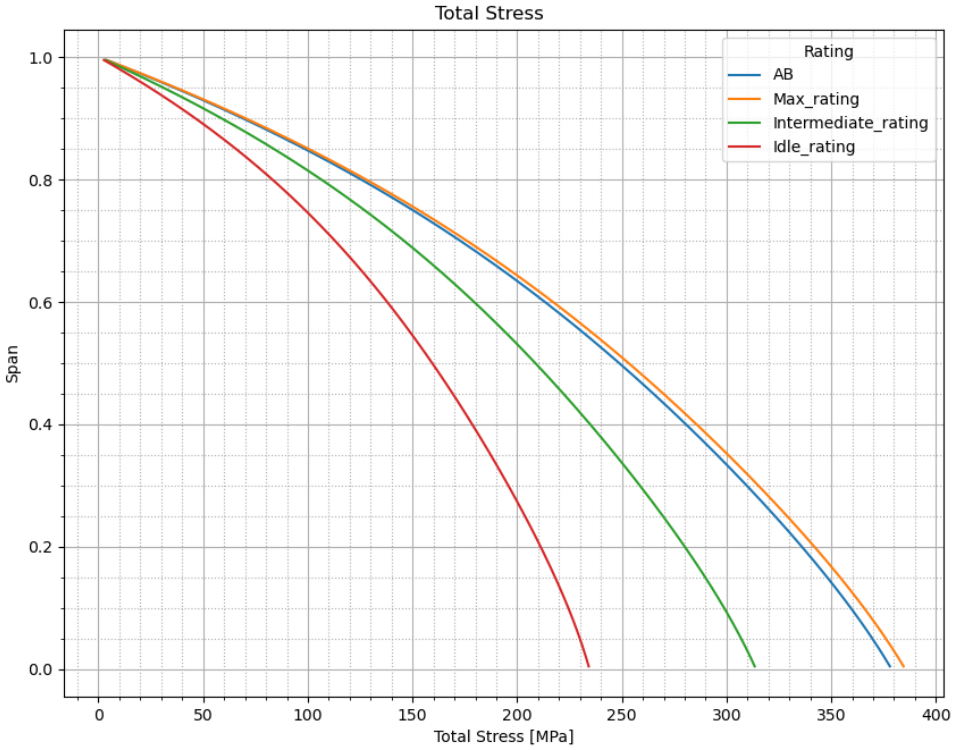

Figure 3-11: Spanwise blade Total Stress for different engine ratings

A notable observation in Figure 3-11 is that that the maximum Total Stress is observed in ”Max_rating”. This is caused by the reduced contribution of bending stress in “AB” due to the pressure gradient on the blade being less intense.

3.7 Failure mechanisms

In order to estimate the damage induced on the engine components during loading, the impact on component life has to be determined based on failure mechanisms acting on the HPT blades.

In the context of this research, three failure mechanisms were studied:

1. Creep
2. Low Cycle Fatigue (LCF)
3. High Cycle Fatigue (HCF)

These mechanisms are assumed to act independently on the blades.

3.7.1 Creep

Creep refers to the time-dependent and permanent deformation that occurs in a material when it is subjected to a constant load or stress at elevated temperatures. This phenomenon is particularly prominent in materials exposed to high temperatures such as these of GTE and occurs over an extended period. Creep is a result of the diffusion of atoms or molecules within the material, leading to gradual changes in the material's shape and dimensions. This deformation under sustained load can compromise the structural integrity of components and is a crucial consideration in the design and engineering of high-temperature applications, such as gas turbine blades, steam turbines, and structural elements in aerospace.

The Larson-Miller Parameter method [46] is a widely used approach to calculate creep life. It correlates the time to failure of a material t_f in a logarithmic scale with LMP.

$$LMP = \frac{T}{1000}\left(log t_f + C\right) \tag{3-48}$$

where T is the temperature and C a material constant.

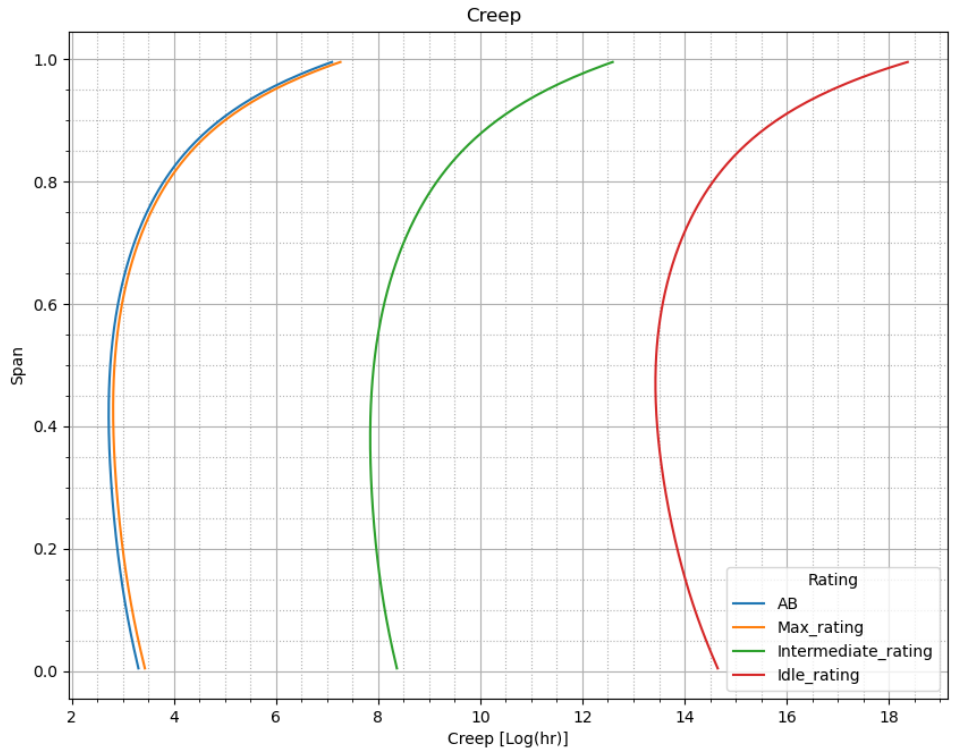

Figure 3-12: Spanwise Creep life in Log(hr) for different engine ratings

Fig. 3-12 shows that despite the mechanical stress being higher in “MAX” rating, the temperature is the dominant factor in creep and thus the damage life of Creep is lower in “AB” rating.

3.7.2 Fatigue

Material fatigue refers to the progressive and localized structural damage that occurs in a material subjected to cyclic loading or stress, typically at lower levels than the material's ultimate strength. The repeated application of loads leads to microscopic cracks or defects within the material, which gradually grow and propagate with each load cycle. Over time, these cracks can reach a critical size, leading to sudden and catastrophic failure, even though the applied stress levels may have been well below the material's yield strength.

Fatigue is a prevalent and significant concern in engineering applications, especially in components that undergo repeated loading or vibrations, such as turbine blades, aircraft wings, automotive components, bridges, and machine parts.

3.7.2.1 Low cycle fatigue

To calculate LCF life estimation Manson's Universal Slope (MUS) [47] was adopted for the needs of this research. It was deemed appropriate as it requires little material specific data. It associates the number of cycles to failure Nf with the strain amplitude experienced by the material. The fatigue life after observation in Figure 3-13 can be expressed as:

$$\Delta\varepsilon = 3.5\frac{\sigma_{UTS}}{E}{N_f}^{-0.12} + D^{0.6}{N_f}^{-0.6} \quad (3\text{-}49)$$

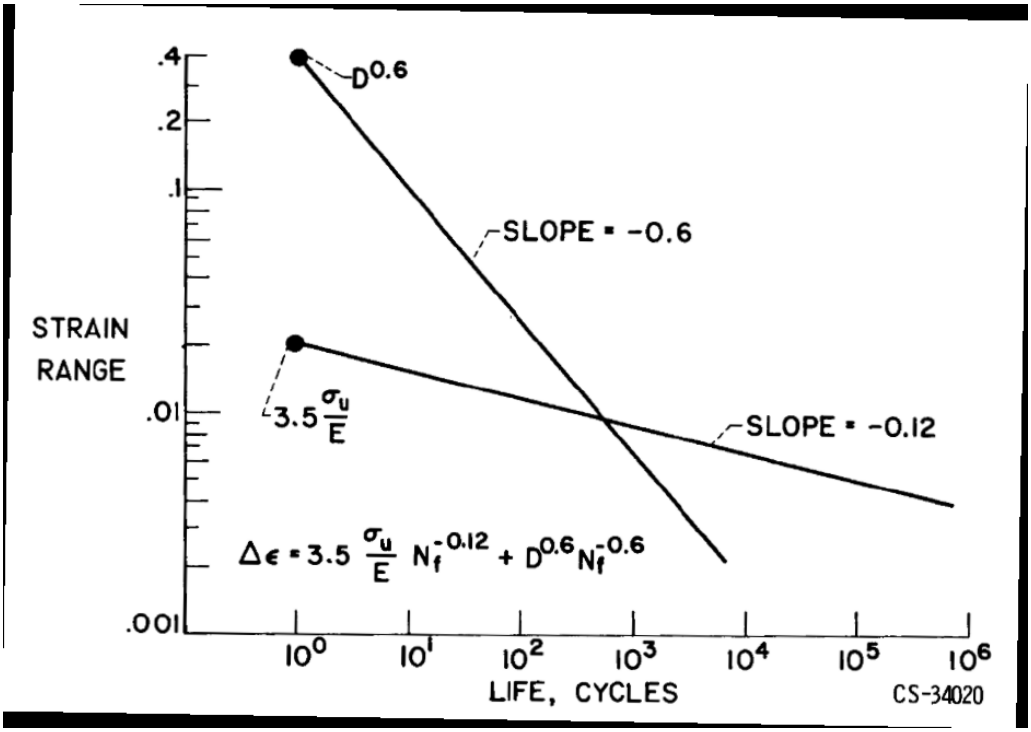

Figure 3-13: Fatigue life method of Universal Slopes [47]

In Equation 3-49:

- D is the true fracture ductility of the material calculated from:

$$D = \ln\left(\frac{1}{1-RA}\right) \quad (3\text{-}50)$$

  where RA is the reduction are of the stressed component.

- E is the Young's modulus material property
- Δε is the total strain range calculated from Neuber's rule [48]

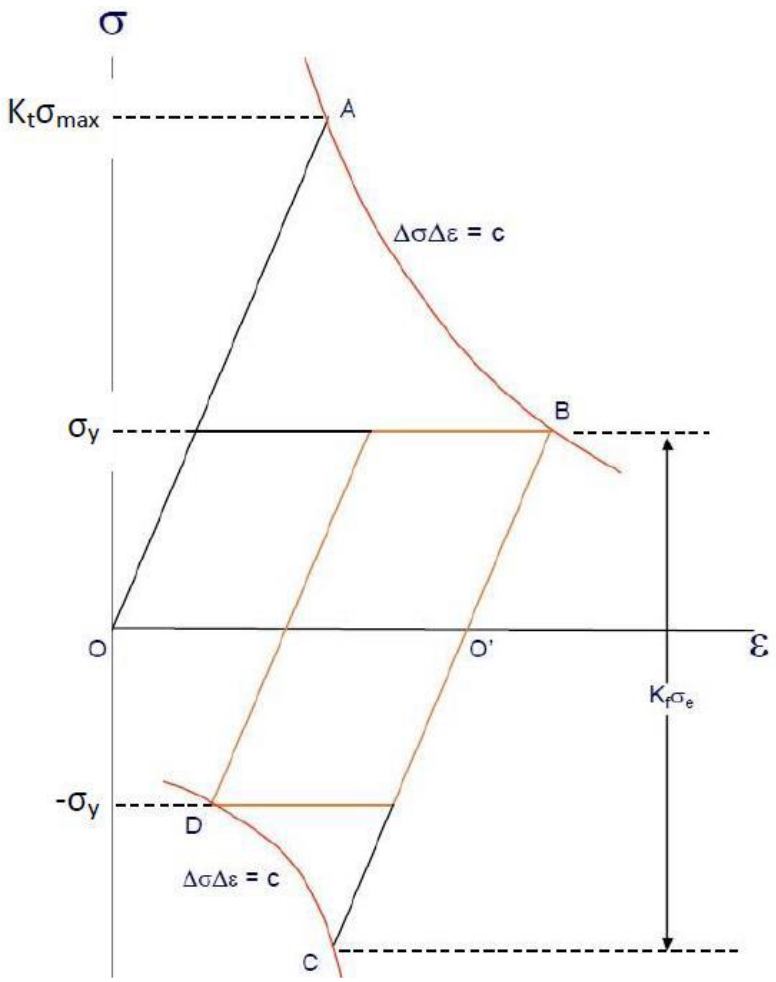

Figure 3-14: Idealized fatigue hysteresis loop displaying Nuebler's Rule [48]

According to Neuber's rule over Figure 3-14:

$$\sigma_A = \sigma_{elastic} = \sigma_{max} K_t \tag{3-51}$$

where σ_{max} is the maximum nominal stress acting on the blade, and Kt is a stress concentration factor. Based on the elastic material property for point A, ε_A could be calculated via elastic modulus E:

$$\varepsilon_A = \frac{\sigma_A}{E} \tag{3-52}$$

The Neuber's Rule is used to relate point A and B:

$$\Delta\sigma\Delta\varepsilon = \sigma_A\varepsilon_A = \sigma_B\varepsilon_B \tag{3-53}$$

Repeating the process for points C and D the total strain can be given as:

$$\Delta\varepsilon = \varepsilon_B - \varepsilon_D = \varepsilon_A + \varepsilon_{CD} \tag{3-54}$$

By applying an iterative procedure in Equation 3-49 for different values of Nf, the correct value for cycles to failure is obtained.

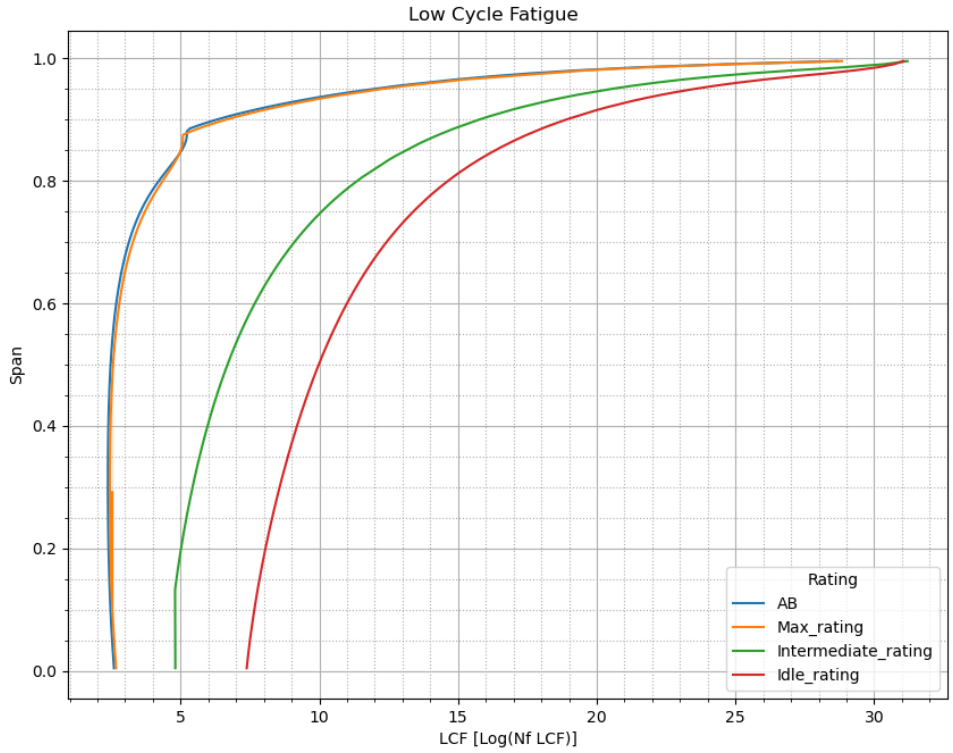

Figure 3-15: Spanwise LCF life in Log(Nf) for different engine ratings

3.7.2.2 High cycle fatigue

The HPT blades, due to the nature of their function experience cyclic stresses each time they are loaded from a different engine rating, they are loaded from the passing behind the stator blades of HPT in every rotation. This high frequency loading is High Cycle Fatigue (HCF).

The stress-life approach was adopted for this research using S-N curves in combination with a double Goodman diagram (Fig 3-16).

3.7.2.2.1 S-N Curves Modelling

Figure 3-17 displays the S-N curve for steel. IT makes the assumptions that endurance strength for the first 10^3 cycle is 90% of the material UTS and 50% of the UTS for the cycles after 10^6. The endurance strength values between these two points can be calculated by:

$$\sigma_{N_f} = \sigma_{N=10^6} \left(\frac{\sigma_{N=10^3}}{\sigma_{N=10^6}} \right)^{\left(2-\frac{1}{3}N_f\right)} \quad (3\text{-}55)$$

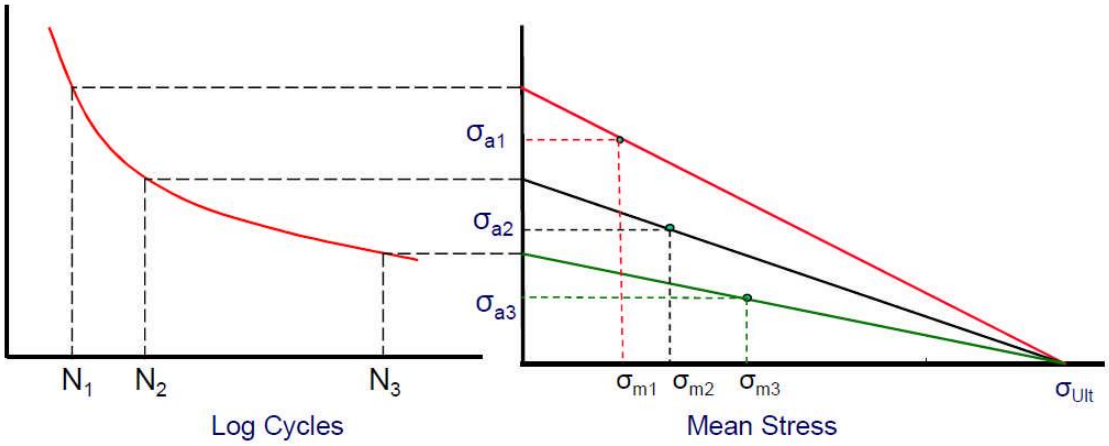

Figure 3-16: Combined Goodman/S-N diagram [48]

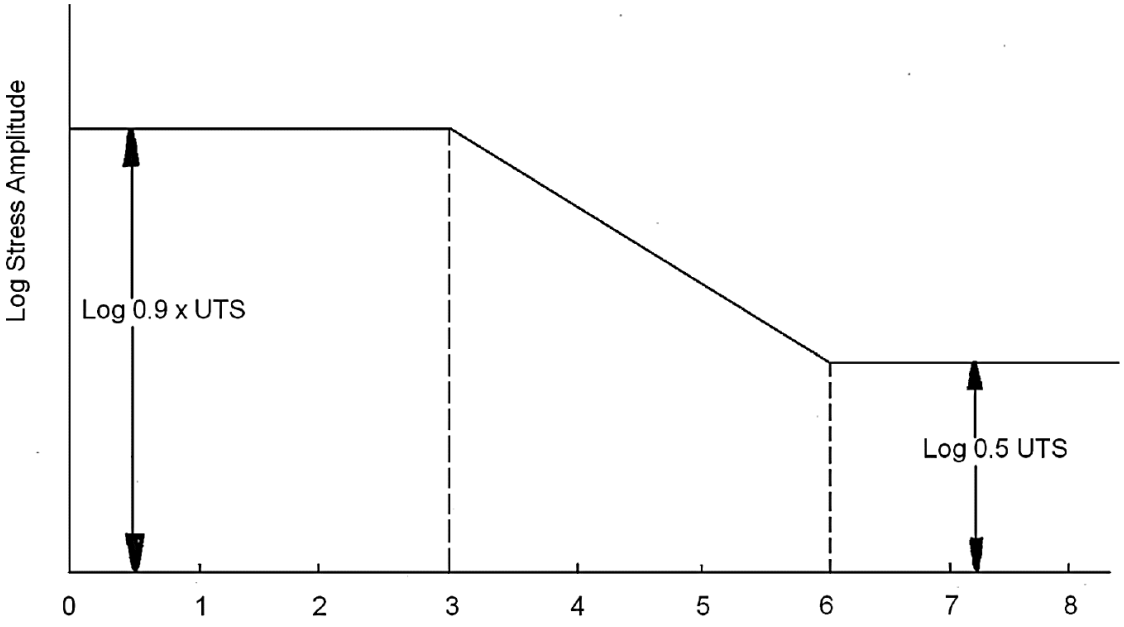

Figure 3-17: Approximation of S-N curve for steel [48]

3.7.2.2.2 Double Goodman Diagram

Stress acting on rotor blades is caused by rotational and aerodynamic forces meaning that the blades are subject to a cyclic and thermal stresses. For HPT, σ_{CF} and $\sigma_{thermal}$ are the constant stresses experienced during a major cycle (ie RPM engine rating) and σ_{BD} is the minor stress experienced every time a blade passes in the wake caused by the stator blades. This combined loading can be visualized in Fig 3-18.

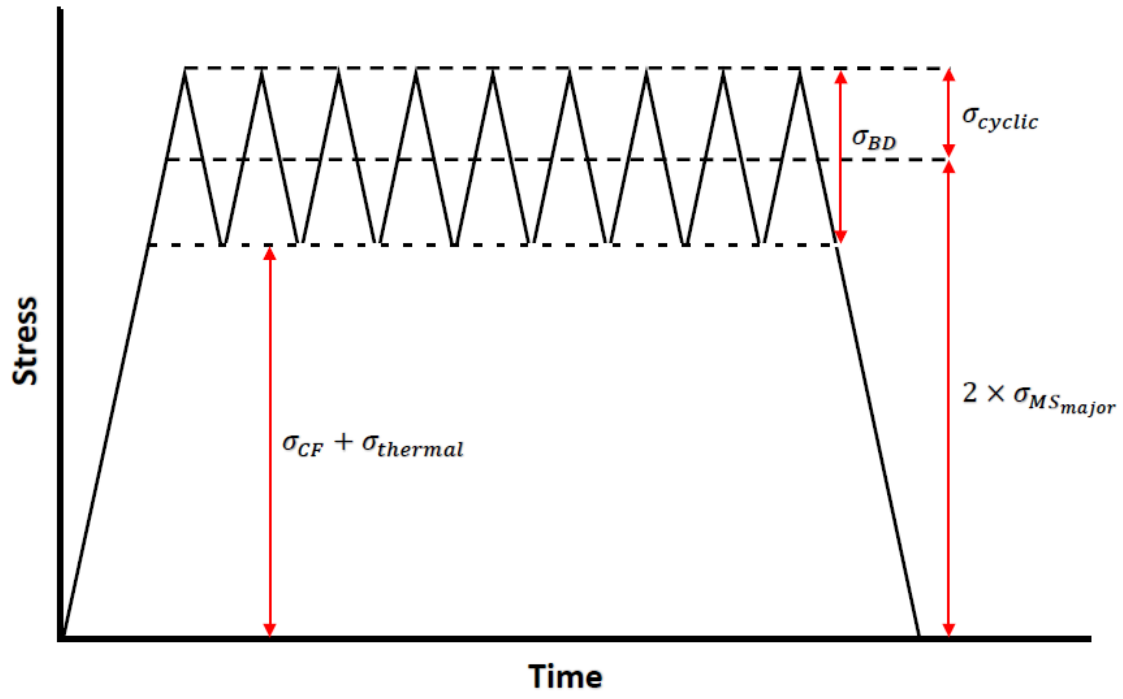

Figure 3-18: Representation of combined cyclic loading [28]

where

$$\sigma_{MS_{major}} = \frac{\sigma_{CF} + \sigma_{cyclic}}{2} \tag{3-56}$$

and

$$\sigma_{cyclic} = \frac{\sigma_{BD}}{2} \tag{3-57}$$

3.7.2.2.3 Major Cycle Goodman Diagram

Since the $\sigma_{MS_{major}}$ is known, the major cycle alternating stress is calculated:

$$\sigma_{Alt_{major}} = K_{f_{design}} \sigma_{MS_{major}} \tag{3-58}$$

where

$$K_{f_{design}} = q(K_t - 1) + 1 \tag{3-59}$$

Finally, from Fig 3-19 the $\sigma_{EMS_{major}}$ can determined with use of similar triangles:

$$\sigma_{EMS_{major}} = \sigma_{MS_{major}} + \frac{\sigma_{Alt_{major}} \sigma_{UTS}}{\sigma_{endurance}} \tag{3-60}$$

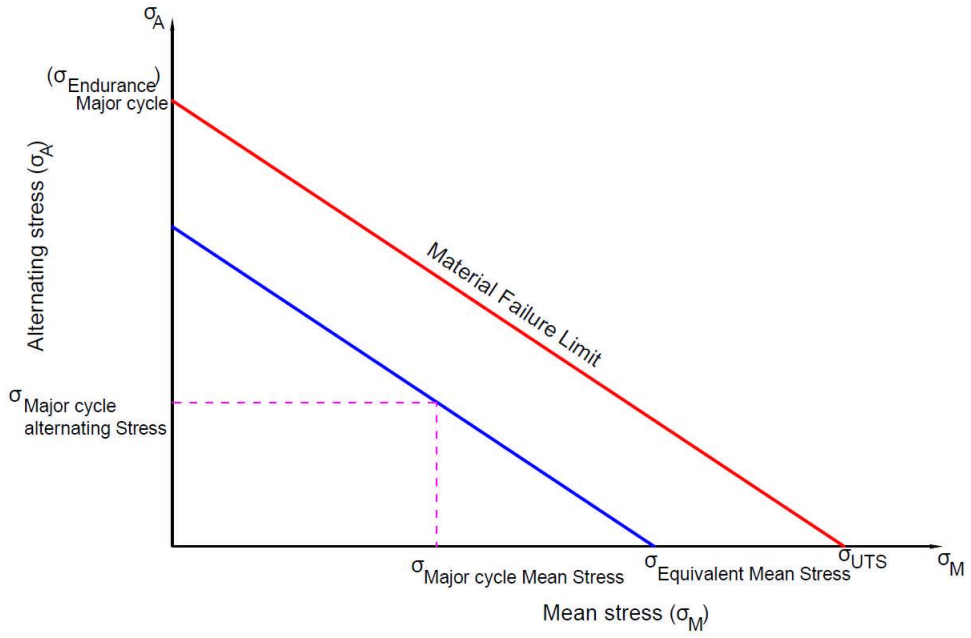

Figure 3-19: Major cycle Goodman diagram [25]

3.7.2.2.4 Minor Cycle Goodman Diagram

To obtain the failure limit of the material for HCF cycles, the minor cycle endurance strength is used along with UTS value is to calculate the equivalent alternating stress for the minor cycle, $\sigma_{EAlt_{minor}}$ along with the alternating stress of the minor cycle, $\sigma_{Alt_{minor}}$ in the second Goodman diagram as shown in Fig 3-20.

$$\sigma_{EMS_{minor}} = \sigma_{EMS_{major}} + \frac{\sigma_{Alt_{minor}}\sigma_{UTS}}{\sigma_{endurance}} \tag{3-61}$$

To calculate the alternating stress of the minor cycle the Eq. 3-58 is used and by similar trianlges in Fig. 3-20 the $\sigma_{EAlt_{minor}}$ is as follows:

$$\sigma_{EAlt_{minor}} = \frac{\sigma_{endurance}\sigma_{EMS_{minor}}}{\sigma_{UTS}} \tag{3-62}$$

The equivalent alternating strees obtained is used in conjction with the S-N diagram to estimate the the total number of cycles to failure N_f. This correlation is shown in Fig 3-21.

The number of HCF cycles the blade experiences for the given input of number of major cycles is given by Equation

$$N_{rating} = No\ of\ NGVs \times rpm \times Nmajor \times t_{cycle} \tag{3-63}$$

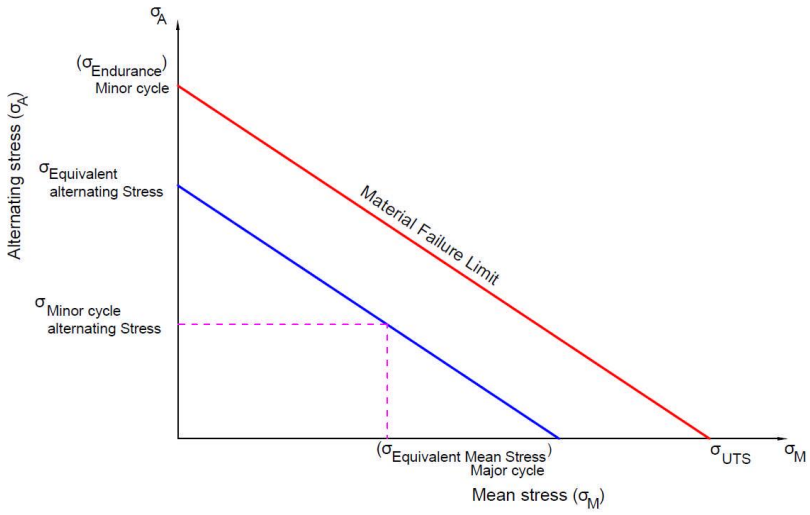

Figure 3-20: Minor cycle Goodman diagram [25]

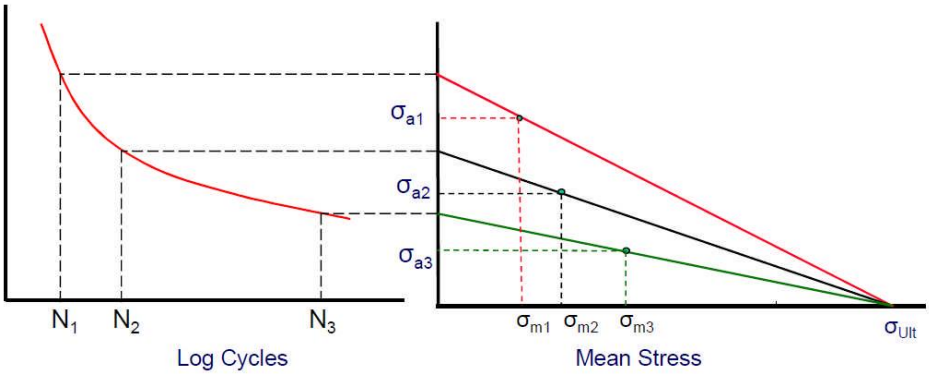

Figure 3-21: S-N/R-M diagram [25]

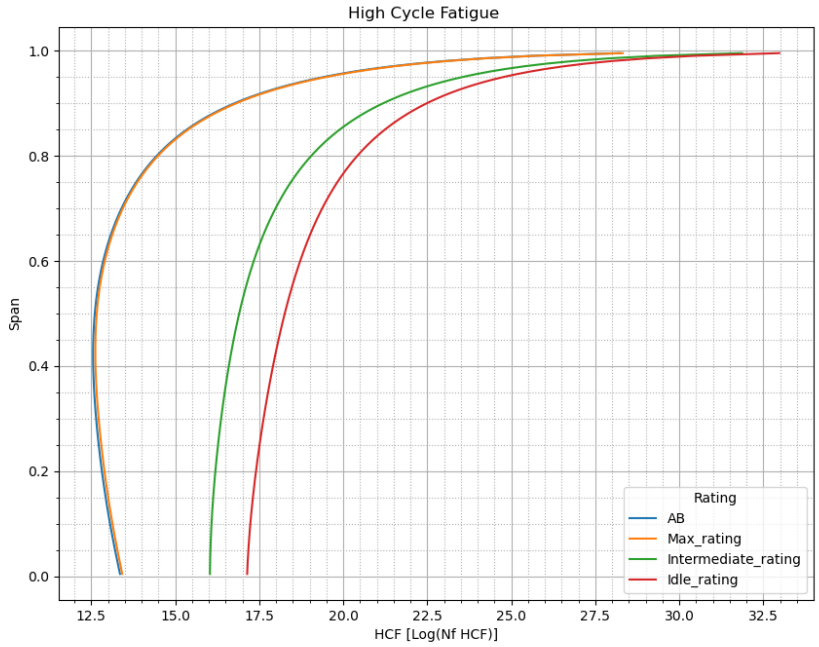

Figure 3-22: Spanwise HCF life in Log(Nf) for different engine ratings

As observed in Fig. (3-22), the life estimation for HCF in “AB” and “MAX” ratings are almost the same. This is caused on by the fact that the two ratings have the same shaft rotational speed and thus experience the same frequency of loading.

3.8 Total damage

In order to calculate the total damage induced on the blades by thermal and mechanical loads, the Palmgren-Miner linear damage theory is used. This theory assumes that failure occurs when the damage fraction reaches unity [49].

$$D = D_{cyclic} + D_{steady} \tag{3-64}$$

Where

$$D = \sum_{i=1}^{phases} \frac{1}{N_f} + \sum_{i=1}^{phases} \frac{t_i}{t_f} \tag{3-65}$$

4 Case Studies

To investigate the implications of optimized performance on engine life certain case studies were performed. The first objective was to investigate different mission profiles from Antonakis [18] and their impact upon engine life. The missions that were modelled are:

1. Training mission: Its performance characteristics are detailed in Fig. 4-1 to Fig. 4-5.

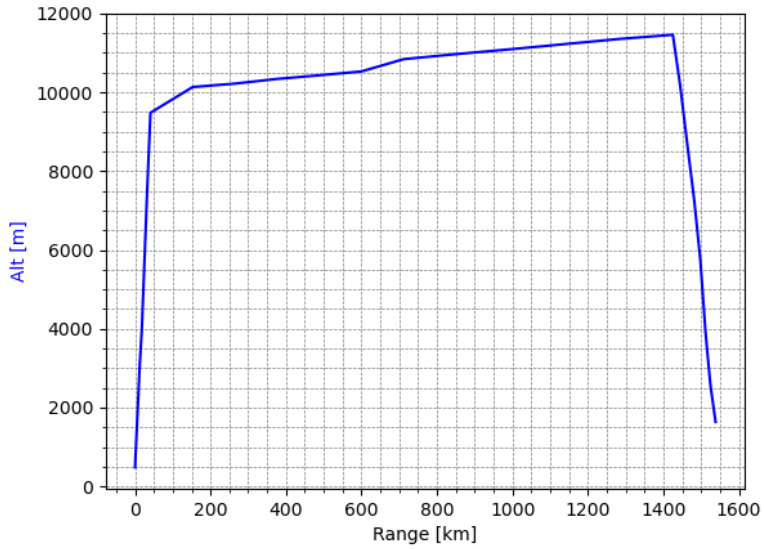

Figure 4-1: Training mission: Alt - Range

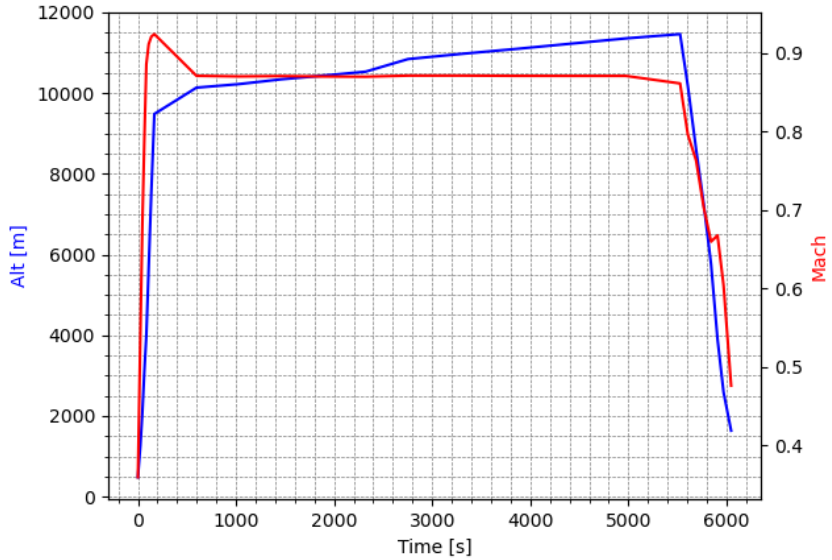

Figure 4-2: Training mission: Alt & Mach - Time

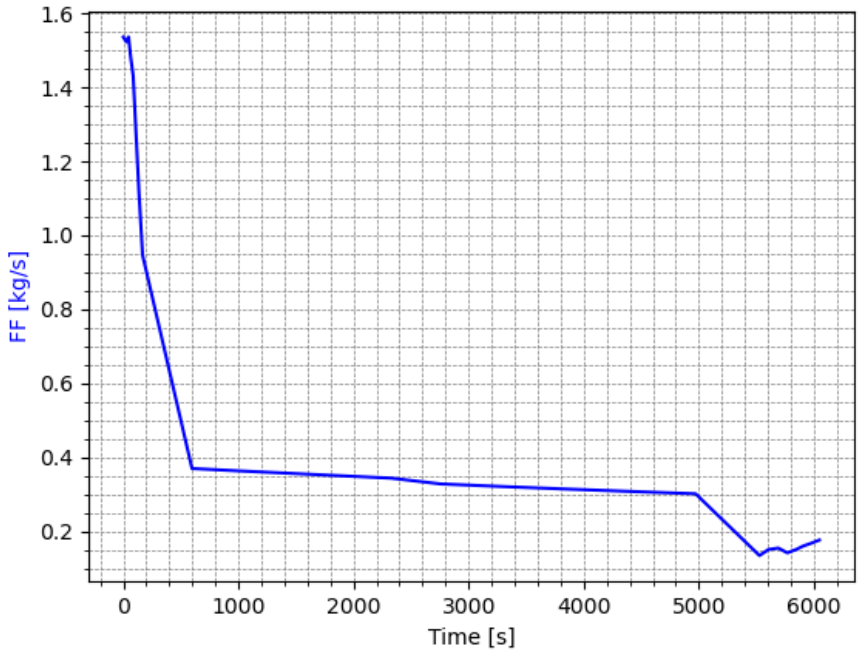

Figure 4-3: Training mission: Fuel Flow – Time

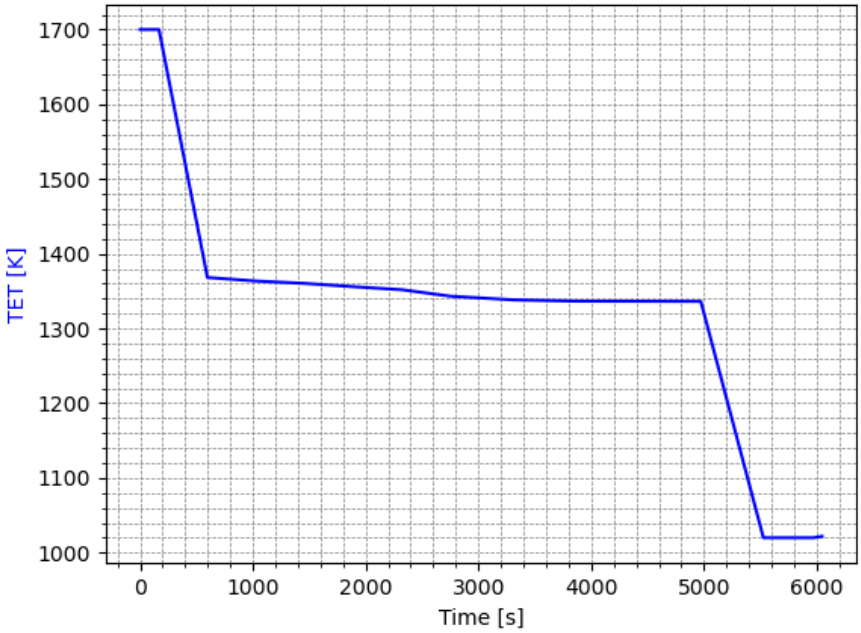

Figure 4-4: Training mission: TET – Time

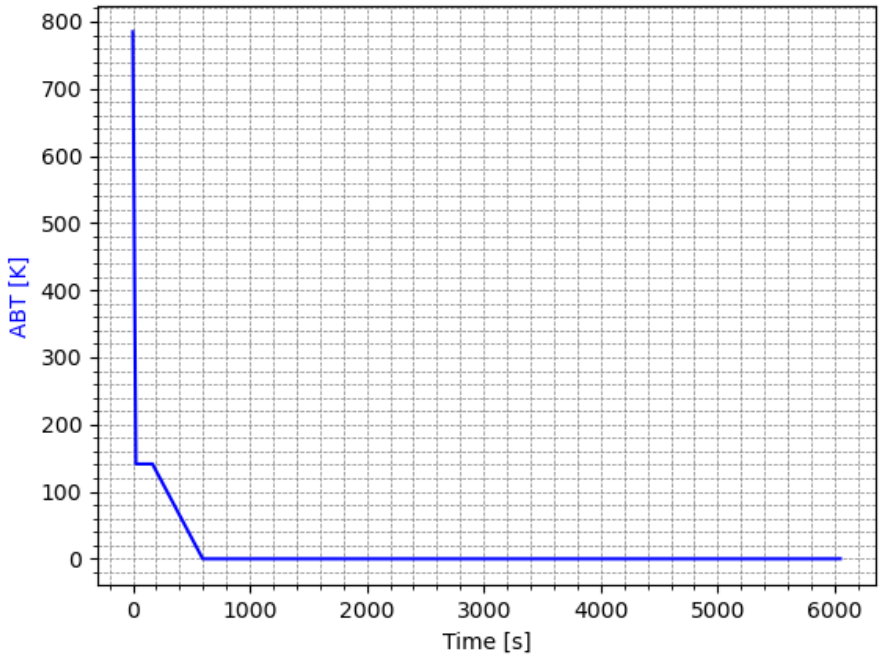

Figure 4-5: Training mission: AB temperature – Time

2. Supersonic interception: Its performance characteristics are detailed in Fig. 4-6 to Fig. 4-10.

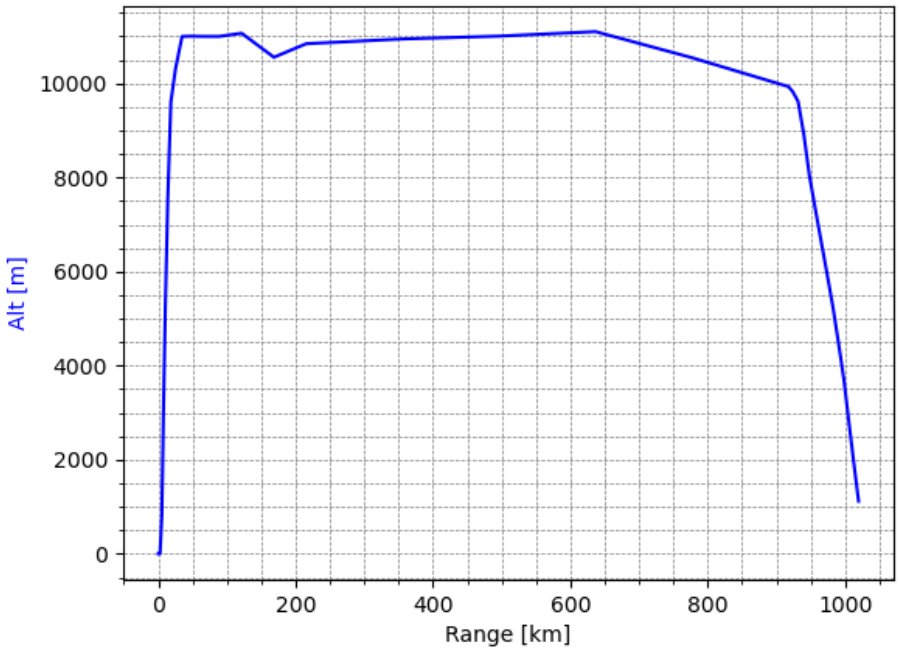

Figure 4-6: Supersonic interception: Alt - Range

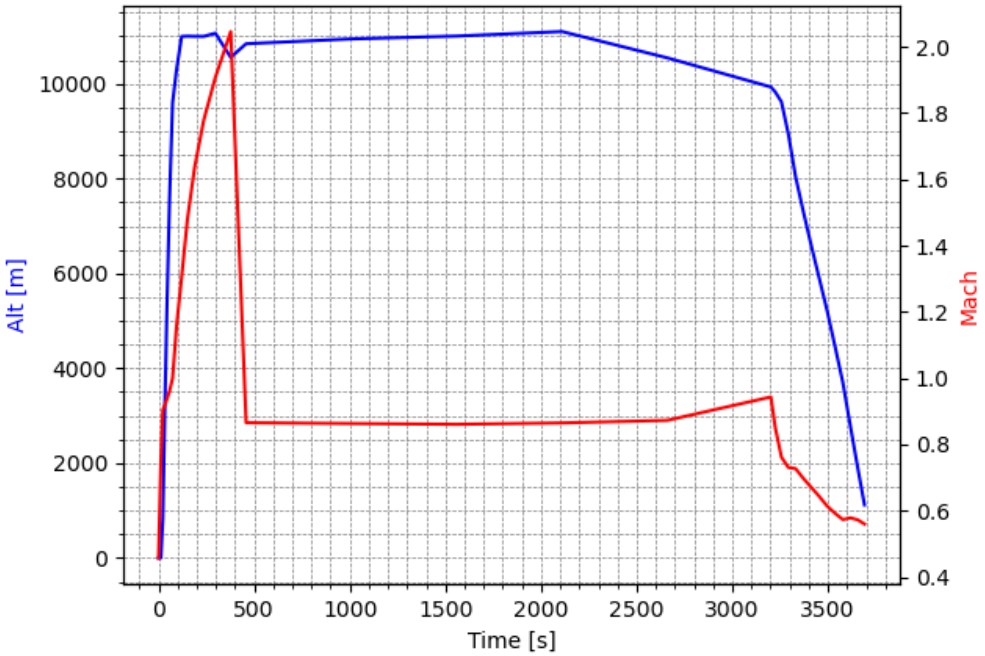

Figure 4-7: Supersonic interception: Alt – Mach

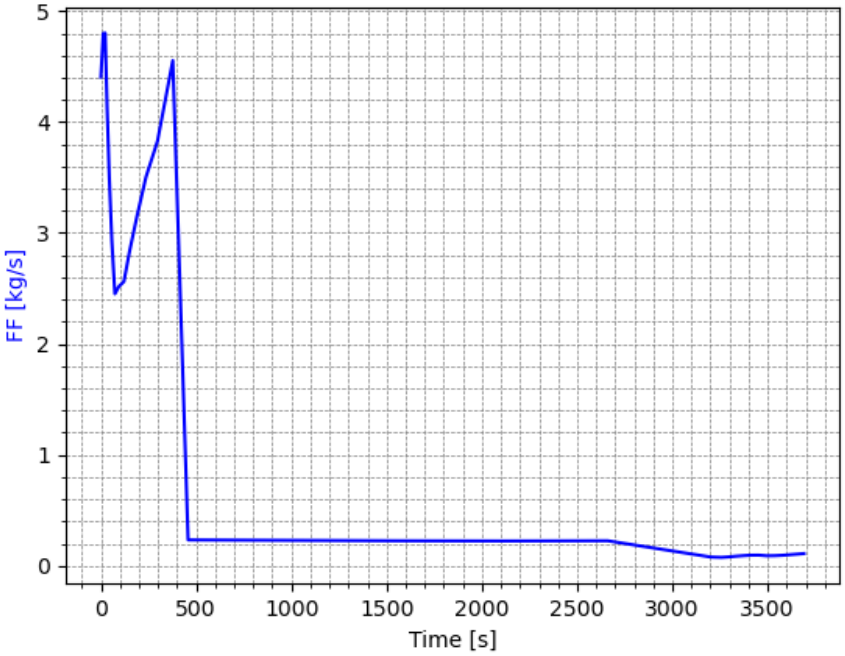

Figure 4-8: Supersonic interception: Fuel Flow – Time

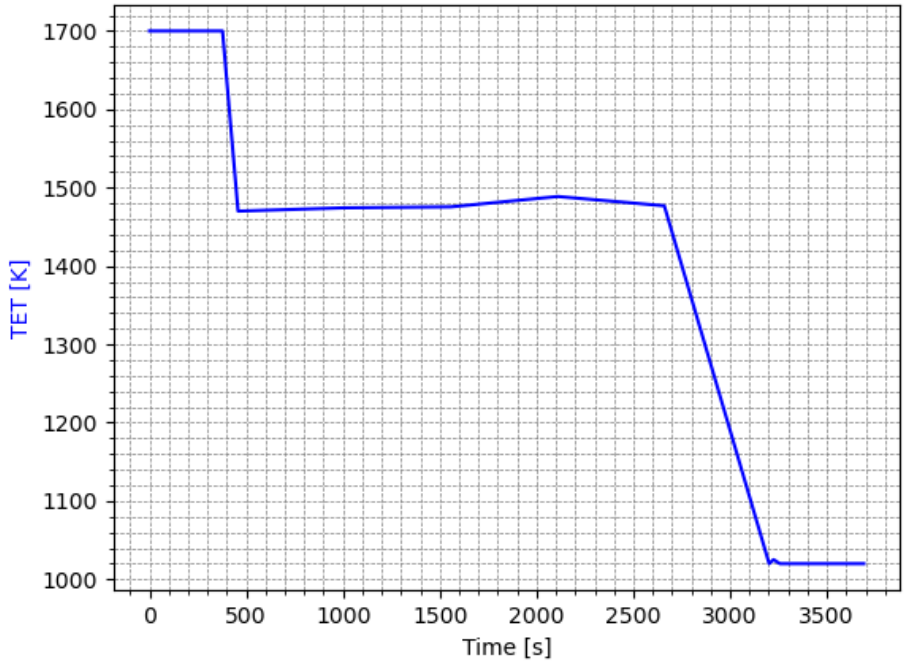

Figure 4-9: Supersonic interception: TET – Time

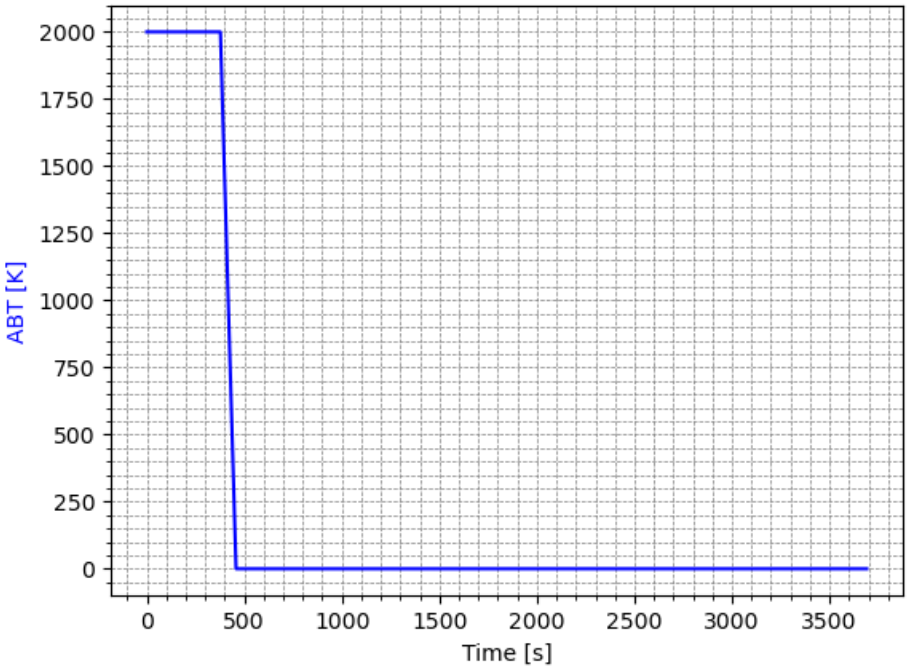

Figure 4-10: Supersonic interception: AB temperature – Time

3. High AoA BFM: Its performance characteristics are detailed in Fig. 4-10 to Fig. 4-11.

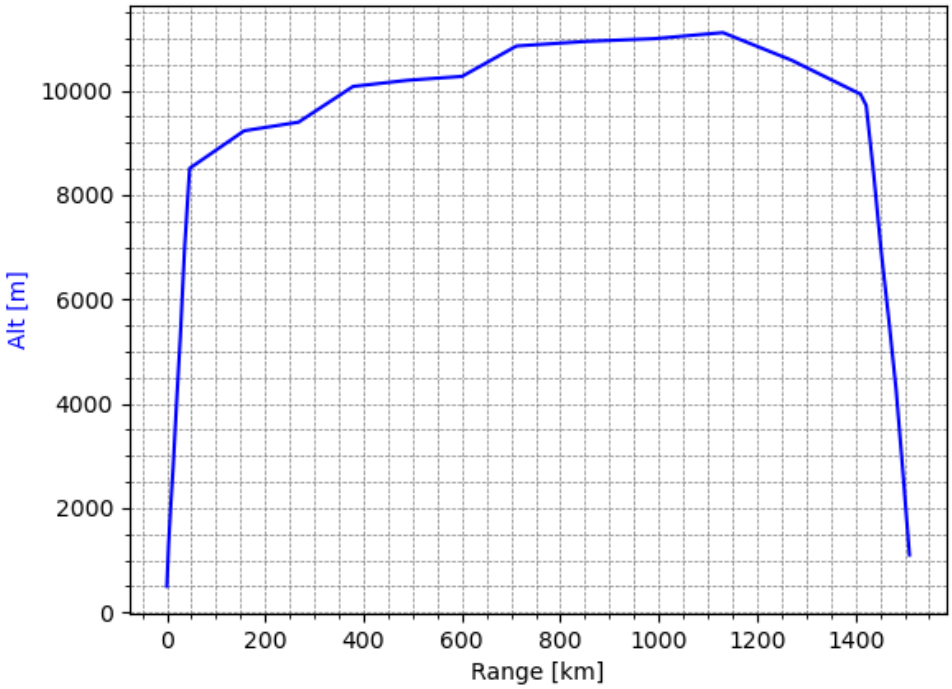

Figure 4-11: High AoA BFM: Alt – Range

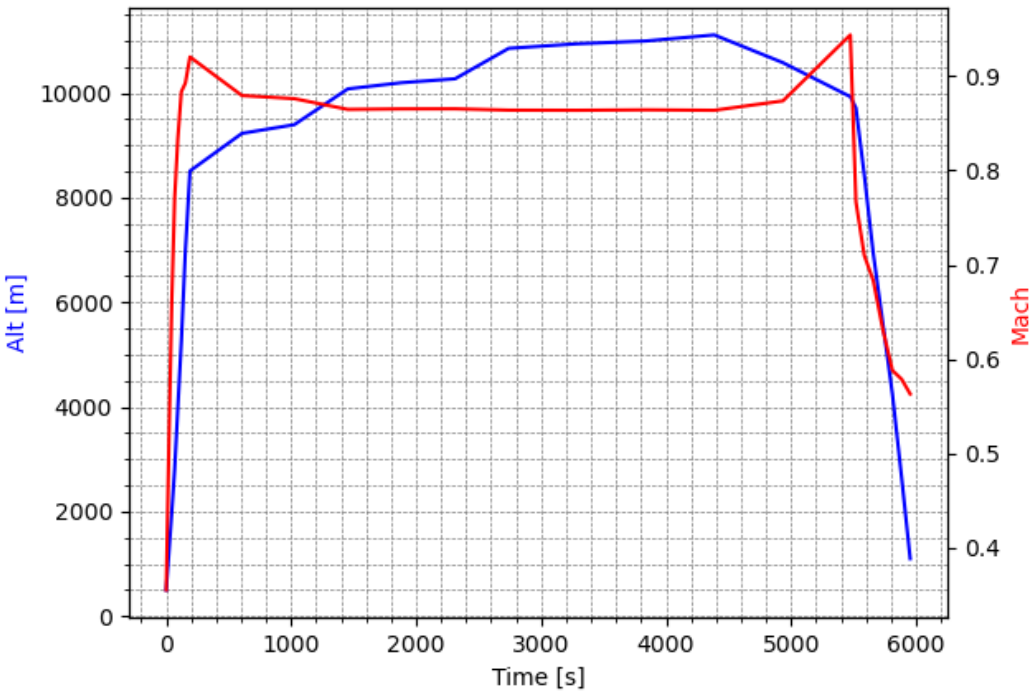

Figure 4-12: High AoA BFM: Alt – Mach

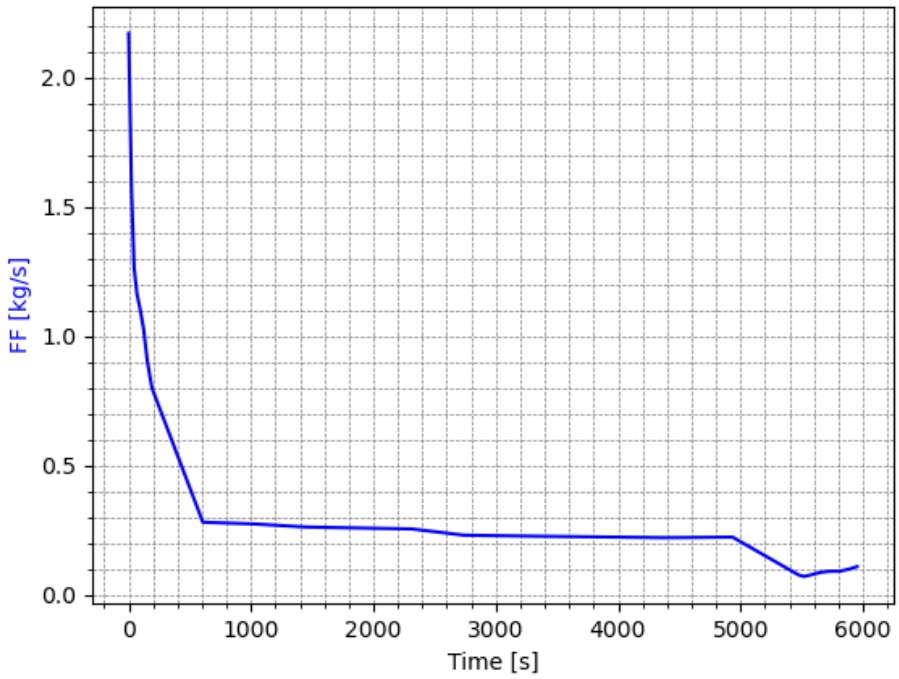

Figure 4-13: High AoA BFM: Fuel Flow – Time

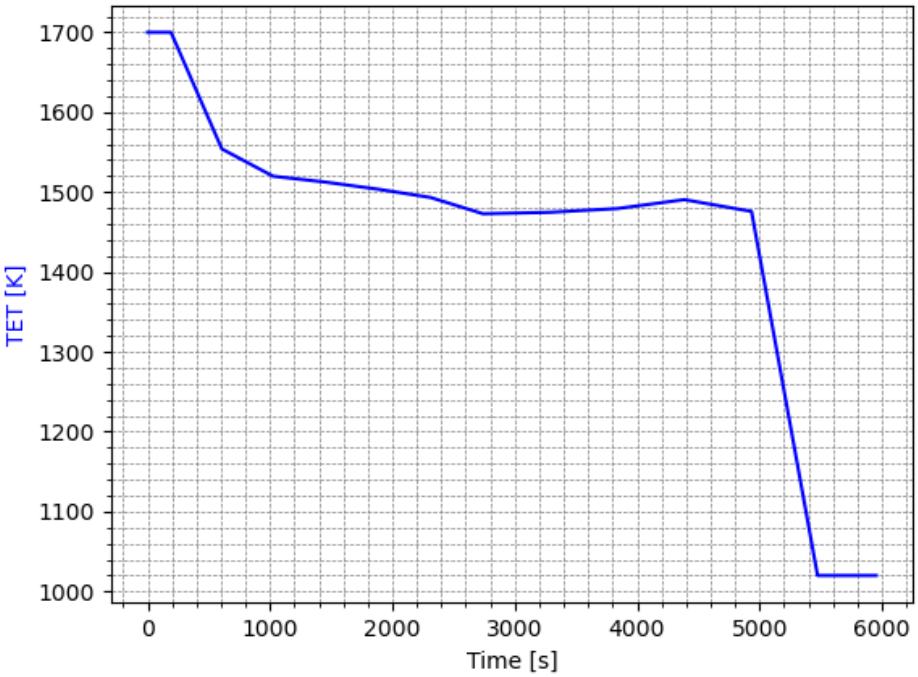

Figure 4-14: High AoA BFM: TET – Time

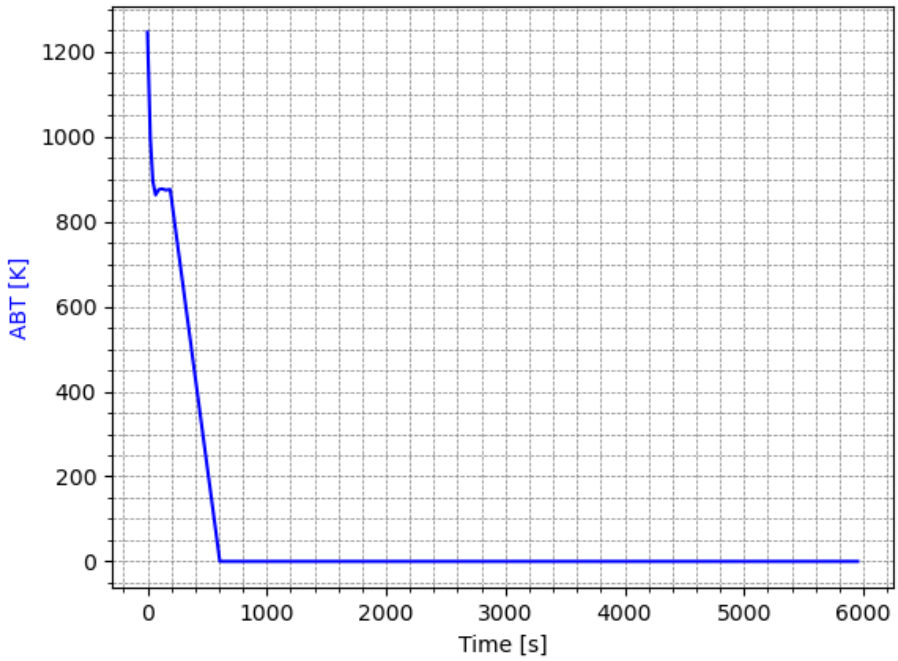

Figure 4-15: High AoA BFM: AB Temperature – Time

In order to reduce the computational cost, the throttle settings applied throughout the mission profiles were chosen to be grouped in four discrete categories:

1. ***AB***: For settings that the afterburner temperature was close to maximum
2. ***Max_Rating:*** For ratings that either correspond to military thrust, with maximum TET temperature or settings that have min AB TLA.
3. ***Intermediate_Rating:*** For settings near 0.87 of TLA
4. ***Idle_Rating:*** For settings near 0.7 TLA

For these settings, the cycles to failure were computed and presented in Figures 4-16 to 4-19.

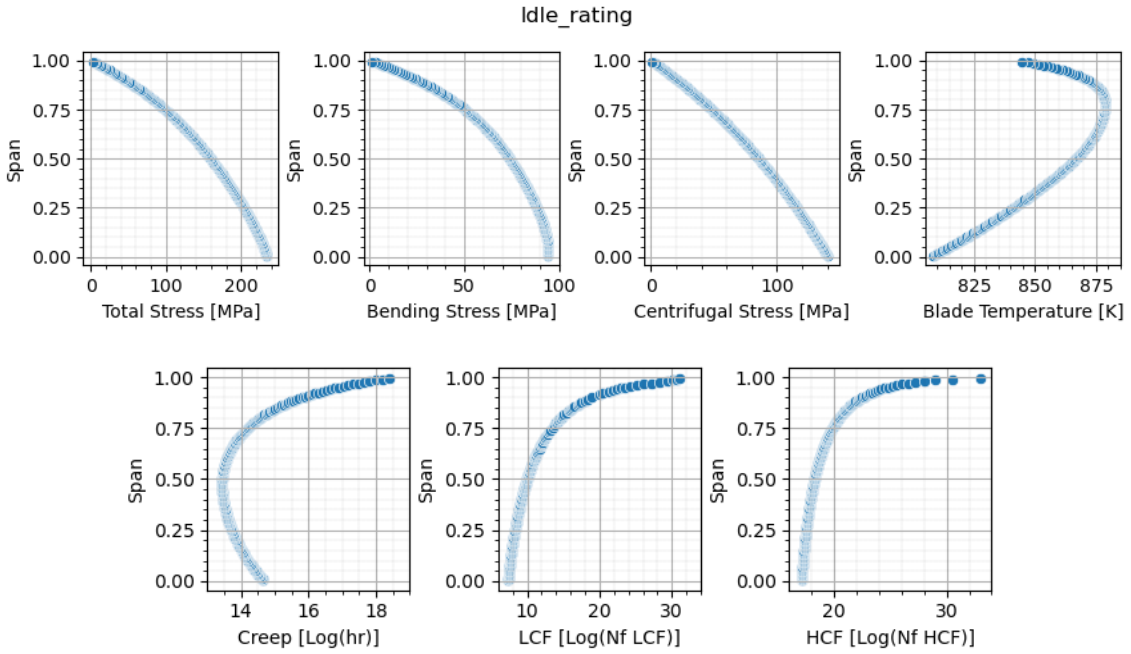

Figure 4-16: Thermo-mechanical analysis at "Idle" rating

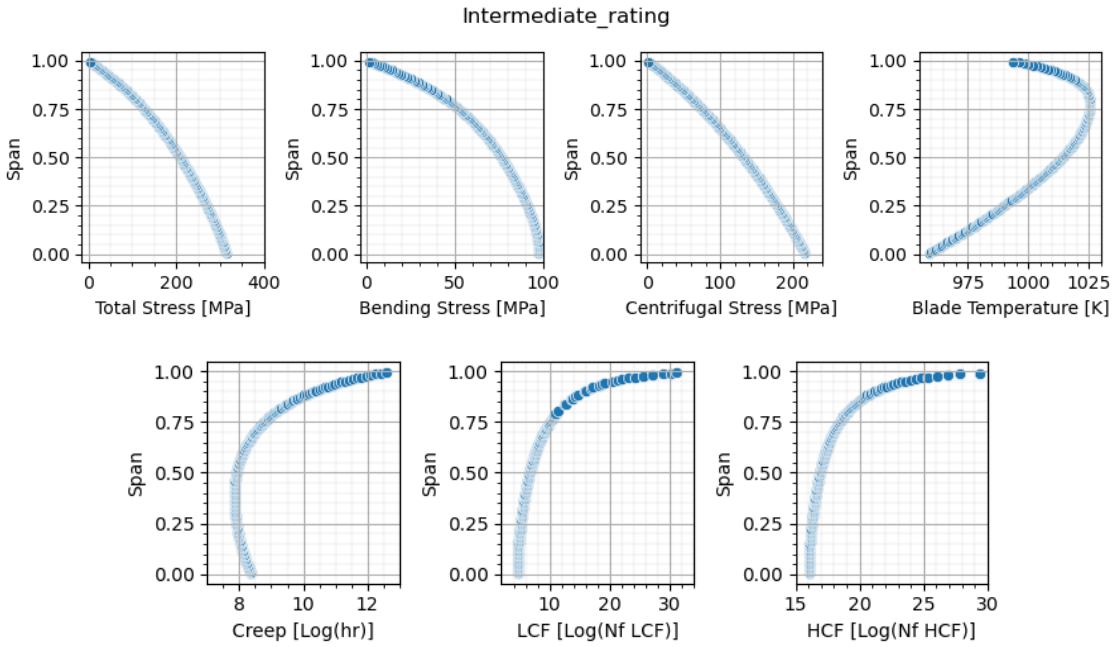

Figure 4-17: Thermo-mechanical analysis at "Intermediate" rating

After observation of graphs 4-16 to 4-19 the assumed approach was deemed appropriate since the chosen ratings are able to closely represent the engine status throughout the operating spectrum. In order to increase the fidelity of the results an interim approach was chosen; interpolation is applied for engine settings between the analyzed ratings. This interim approach was applied since Figures 3-7 and 3-8 to 3-11 displayed a liner change in the measured loads.

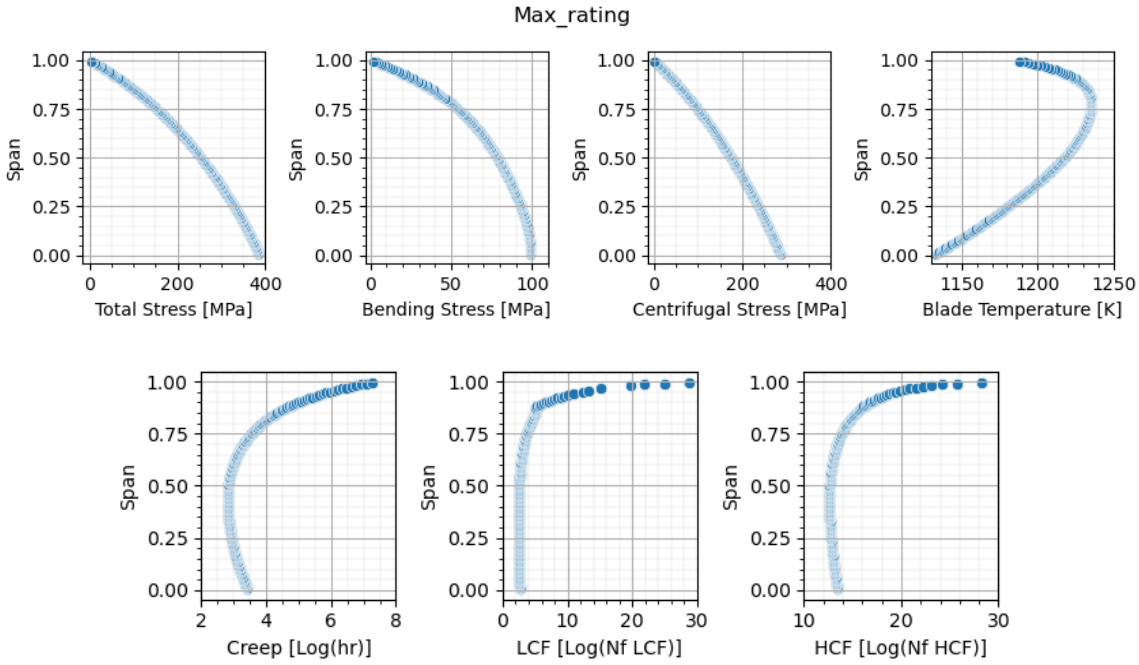

Figure 4-18: Thermo-mechanical analysis at "Max" rating

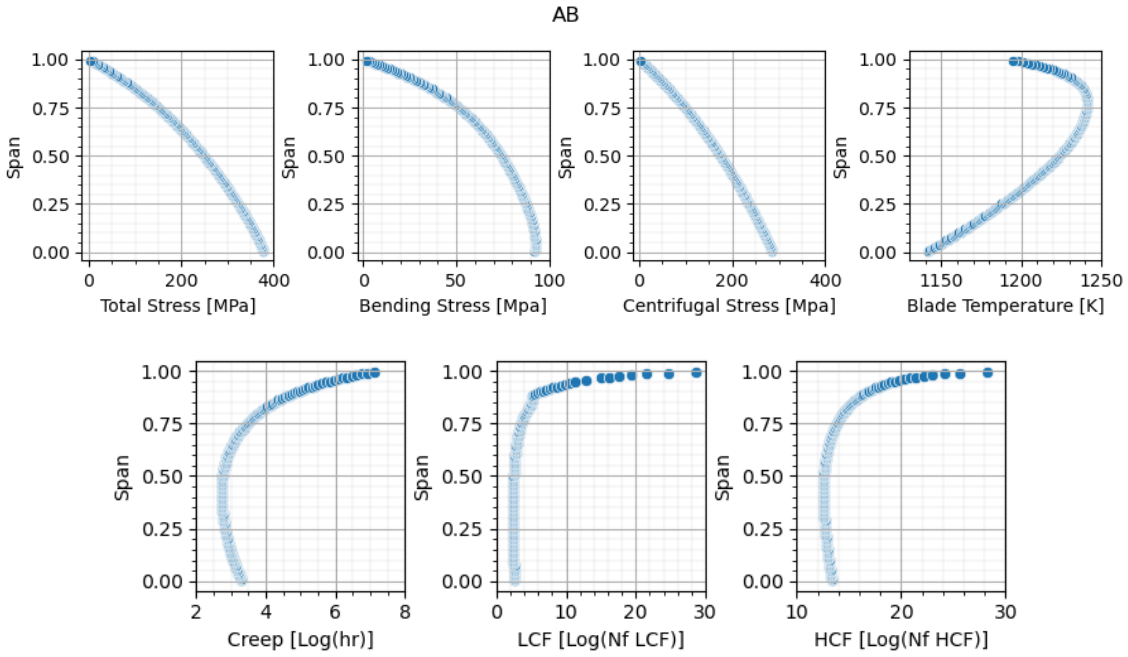

Figure 4-19: Thermo-mechanical analysis at "AB" rating

For each of these missions the life expectancy to failure was calculated for each of the failure mechanisms. In Fig. 4-20 to 4-22 the cycles to failure are plotted against the blade span.

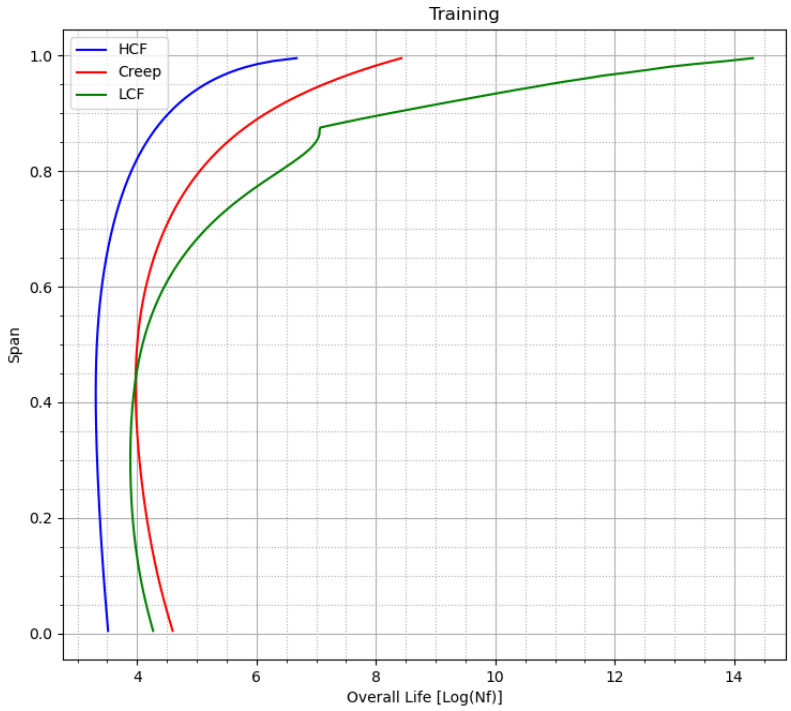

Figure 4-20: Training mission cycles to failure

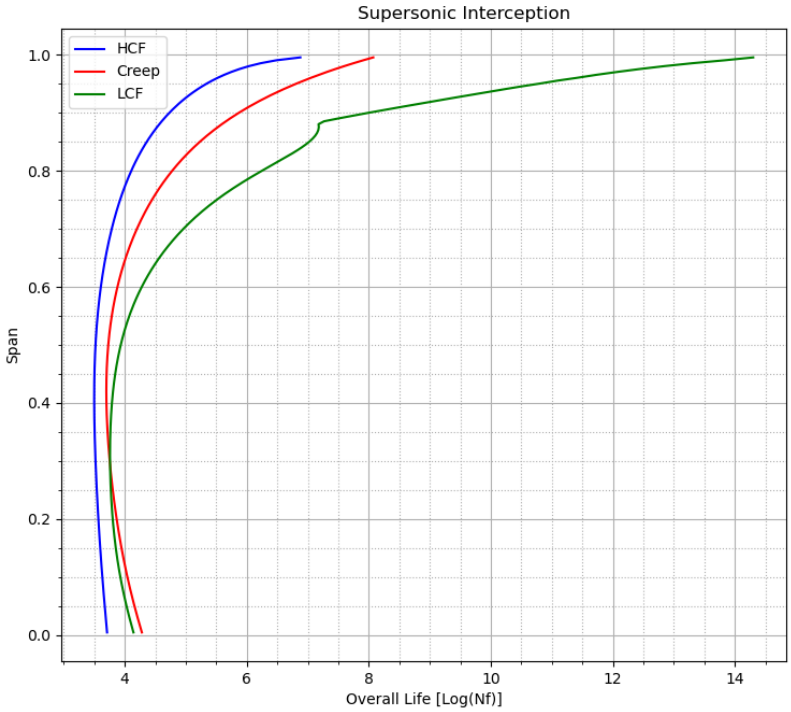

Figure 4-21: Supersonic interception cycles to failure

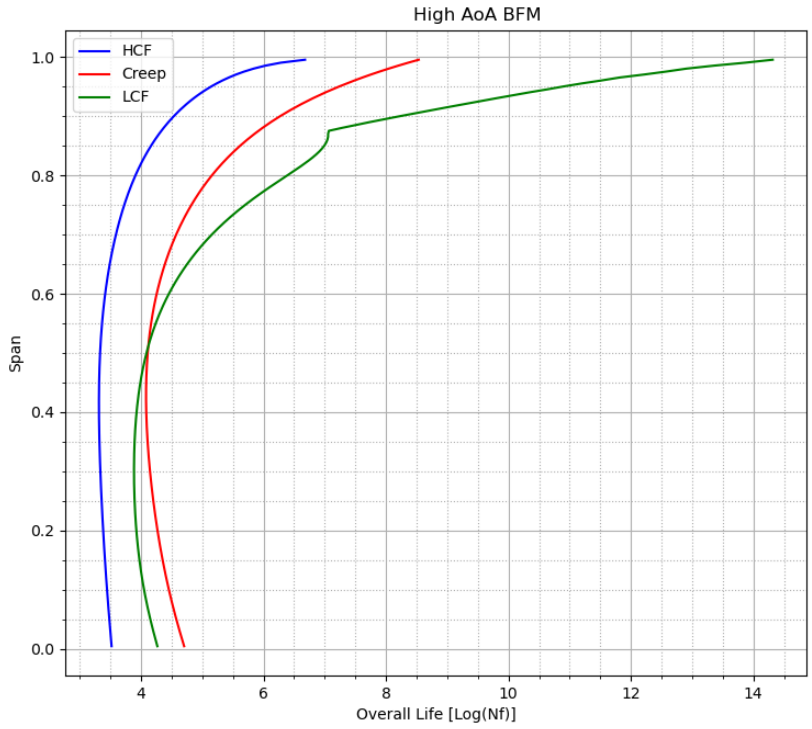

Figure 4-22: High AoA BFM cycles to failure

The respective critical points for every failure mechanism in each mission are shown in Table 4-1.

Missions	Creep cycles	Span	LCF cycles	Span	HCF cycles	Span	Flight Hours	Span
Training	9420	43%	7699	30%	2027	41.5%	2344	38.5%
Supersonic	4996	42%	5741	31%	3161	41%	1510	38%
High AoA BFM	12108	43%	7699	30%	2060	41.5%	2411	38.5%

Table 4-1: Life critical points

Figures 4-20 to 4-22 display the life consumption occurred for each rating for all failure mechanisms. In these graphs, it easily observed the heavy dependence of life consumption on engine rating as “AB” and “Max_rating” being the most severe ones in terms of rotational speeds and temperatures, dominate the life consumption.

It is also notable the difference in life consumption in relation to the mission duration. Although the “Supersonic Interception” is almost 40% shorter than the other two, the “Creep” and “LCF” life cycles are greatly diminished due to the increased duration of afterburner usage.

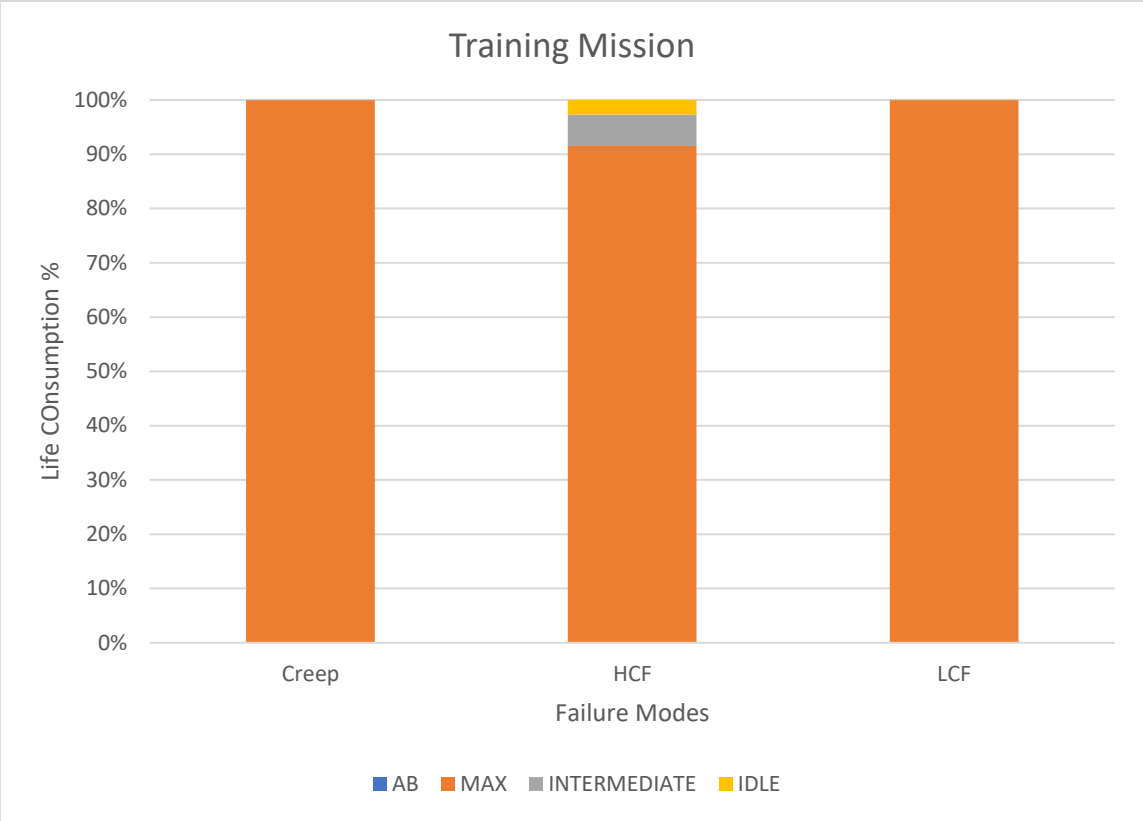

Figure 4-23: Training mission life consumption

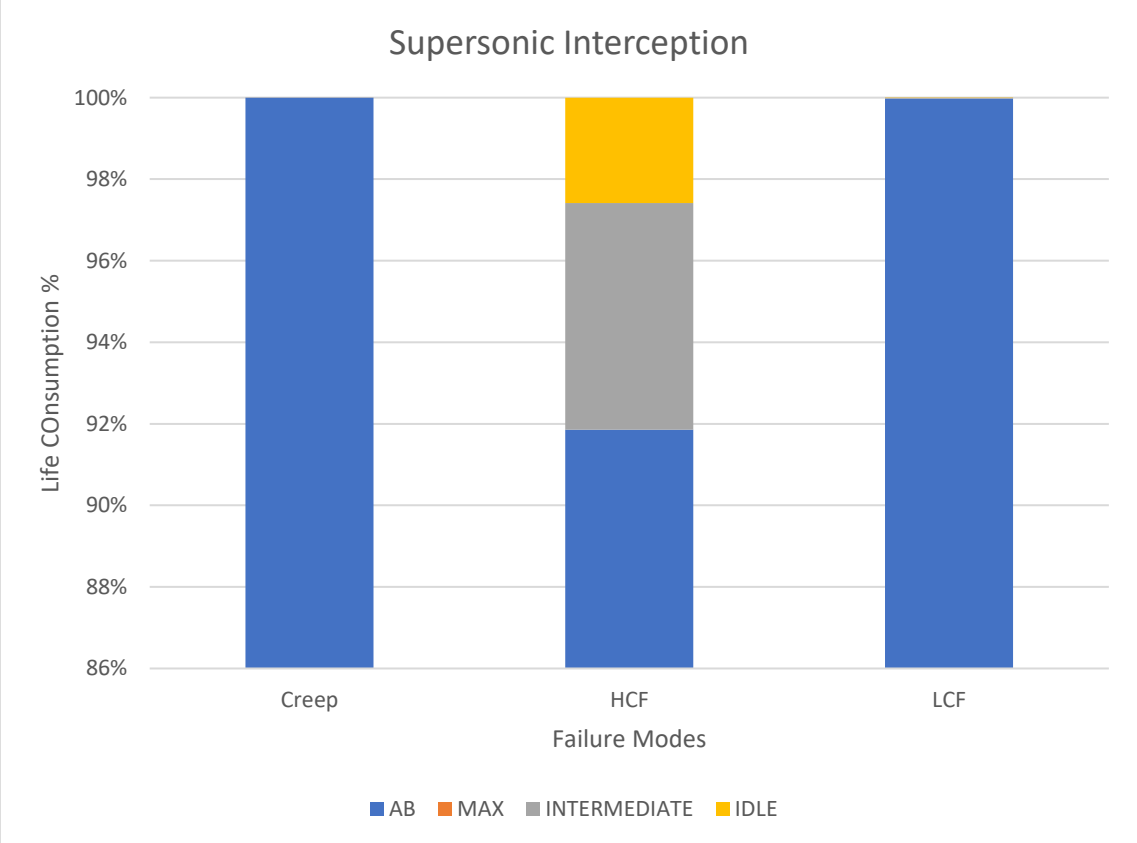

Figure 4-24: Supersonic interception life consumption

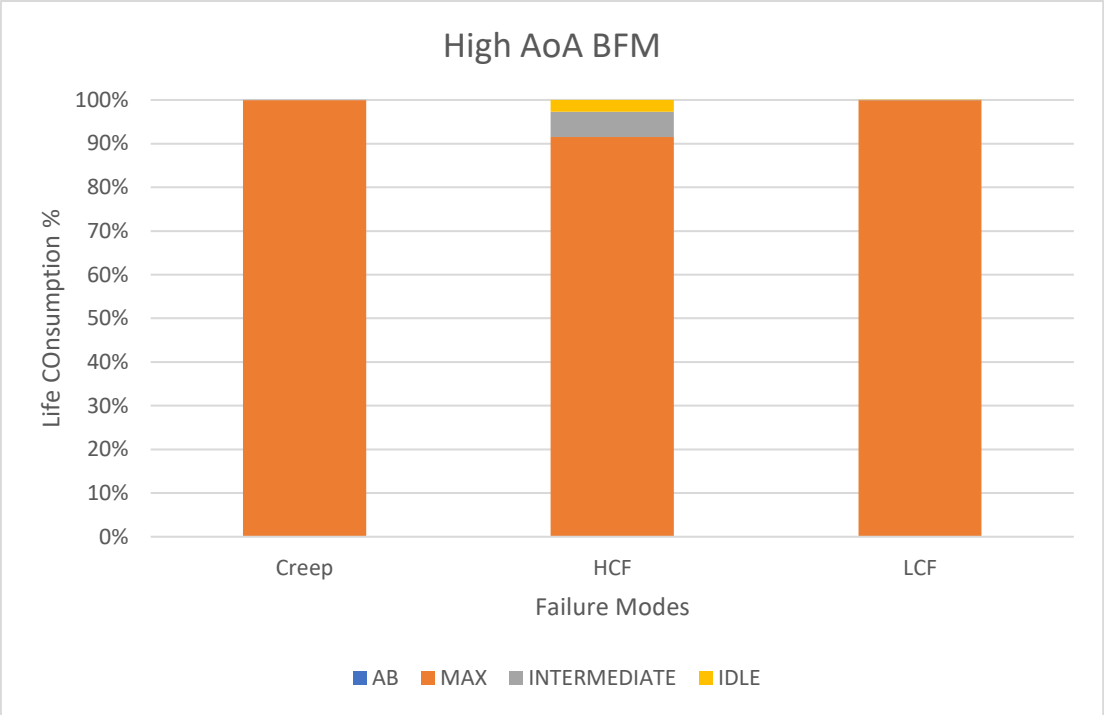

Figure 4-25: High AoA BFM life consumption

From Fig. (4-23) to (4-25) and in conjunction with table (4-1), it is apparent that life consumption is dominated by high-temperature and high-rpm ratings despite them constituting settings of lower usage time.

4.1 Optimal climb profiles

The second objective of this research was to investigate the impact of optimal climb profile on engine life. For this purpose, the climb profiles from Antonakis [18] were studied in a similar way to the full mission cases. In this test case, five climb profiles were analyzed for their respective influence on engine damage life. These profiles are:

1. Max range
2. Min fuel
3. Min IR
4. Min noise
5. Min time

Similarly to full mission profiles, their performance characteristics are detailed below:

1. Maximum mission range

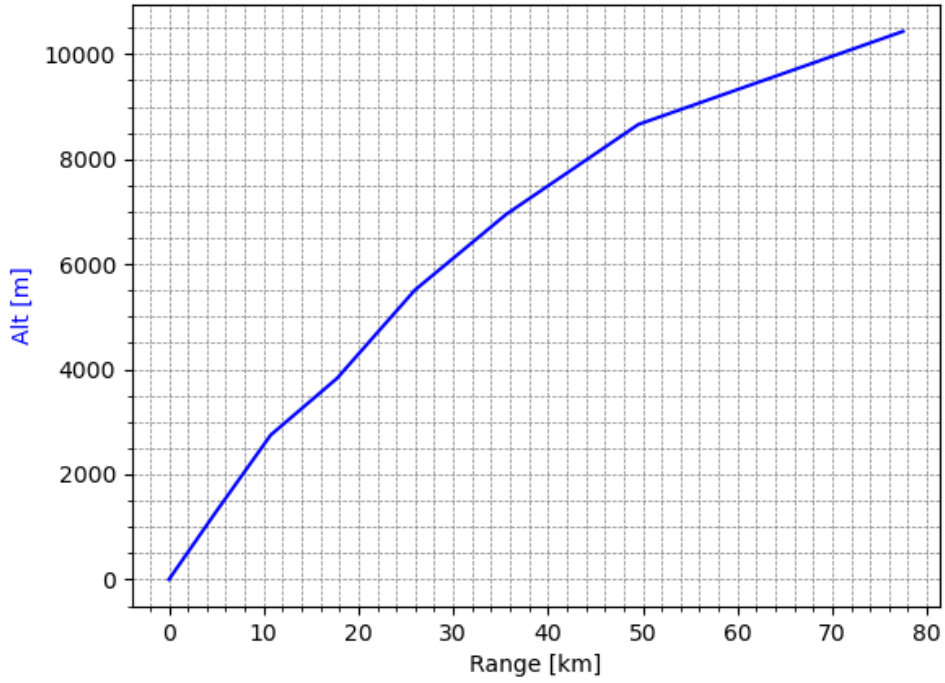

Figure 4-26: Max Range: Alt-Range

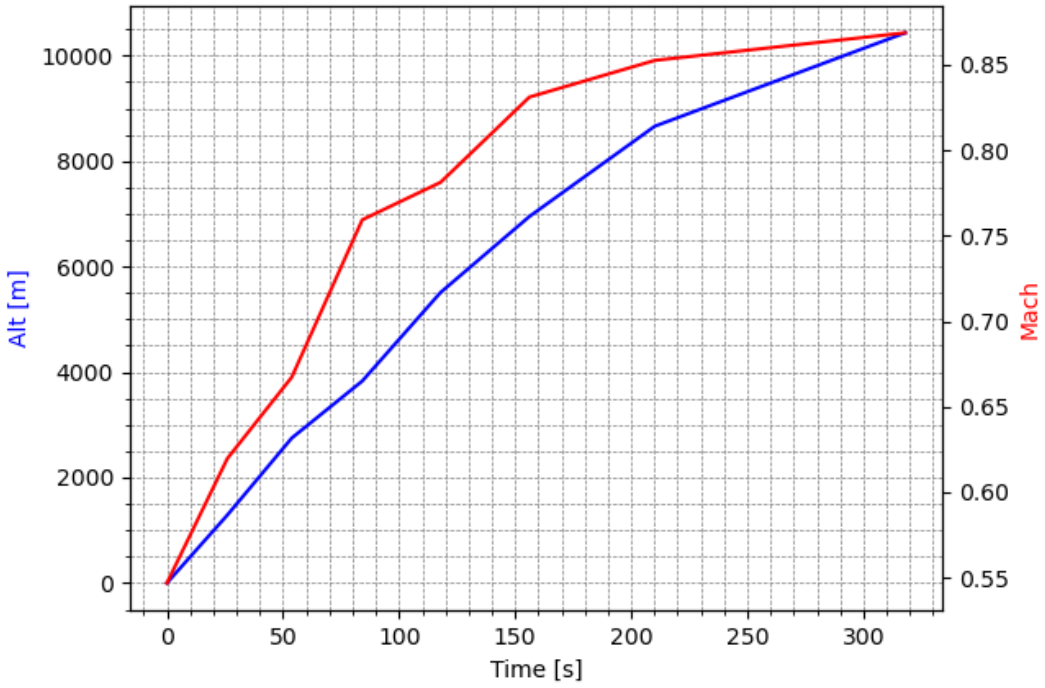

Figure 4-27: Max Range: Alt-Mach

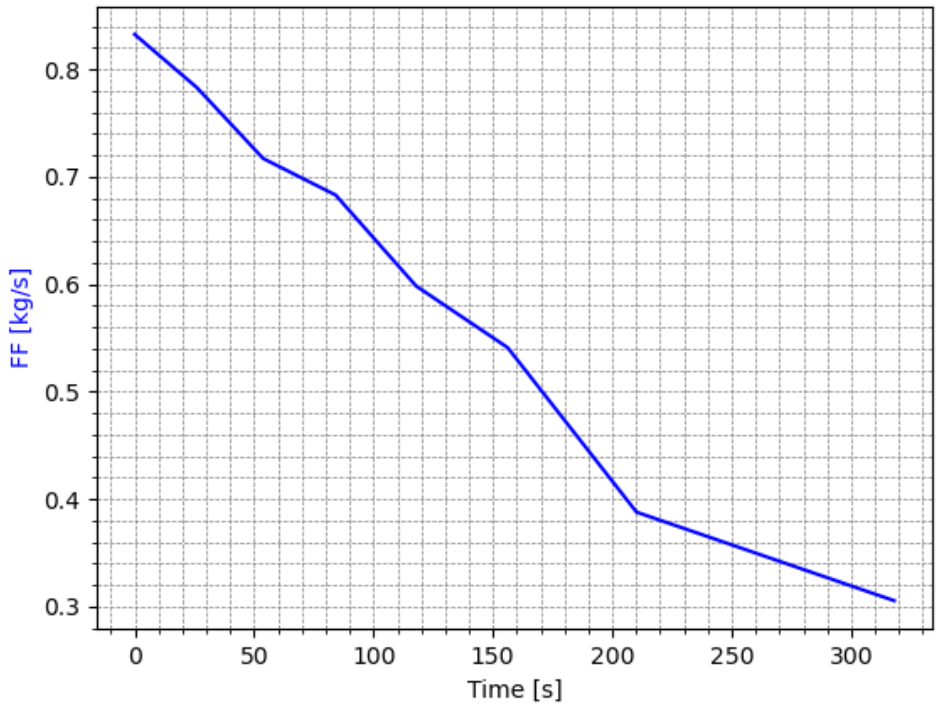

Figure 4-28: Max Range: Fuel Flow-Time

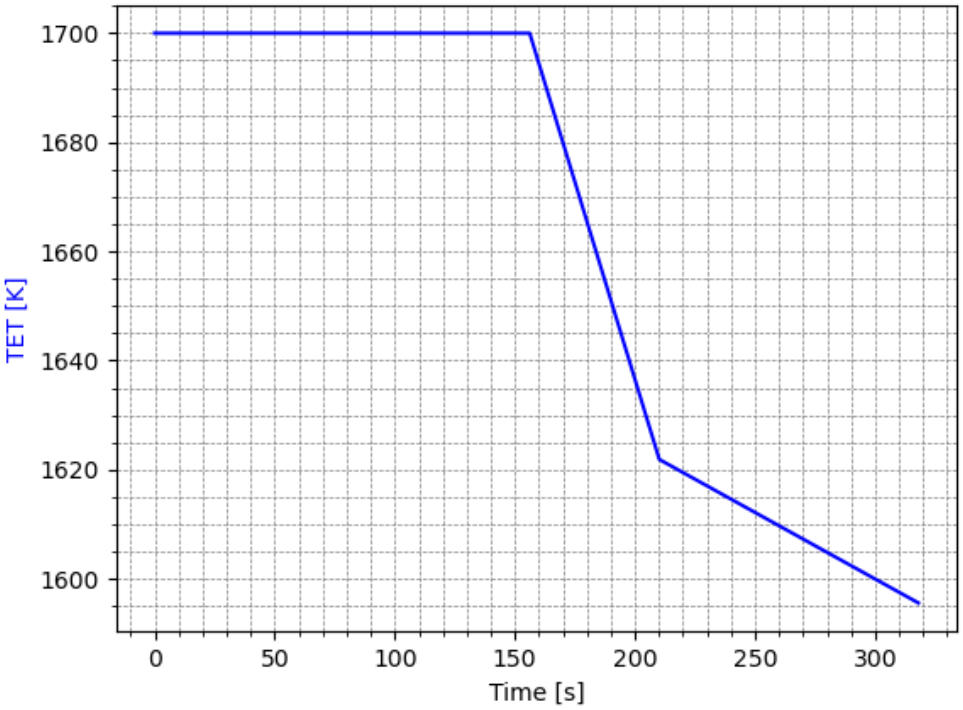

Figure 4-29: Max Range: TET-Time

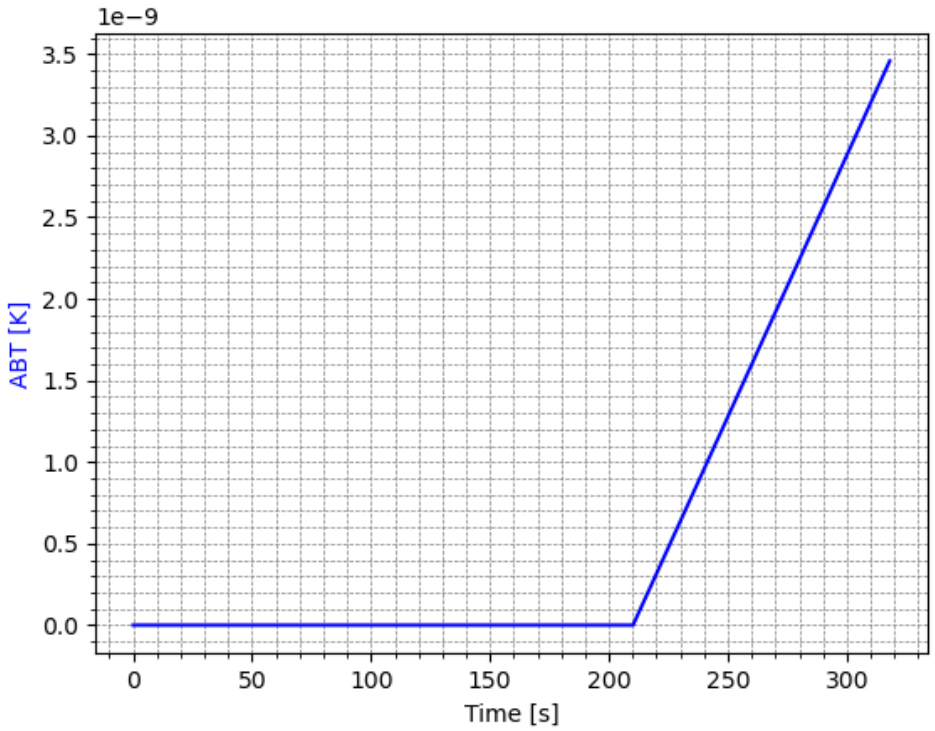

Figure 4-30: Max Range: AB Temperature-Time

2. Minimum fuel climb

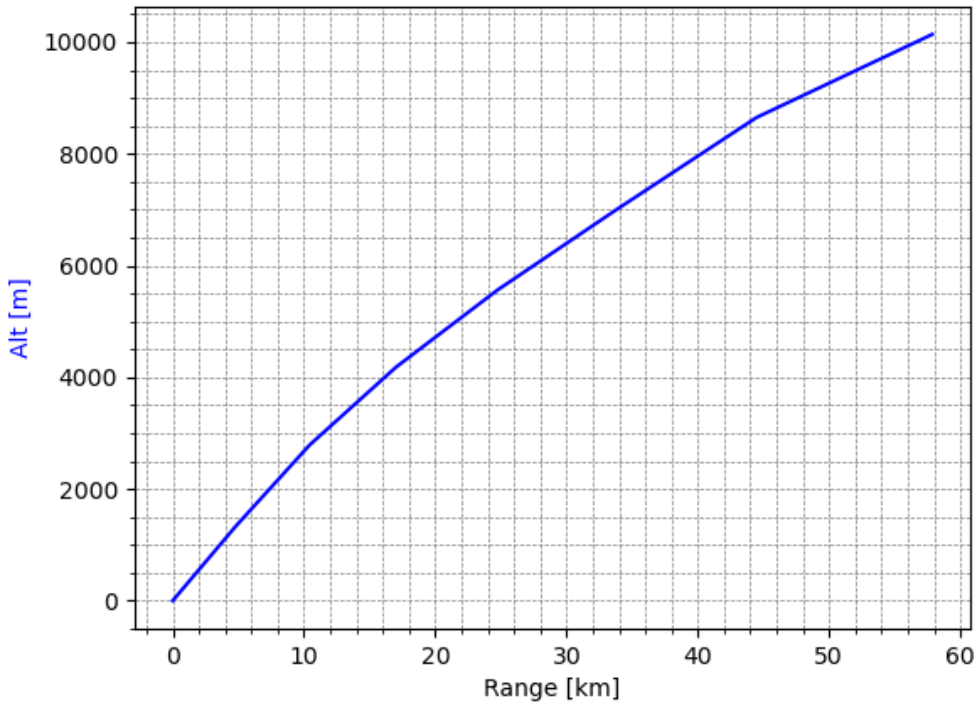

Figure 4-31: Min Fuel: Alt-Range

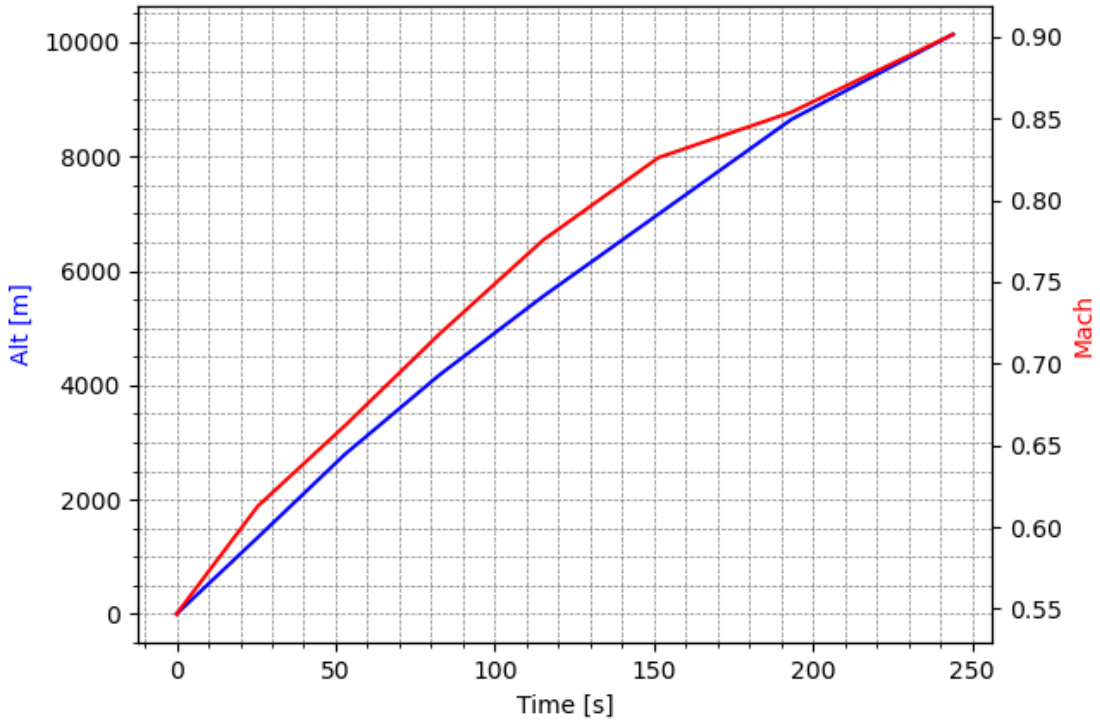

Figure 4-32: Min Fuel: Alt-Mach

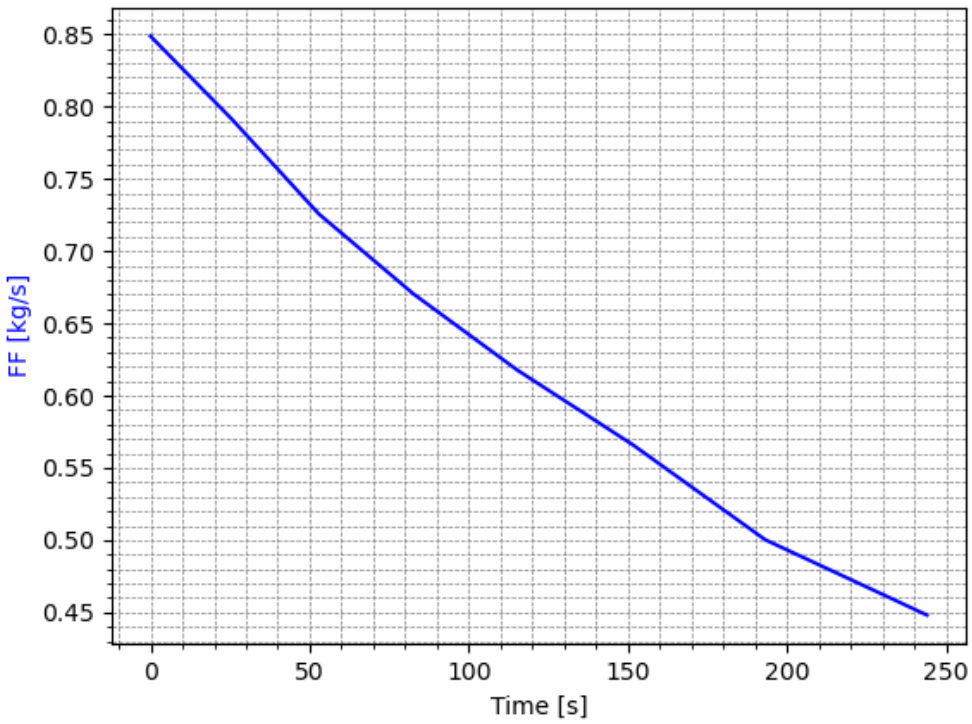

Figure 4-33: Min Fuel: Fuel Flow-Time

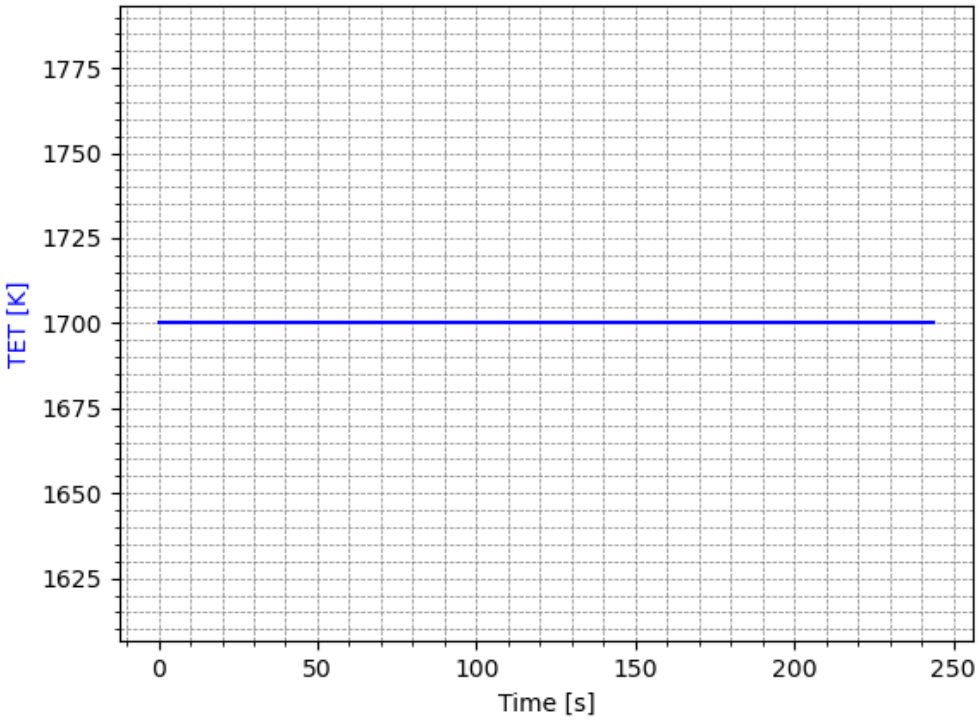

Figure 4-34: Min Fuel: TET-Time

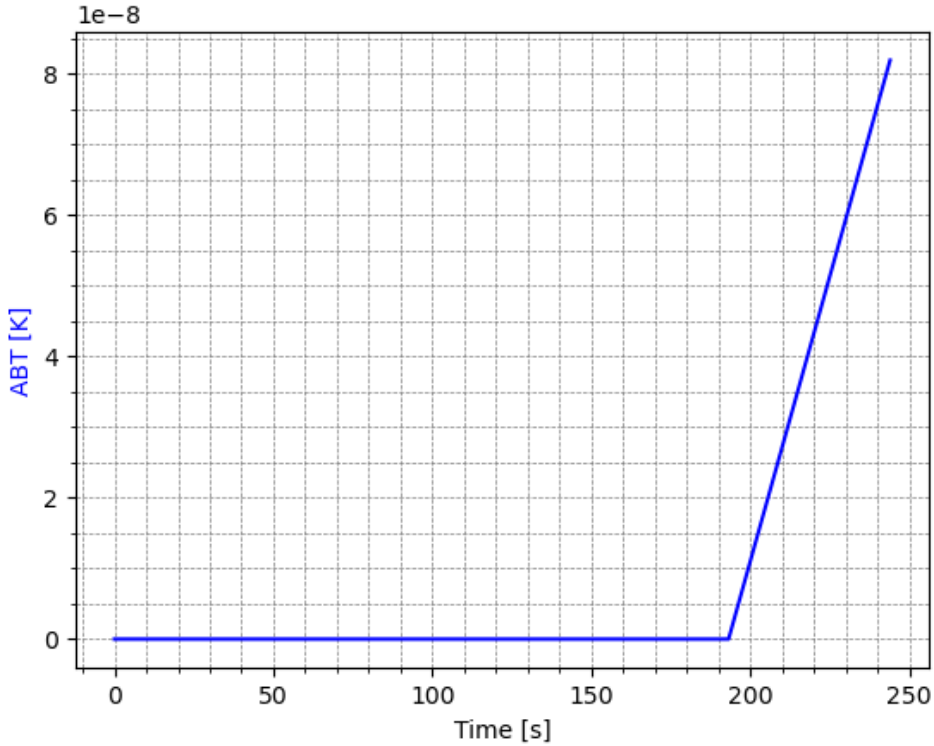

Figure 4-35: Min Fuel: AB Temperature - Time

3. Minimum IR signature

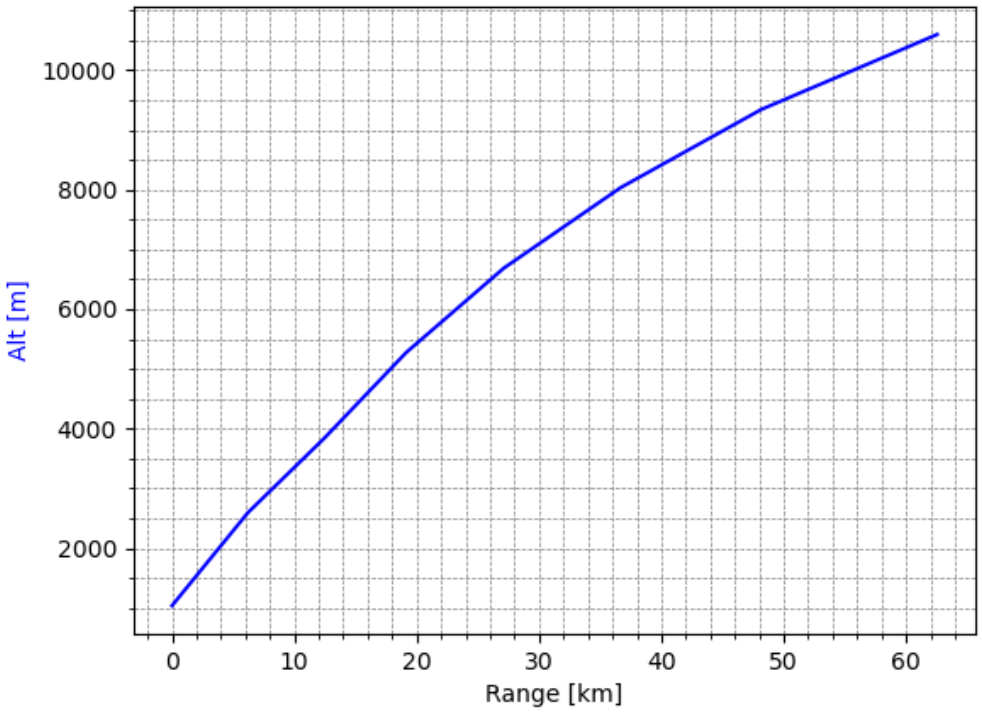

Figure 4-36: Min IR:Alt-Range

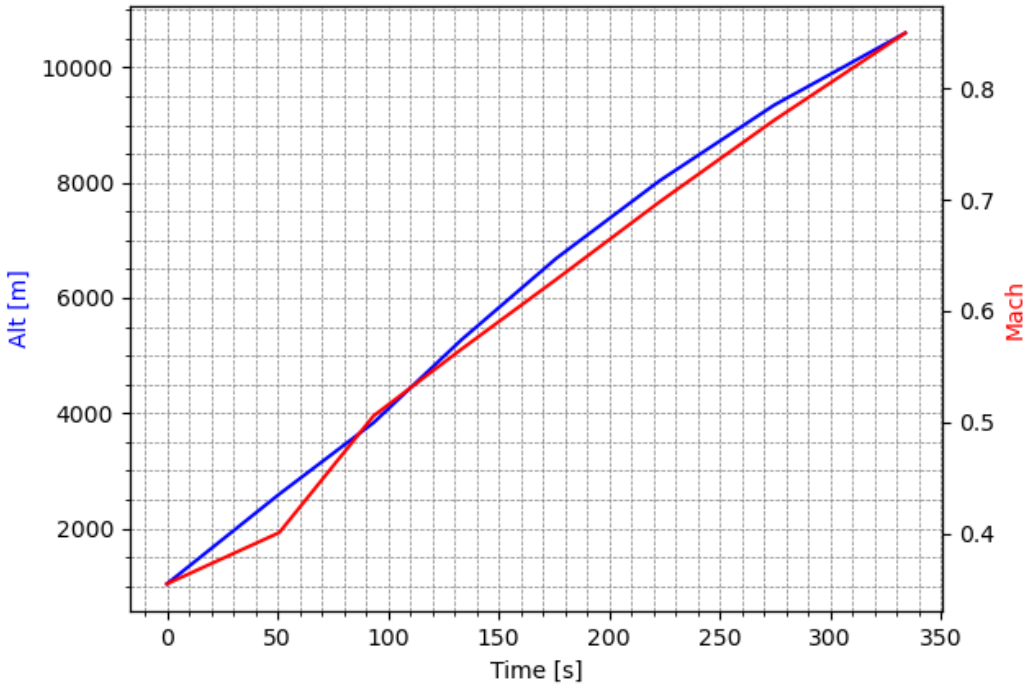

Figure 4-37: Min IR: Alt- Mach

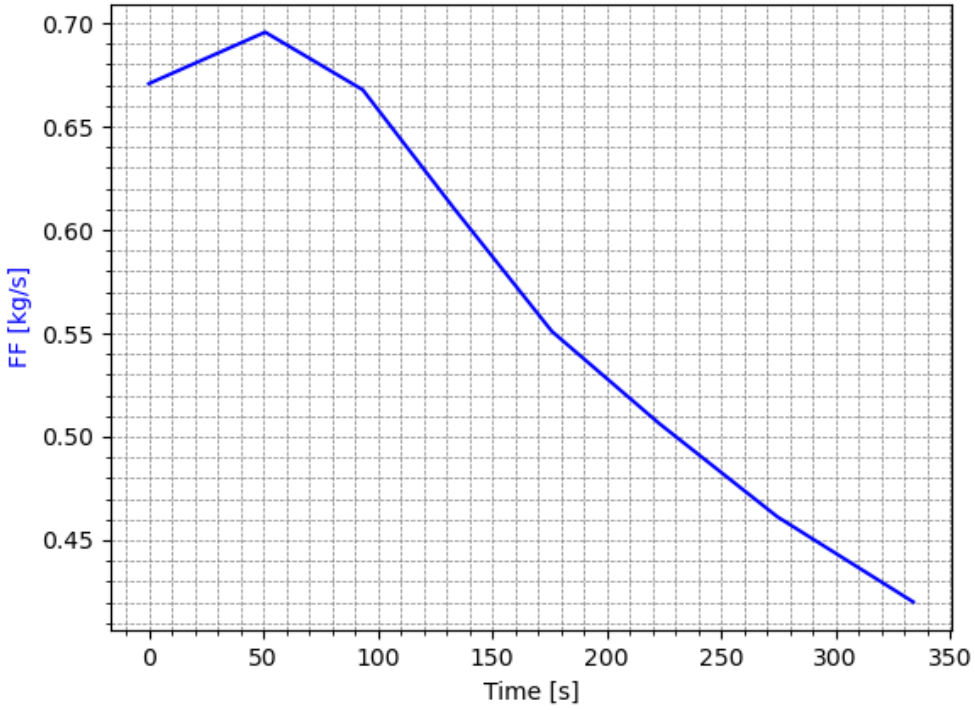

Figure 4-38: Min IR: Fuel Flow-Time

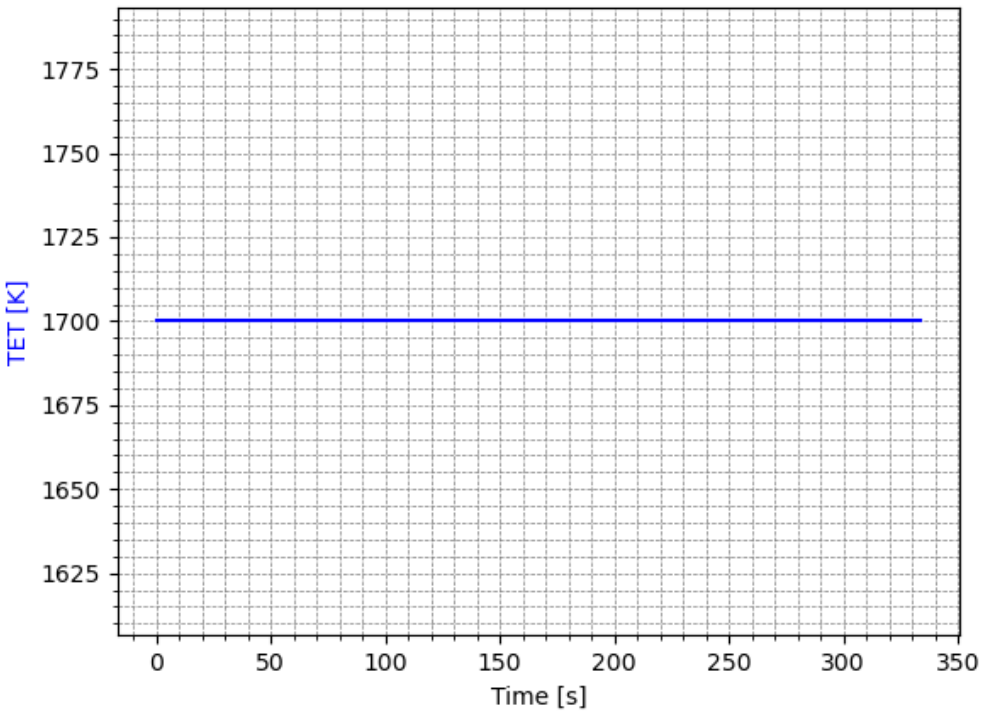

Figure 4-39: Min IR: TET-Time

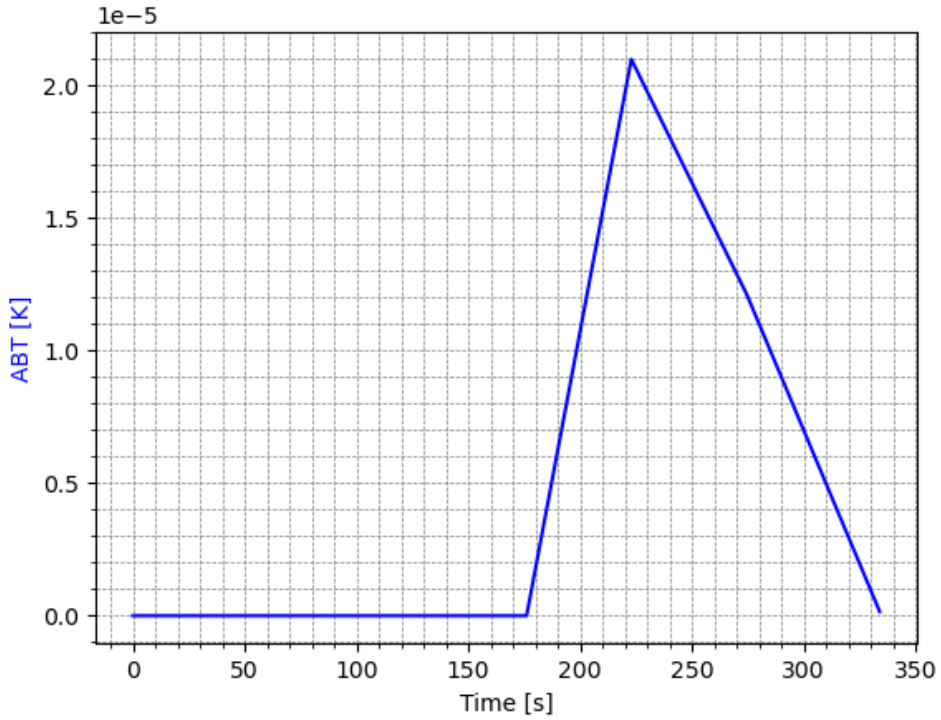

Figure 4-40: Min IR: AB Temperature-Time

4. Minimum noise

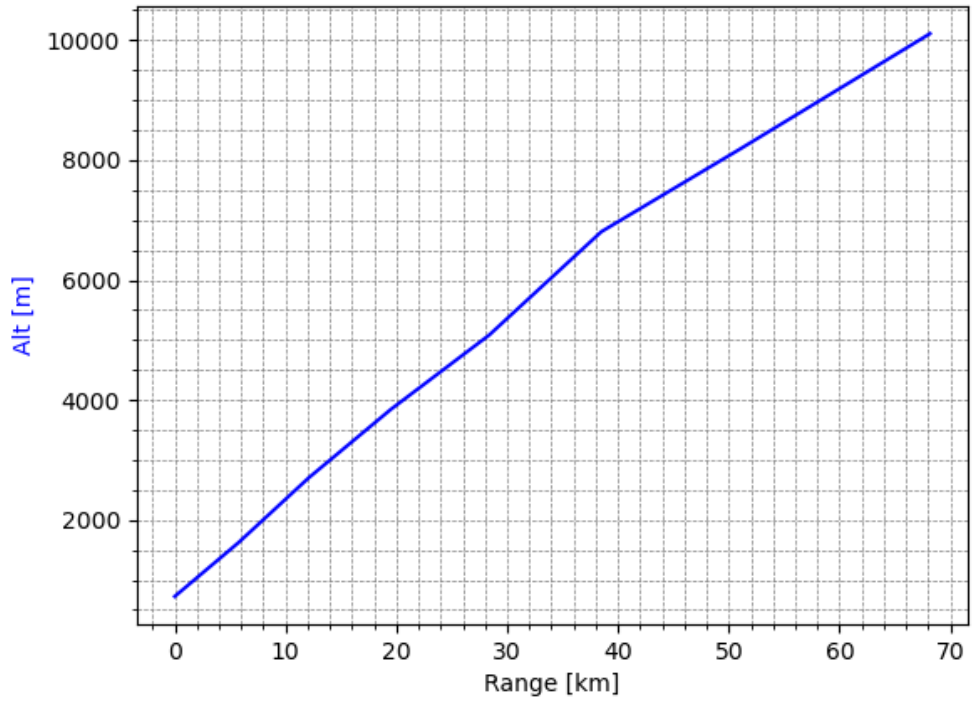

Figure 4-41: Min Noise: Alt-Range

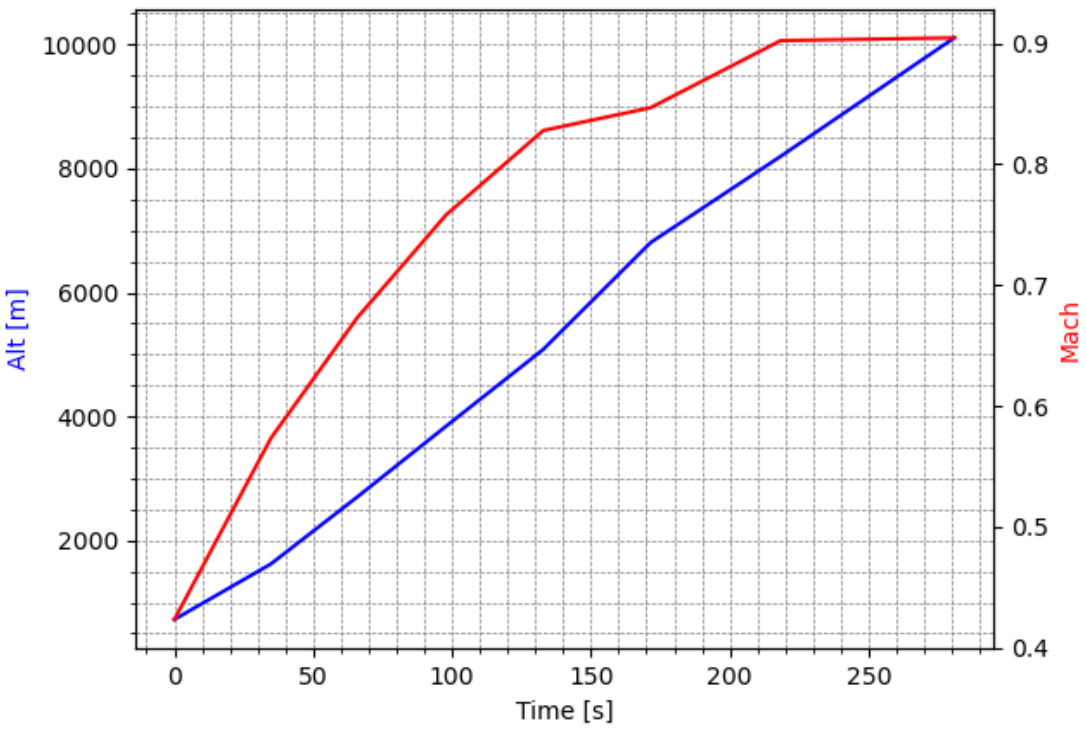

Figure 4-42: Min Noise: Alt-Mach

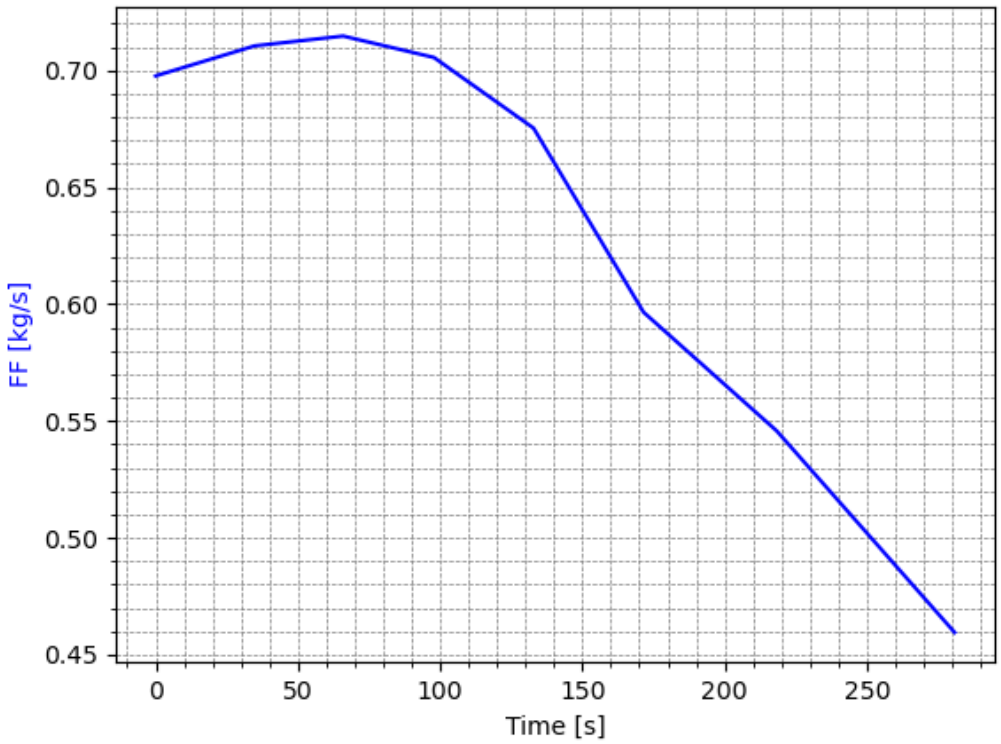

Figure 4-43: Min Noise: Fuel Flow-Time

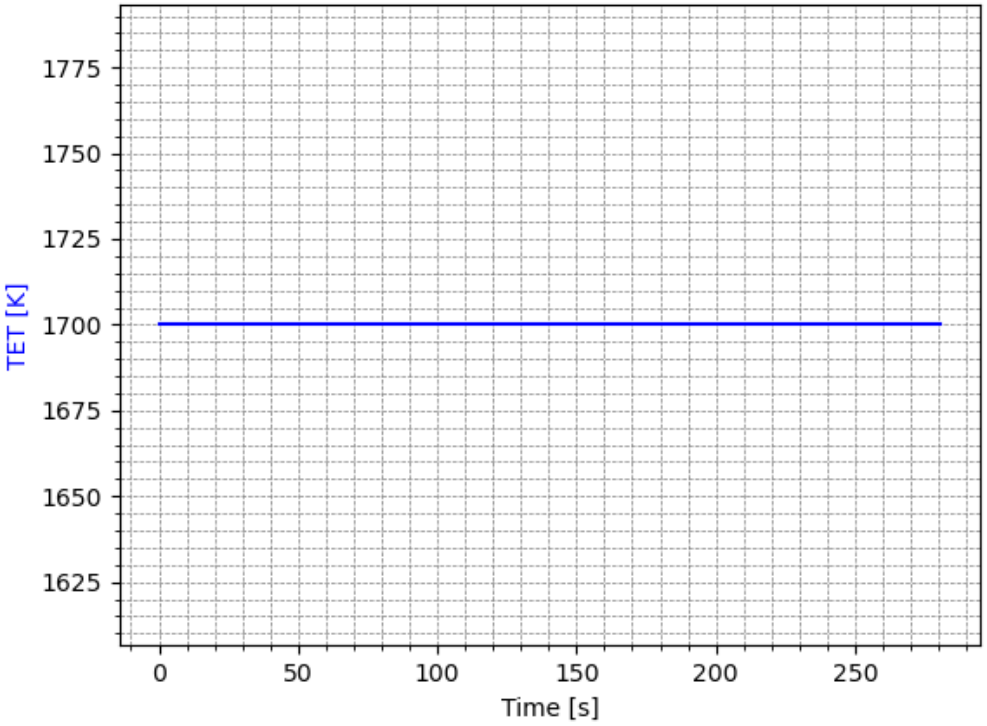

Figure 4-44: Min Noise: TET-Time

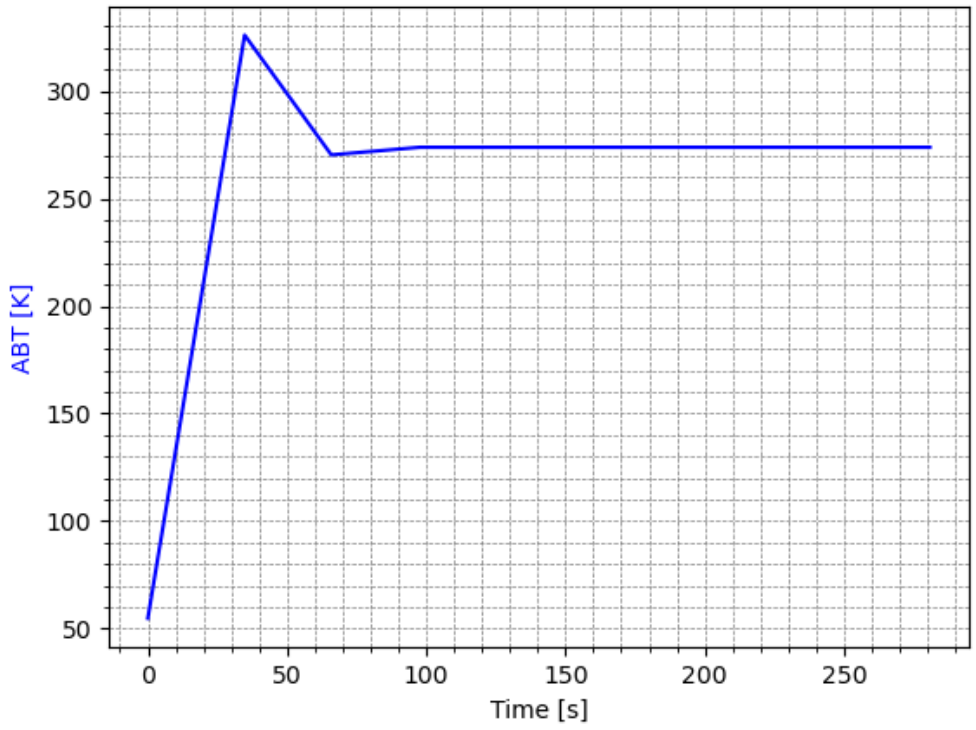

Figure 4-45: Min Noise: ABT-Time

5. Minimum time

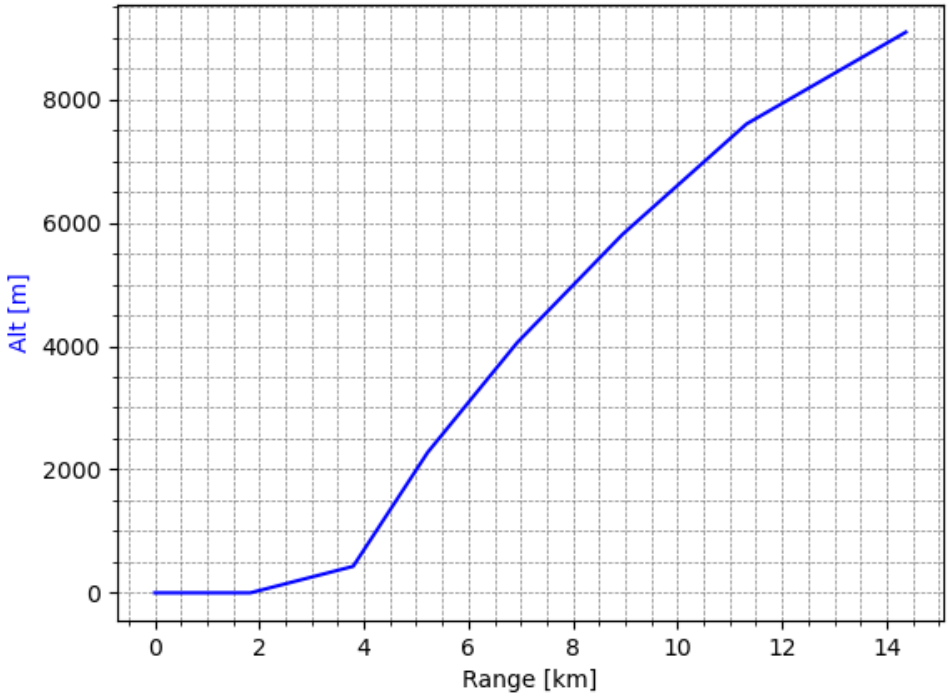

Figure 4-46: Min Time: Alt-Range

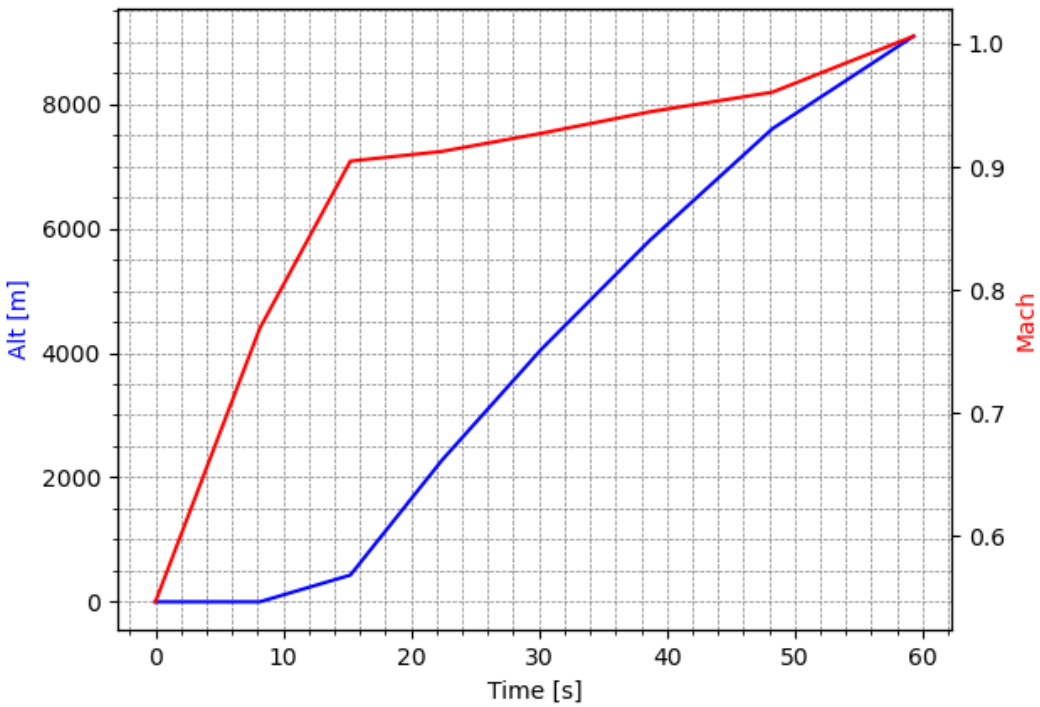

Figure 4-47: Min Time: Alt-Mach

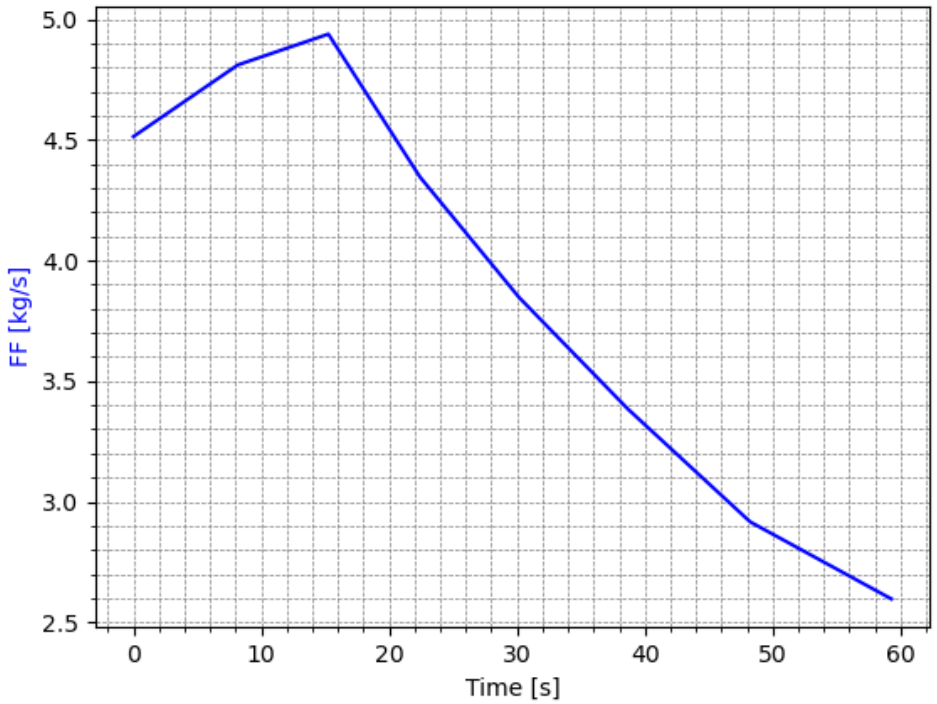

Figure 4-48: MIn Time: Fuel Flow-Time

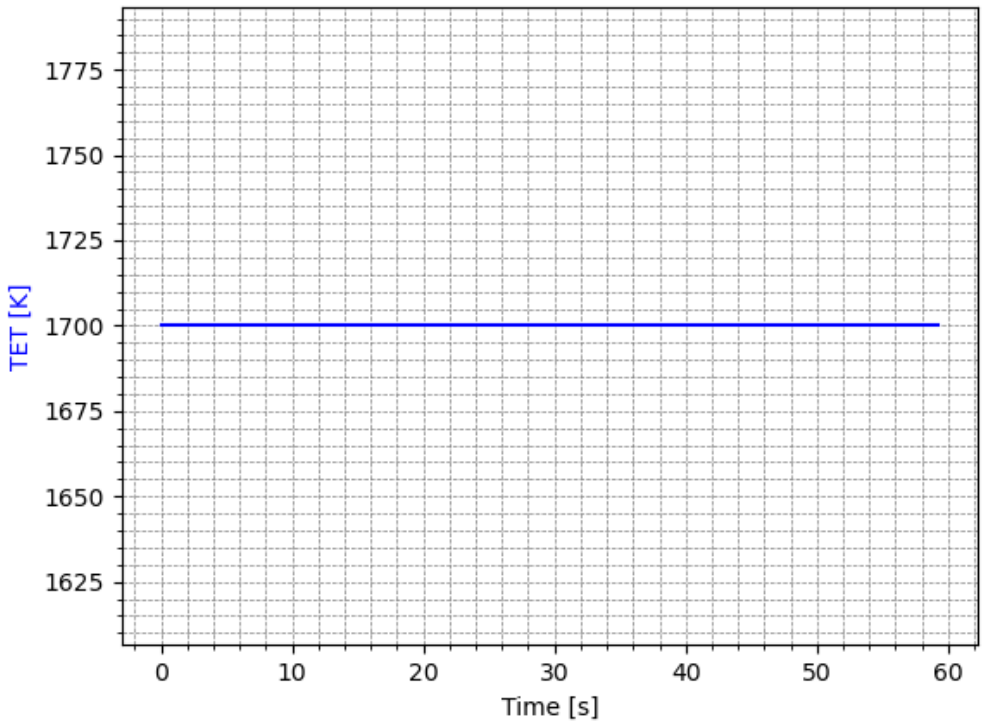

Figure 4-49: Min Time: TET-Time

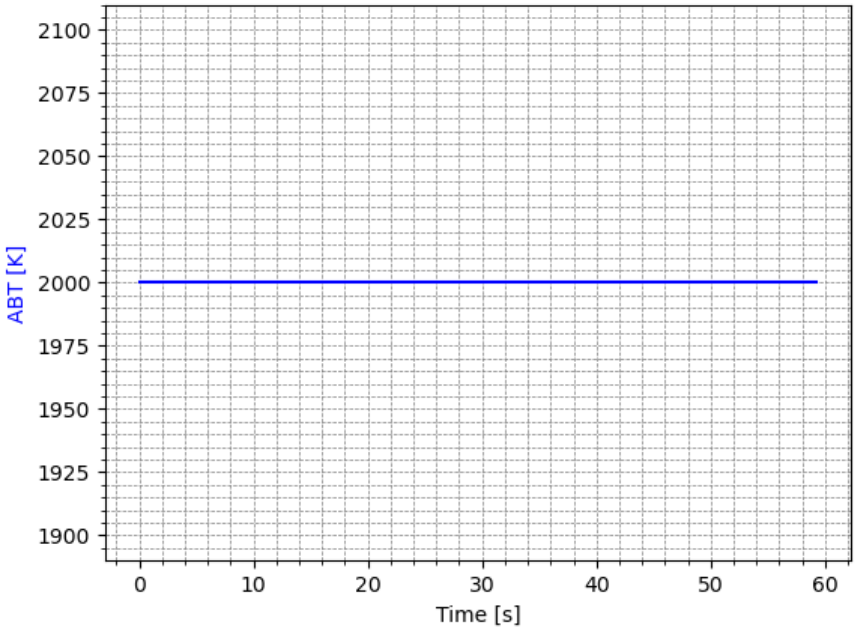

Figure 4-50: Min Time: AB Temperature-Time

Similar to full mission profiles, the life expectancy for each failure mechanism for each of these profiles was calculated. Figures 4-51 to 4-55 display the cycles to failure against blade span for each of the simulated profiles.

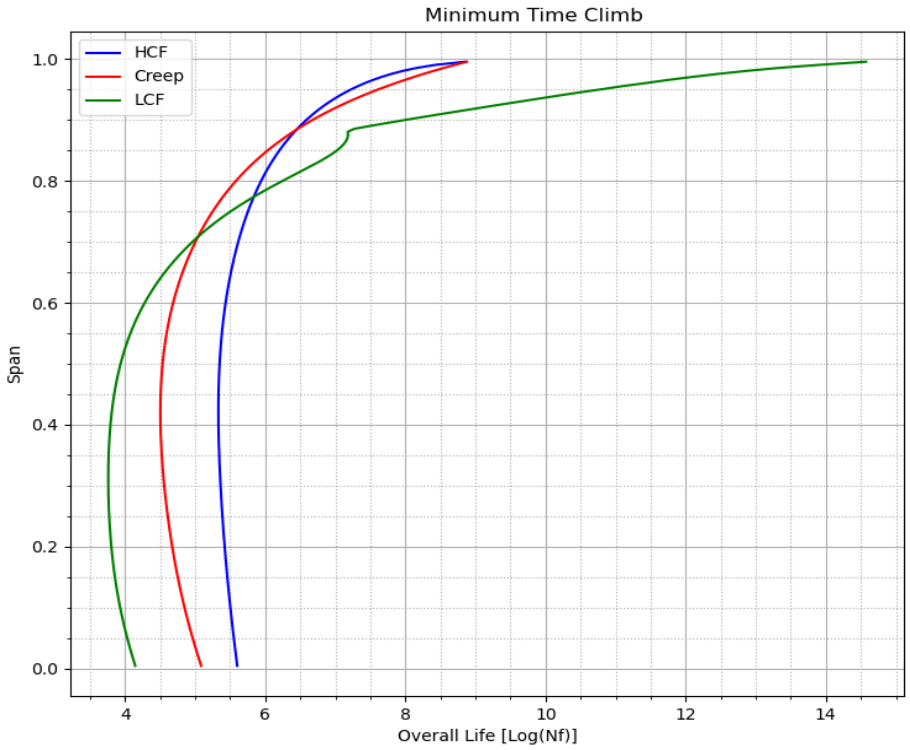

Figure 4-51: Minimum Time Climb cycles to failure

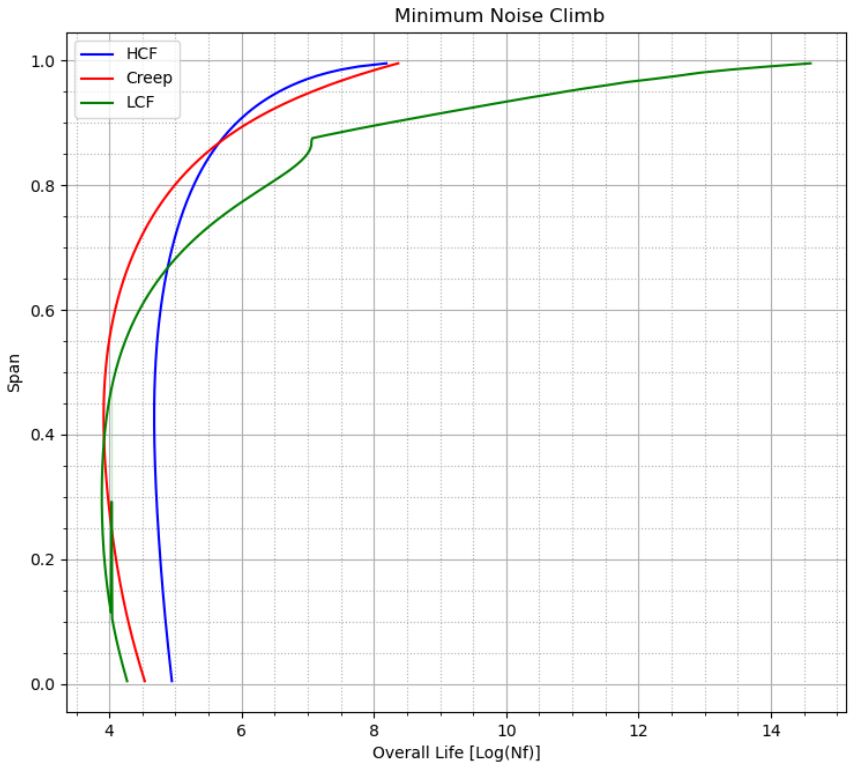

Figure 4-52: Minimum Noise Climb cycles to failure

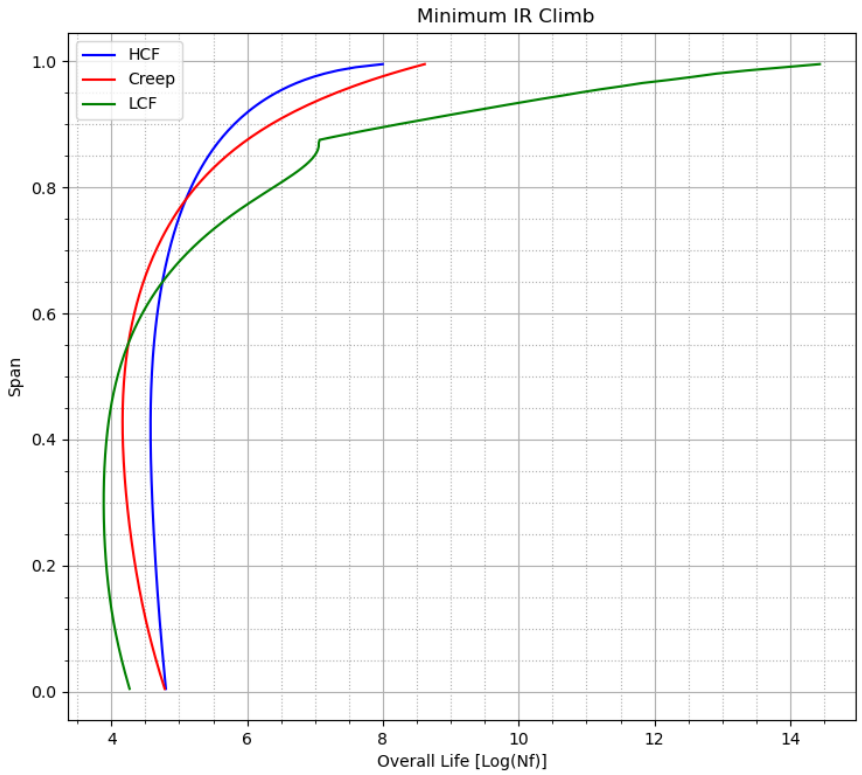

Figure 4-53: Minimum IR signature Climb cycles to failure

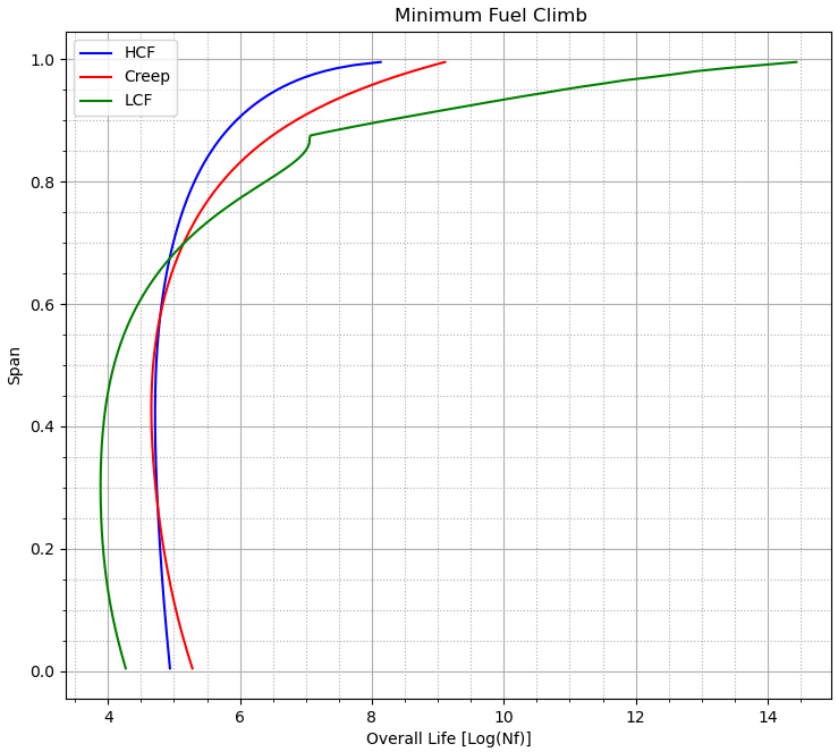

Figure 4-54: Minimum Fuel Climb cycles to failure

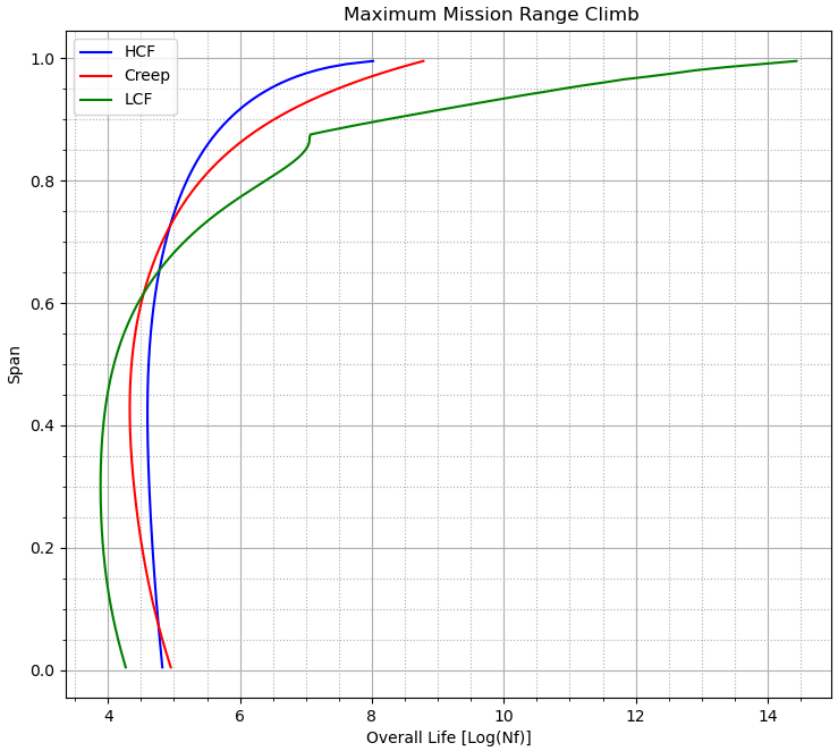

Figure 4-55: Maximum Mission Range cycles to failure

The respective critical points for every failure mechanism in each climb profile are shown in Table 4-2. The cycles mentioned are the limit where life of the material is expected to end.

Missions	Creep cycles	Span	LCF cycles	Span	HCF cycles	Span	Flight Hours	Span
Min Time	31811	42%	5742	31%	214081	42%	80	33%
Min Noise	8204	43%	7701	30%	47666	43%	297	36.5%
Min IR	14596	43%	7699	30%	37739	42%	426	34.5%
Min Fuel	45369	43%	7699	30%	51668	42%	404	32.5%
Max Range	21359	43%	7699	30%	39630	42%	450	34%

Table 4-2: Life critical points

Going through figures 4-26 to 4-55 in relation to table 4-2, it is evident that “AB” usage is dominant in life consumption. Even though that “Minimum Time” climb is the shortest in duration, even by 5 times comparatively to other optimal climb profiles, the predominant thermal and mechanical stress experienced make it the most critical profile. Worth the attention is also the fact that even though “Creep” and “HCF” life limits are not by any means critical for this profile, the impact on “LCF” is enough to drastically lower the engine’s life expectancy.

5 Results Discussion

This research was part of an effort to enhance the capabilities of Cranfield's TERA module for military aircraft. As a result, the main goal was to explore the possibilities of engine life estimation methods on modern fighter aircraft. To achieve this goal, a composition was made between well-established methods for aircraft mission performance and engine lifecycle estimation.

The product of this work is the development of a modular computational framework for the quantification of optimal mission performance on engine life. This framework is comprised of a module for gas turbine engine design suitable for military applications and a module for mission analysis on HPT rotor life estimation. This study focused on the development of computationally cost-effective solutions for the estimation of damage on the blades of HPT. The results produced by this effort, are presented below:

- The development of a module for gas turbine design suitable for military applications is possible using a combination of published data from civil GTE correctly scaled for low by-pass engines. This was proved by the calculation of reasonable values both for mechanical/thermal loads and most importantly by the production of logical life estimation results.
- Implications of optimal profiles on engine life have to be analyzed, as indicated by the variance of results from the studied failure mechanisms. In particular, a maximum difference of almost 35000 cycles was observed for Creep estimation and almost 150000 major cycles for HCF. The points of failure remain almost at the same spanwise position of the blade for all different profiles.
- In the same context, missions induce different results on the turbine blades.
- Regarding the TET, it was found to have a disproportionately greater effect on the damage of the blades. As TET increases, the stresses on the blade develop at a much higher pace than the rise of blade's temperature.

- As expected, TET is directly connected to Creep life. Profiles that include long periods of time in high temperature ratings are negatively influenced by Creep
- The use of A/B as an operating point was found to have little effect on engine life compared to military thrust setting (“Max_Rating”). This was proved by both the operating point lifing results and the simulation of climb and full mission profiles. This observation is related to the fact that the actual thrust increase is caused by a rise of temperature downstream the HPT. Therefore, this rise of temperature doesn’t affect much the conditions experienced by HPT.
- The previous observations is limited in terms of usage period meaning that in cases where AB is heavily used such as the “Supersonic Interception” mission, this effect is amplified and can result in greatly reduced life. This can be observed in the life expectancy of critical points where the use of AB has a great influence on the Creep and LCF life expectancy. HCF remains independent as it is mainly influenced by the mechanical stresses on the blades and the time period exposed to them. This is evident by the reduced HCF life expectancy for “Training” and “High Aoa BFM” missions where the duration of the mission is almost double the duration of ”Supersonic Interception”
- As expected, life consumption on all missions is mainly influenced by the use of high-power ratings (AB, Max_rating) as they have the biggest impact on failure mechanisms. It was found that life consumption during these two ratings can be as much as 85% both for full mission and climb profiles.
- HCF as a failure mechanism is heavily influenced by the rotational speed of the engine and the duration of operation. This is the reason why it was found that profiles such as “Max Range” and “Min IR” climb paths have reduced life expectancy in terms of HCF in relation to other profiles.

6 Future work

As previously discussed in the context of this study, the employment of low-fidelity but computationally cost-effective tool was chosen as a means to focus on the exploration of the possibilities around the topic of mission induced implication on the rotor blades of HPT.

The limitations of this framework are inherently in the choice of low fidelity tools. In order for this research to be expanded, the need of a more comprehensive engine design module is needed. In addition, the incorporation of HPT rotor disc in the lifing procedure would present a more holistic approach to lifing problem.

Regarding the failure mechanisms, Oxidation could be an interesting addition to military related TERA as multirole fighter can operate over different terrains and at low altitudes.

The author recommends that research be conducted in materials suitable for military applications and the construction of a database providing easily accessible information.

Regarding the engine life and the predictions made for component life expectancy, the incorporation EGT margin to account for inherent engine performance deterioration would create a more detailed view on the lifecycle of the engine and the costs surrounding the operation of the engine.

As it was showcased, different flight profiles, even if they share some common attributes can have diverse effects on the engine life consumption. Decision makers should be able to opt for specific profiles depending on the mission when operational demands are met. In this framework, optimal flight profiles for different flight phases could be explored for their potential benefits in engine life. This study proved that during the climb phase, optimal profiles can impact the engine life and so potentially can other flight phases.

Finally, in order to explore the potential links between mission sequence execution, SVR and life expectancy, it would be beneficial according to the author a model to be developed that will account for all these parameters and potentially simulate random mission execution sequences to study the interconnection between mission severity and life deterioration.

7 References

[1] M. Verhoeffa, W. Verhagen and R. Curran, "Maximizing operational readiness in military aviation by optimizing flight and maintenance planning," 18th Euro Working Group on Transportation, Delft, The Netherlands, 2015.

[2] Y. Macheret, P. Koehn and D. Sparrow, "Improving reliability and operational availability of military systems," IEEE, 2004.

[3] J. F. Montgomery, T. R. Sewall and J. Batka, "Aircraft usage and effects on engine life," THE AMERICAN SOCIETY OF MECHANICAL ENGINEERS, 1983.

[4] A. Gad-Briggs, A. Haslam and P. Laskaridis, "Effect of change in role of an aircraft on engine life," Aeronautical journal, 2013.

[5] D. Mavris and D. DeLaurentis, "An integrated approach to military aircraft selection and concept evaluation," AIAA, 1995.

[6] A. Seitz, "Advanced Methods for Propulsion System Integration in Aircraft Conceptual Design, PhD Thesis," Techische Universitat Munchen, Munchen,, 2011.

[7] W. Lammen, P. Kupijai, D. Kickenweitz and T. Laudan, "Integrate Engine Manufacturer's Knowledge into the Preliminary Aircraft Sizing Process," NLR-TP-2014-428, NLR, Amsterdam,, 2014.

[8] S. Ogaji, P. Pilidis and R. Hales, "TERA - A Tool for Aero-engine Modelling and Management," 2nd World Congress on Engineering Asset Management and the 4th International Conference on Condition Monitoring, Harrogate, 2007.

[9] P. Laskaridis, "Performance Investigations and Systems Architectures for the More Electric Aircraft, PhD Thesis," Cranfield University, 2004.

[10] T. Nikolaidis, "The TURBOMATCH 2.0 Scheme for Gas Turbine Performance Calculations," Cranfield University, 2015.

[11] H. Moon, "Military aircraft engine integration & mission performance, MSc Thesis," Cranfield University, 2019.

[12] P. Rolph, "Modelling of a severity dependent shop visit rate for a military turboprop engine, MSc Thesis," Cranfield University, 2022.

[13] R. G. Grant, "Flight: The complete History," Dorling Kindersley Limited, 2010.

[14] US Department of Defence, "Standard Aircraft Characteristics and Performance, Piloted Aircraft (Fixed Wing)," MIL-C-005011B, Washington DC, 1951.

[15] J. R. Boyd, T. P. Christie and J. E. Gibson, "Energy-Manoeuvrability," AD372287, Air Proving Ground Center Eglin AFB, 1966.

[16] E. Rutowski, "Energy Approach to the General Aircraft Performance Problem," Journal of the Aeronautical Sciences, vol. 21, no. 3, pp. 187-195, 1954.

[17] MIL-STD-3013, "Glossary of Definitions, Ground Rules and Mission," US Department of Defence, Washington DC, 2003.

[18] A. Antonakis, "Multi-disciplinary performance studies on propulsion system integration for military aircraft, PhD Thesis," Cranfield University, 2019.

[19] T. Takahashi, "Optimal Climb Trajectories through Explicit Simulation," Proceedings of the 15th AIAA Aviation Technology, Integration and Operations Conference, 2015.

[20] J. T. Betts, " Practical Methods for Optimal Control and Estimation Using Nonlinear Programming," SIAM, 2010.

[21] R. R-2103-AF, "Life-cycle analysis of aircraft turbine engines: Executive summary," USAF, 1977.

[22] M. Naeem, "Implications od aero-engien deterioration for a military aircraft's performance, PhD Thesis," Cranfield University, 1999.

[23] R. A. Matchett, "Life usage of a military turbofan, MSc Thesis," Cranfield University, 1999.

[24] M. Maxwell, "F404-GE-400 LPT Blade Lifing Study, MSc Thesis," Cranfield University, 2013.

[25] R. Tamma, "HPT Blade Life Study for a Low Bypass Turbofan Engine, MSc Thesis," Cranfield University, 2014.

[26] N. Khani, "Influence of airport factors and mission fuel burn optimised aircraft trajectories on severity and engine life, PhD Thesis," Cranfield University, 2014.

[27] H. Hanumanthan, "Severity estimation and shop visit prediction of civil aircraft engines, PhD Thesis," Cranfield University, 2009.

[28] A. Qigang, "Life Cycle Studies for Civil Turbofan Aero Engines, MSc Thesis," Cranfield University, 2021.

[29] R. Xu, "Life study of energy efficient engine 1st stage turbine disk, MSc Thesis," Cranfield University, 2020.

[30] R. Heffley and F. Wayne, "Aircraft Handling Qualities Data," NASA CR-2144, NASA, 1972.

[31] E. Haering and F. Burcham, "Minimum Time and Fuel Flight Profiles for an F-15 Airplane with a Highly Integrated Digital Electronic Control System," NASA-TM-88042, NASA Ames Research Center, 1984.

[32] T. NIkolaidis, "The TURBOMATCH 2.0 Scheme for Gas Turbine Performance Calculations," Cranfield University, Cranfield, UK, 2015.

[33] G. Farin, "Curves and Surfaces for CAGD: A Practical Guide, 5th ed.," Morgan-Kaufmann, San Francisco, California, 2002.

[34] J. Kennedy and R. Eberhart, "Particle swarm optimization," Proceedings of IEEE International Conference on Neural Networks 4, Piscataway, New Jersey, 1995.

[35] P. Sujit, S. Saripalli and J. Sousa, "An Evaluation of UAV Path Following Algorithms," European Control Conference, Zurich, Switzerland, 17-19 July 2013.

[36] H. Cohen, G. Rogers, H. Saravanamuttoo and P. Straznicky, "Gas turbine theory, 6th edn.," Pearson Education Limited, Essex, 2009.

[37] P. P. Walsh and P. Fletcher, "Gas Turbine Performance. 2nd edn.," Blackwell Science Ltd, 2004.

[38] J. Horlock, "Axial flow turbines thermodynamics and fluid dynamics," Hungtington: Robert E. Krieger Publishing Co., 1966.

[39] D. MacManus, P. Rubini and P. Zachos, "Turbomachinery and blade cooling notes," Cranfield University, 2019.

[40] R. D. Thulin, D. C. Howe and I. D. Singer, "Energy Efficient Engine High-Pressure Turbine Detailed Design Report," Cleveland, OH, US, 1982.

[41] S. W. Bartlett and P. F. Braun, "A Feasibility Study of Expanding the F404 Aircraft Engine Repair Capability at the Aircraft Intermediate Maintenance Department," NAVAL POSTGRADUATE SCHOOL MONTEREY CA, 1993.

[42] "https://en.wikipedia.org/wiki/Degree_of_reaction".

[43] A. C. Stitt, "A physics-based maintenance cost methodology for commercial aircraft engines, PhD Thesis," Cranfield University, 2014.

[44] L. Torbidoni and J. H. Horlock, "A New Method to Calculate the Coolant Requirements of a High-Temperature Gas Turbine Blade," Journal of Turbomachinery-transactions of The Asme, 2005.

[45] J. H. Horlock and L. Torbidoni, "Turbine Blade Cooling: The Blade Temperature Distribution," Proceedings of the Institution of Mechanical Engineers, Part A: Journal of Power and Energy. SAGE PublicationsSage, London, England, 2006.

[46] F. R. Larson, and J. Miller, "A time-temperature relationship for rupture and creep stresses," Trans. ASME, 1952.

[47] S. Manson, "Fatigue: a complex subject - some simple approximations," NASA TM X-52084, 1964.

[48] R. A. Cookson, and A. Haslam., "Fatigue and Fracture (unpublished," School of Engineering, Cranfield University, 2013.

[49] J. A. Collins,, "Failure of Materials in Mechanical Design: Analysis, Prediction, Prevention," Wiley., 1993.

[50] J. SZWEDOWICZ, "High Cyclic Fatigue," NATO, RTO-EN-AVT-207.

[51] R. Kurz and K. Brun, "Degradation in gas turbine systems," ASME, 2001.